General Disclaimer

One or more of the Following Statements may affect this Document

- This document has been reproduced from the best copy furnished by the organizational source. It is being released in the interest of making available as much information as possible.

- This document may contain data, which exceeds the sheet parameters. It was furnished in this condition by the organizational source and is the best copy available.

- This document may contain tone-on-tone or color graphs, charts and/or pictures, which have been reproduced in black and white.

- This document is paginated as submitted by the original source.

- Portions of this document are not fully legible due to the historical nature of some of the material. However, it is the best reproduction available from the original submission.

Produced by the NASA Center for Aerospace Information (CASI)

NASA CONTRACTOR REPORT 166607

(NASA-CR-166607) PERIODIC CONTROL OF THE INDIVIDUAL-BLADE-CONTROL HELICOPTER ROTOR Ph.D. Thesis (Massachusetts Inst. of Tech.) 192 p HC A09/MF A01 CSCL 20K

N84-34771

Unclas
G3/39 22949

Periodic Control of the Individual-Blade-Control Helicopter Rotor

Robert M. McKillip Jr.

CONTRACT NSG-2266
August 1984

NASA

NASA CONTRACTOR REPORT 166607

Periodic Control of the Individual-Blade-Control Helicopter Rotor

Robert M. McKillip Jr.
Massachusetts Institute of Technology
Cambridge, Massachusetts

Prepared for
Ames Research Center
under Grant NSG-2266

National Aeronautics and
Space Administration

Ames Research Center
Moffett Field, California 94035

PERIODIC CONTROL OF THE INDIVIDUAL-BLADE-CONTROL HELICOPTER ROTOR

by

ROBERT MILLER McKILLIP, JR.

Submitted to the Department of
Aeronautics and Astronautics on August 20, 1984,
in partial fulfillment of the requirements for
the degree of Doctor of Philosophy in
the Field of Estimation and Control

ABSTRACT

Results of an investigation into methods of controller design for an individual helicopter rotor blade in the high forward-flight speed regime are described. This operating condition poses a unique control problem in that the perturbation equations of motion are linear with coefficients that vary periodically with time. The design of a control law was based on extensions to modern multivariable systhesis techniques and incorporated a novel approach to the reconstruction of the missing system state variables. The controller was tested on both an electronic analog computer simulation of the out-of-plane flapping dynamics, and on a four foot diameter single-bladed model helicopter rotor in the M.I.T. 5x7 subsonic wind tunnel at high levels of advance ratio. It is shown that modal control using the IBC concept is possible over a large range of advance ratios with only a modest amount of computational power required.

Thesis Committee:

Professor N. Ham (Chairman)
Professor W. Widnall
Professor J. Dugundji

ACKNOWLEDGEMENTS

Six years of effort, experiences, education and enjoyment make it exceedingly difficult to express my thanks in just a few short paragraphs to all those who made this thesis a reality, but I would be remiss not to try. First, the author would like to thank Professor Norman Ham for his unfaltering support of my sometimes hapless efforts to make our model helicopter behave the way I thought it should. His ability to provide sage counsel and direction kept me from stumbling over conceptual hurdles, while his trust in my efforts allowed me to learn a great deal by exploring many areas previously foreign to me. Thanks are also due to Professor Widnall and Professor Dugundji for their suggestions and advice during the progression of this research effort.

Mr. Paul Bauer deserves a special thanks for all the selfless assistance provided me throughout my stay here at M.I.T. He showed me the importance of being able to laugh at myself, and shared some of his vast wealth of practical expertise that allowed me to eventually complete this work. Mr. Christopher Cole also merits appreciation for the help he provided with some of the system's electronic components.

To Professors R. John Hansman and Edward Crawley, the author would like to extend his thanks for their friendship and encouragement that are so important in any undertaking such as this. Fellow graduate and undergraduate students, too numerous to mention, also helped make this experience so rewarding.

And finally, the author would like to express his love and appreciation to his wife Melissa. Her devotion and patience while this work was in progress have convinced him that he is indeed a very lucky man.

The author would like to dedicate this thesis in loving memory of his mother, and to his father, who got him interested in all this airplane business in the first place.

CONTENTS

LIST OF ILLUSTRATIONS

1. INTRODUCTION

1.1 The Individual-Blade-Control Concept

To further expand the utility and performance of the modern helicopter, improvements must be made in the response of the aircraft to the many and varied disturbances present in its normal operation. These responses are primarily of aerodynamic origin, and are transmitted to the vehicle through its rotating blades. Thus, if sufficient action is taken at the source of these problems, it would appear possible to considerably improve the helicopter's handling qualities, reduce vibration and increase overall stability. Recent efforts to apply active control technology to rotary wings have shown promise in reducing response due to atmospheric turbulence [Ham and McKillip,1980; Zwicke,1980], retreating blade stall [Ham and Quackenbush,1981], vibration suppression [Shaw and Albion,1980; Wood,1983], blade-fuselage interference [Rahnema,1981], and flap-lag modal damping enhancement [Ham, Behal and McKillip, 1983].

These applications have all used the method of active pitch control to produce counteracting aerodynamic forces, but the generation of the control actuation can be divided into two fundamentally different approaches. The first and

currently more widely used in vibration suppression is Higher-Harmonic-Control (HHC) [Shaw and Albion,1980; Wood,1983; Molusis, Hammond and Cline,1981; Johnson,1982; Taylor, et. al.,1980], where integral multiples of rotor rotational frequency are appropriately scaled and phase shifted so as to generate pitch commands, either open- or closed-loop, that approximately cancel the harmonics of vibration passed down from the rotor to the fuselage. The second and more versatile of the two is Individual-Blade-Control (IBC) [Ham and McKillip,1980; Ham and Quackenbush,1981; Rahnema,1981; Ham, Behal and McKillip,1983; Kretz,1976; Ham,1980; Guinn,1982; Ham,1983], involving the use of actuators on each blade to control the pitch individually in the rotating frame of reference. This latter approach is essentially a "broad-band" control of the rotor blade dynamics, as opposed to the HHC limitation of discrete frequency disturbance suppression, and as such is capable of aeroelastic control of the blade modal responses to both external disturbances and pilot commands.

However, this increased functionality of the IBC concept is not without its price. Since the control and the motion sensing of the IBC system is done in the rotating blade's frame of reference, the equations describing the dynamics will contain coefficients that are periodic functions of

blade azimuth angle due to the rotor's non-uniform flowfield in forward flight [Johnson,1980; Gessow and Meyers,1967]. This time dependence of the system dynamics thus makes the use of standard time-invariant controller design techniques invalid for flight speeds exhibiting moderate levels of periodicity. Hence, a definite need exists for rules and guidelines in the selection of a controller design for systems with periodic coefficients if the IBC concept is to become a piece of flight hardware.

1.2 Periodic Coefficient Systems

The linearized small displacement equations of motion of the rotor blade containing periodic coefficients are by no means unique -- the general form of the solution to linear periodic equations was first stated in a set of theorems over a century ago, known collectively as Floquet theory [D'Angelo,1970; Meirovitch,1970; DeRusso, Roy and Close,1965]. Common special cases of these equations are Hill's equation and the Mathieu equation, both only second-order, with the second a subset of the first [Magnus and Winkler,1979]. Applications of such equations to physical phenomena abound, ranging from astronomy and orbital mechanics [Meirovitch,1970; Kern,1980; Nishimura,1972; Wiesel and Shelton,1983], electric circuits and solid-state physics

[Haug,1972] to biolgical cycles [Emanuel and Mulholland,1976], aircraft cruising flight optimization [Evans,1980; Gilbert,1982; Speyer and Evans,1981], chemical reactor process control [Fjeld,1969; Rinaldi,1970; Marzollo,1972], and parametrically excited mechanical systems [Wang,1983; Peters and Hohenemser,1971; Nafeh and Mook,1979].

Analytic solutions for these equations are not possible, except for a few scattered special cases [Wu,1980; Dasarathy and Srinivasan,1968; Junkins,1978] and so one often needs to resort to numerical methods to integrate these equations forward in time [Friedmann, Hammond and Woo,1977; Gaonkar, Sinha-Prasad and Sastry,1981; Vepa and Balasubramanian,1980; Dugundji and Wendell,1983]. Approximate methods such as those of peturbation theory [Nafeh and Mook,1979; Johnson,1972; Nafeh,1981], or a similar technique of harmonic expansion [Dugundji and Wendell,1983; Peters and Ormistron,1975; Hohenemser and Yin,1972; Wendell,1982] are possible if one is interested either in solutions valid over a short time interval or at steady-state.

1.3 Periodic Control Theory

Due to the time-varying nature of the equations, control systems are not easily designed for periodic processes using

classical frequency-domain approaches. However, modern control theory [Bryson and Ho,1975; Kwakernaak and Sivan,1972] is capable of handling time-varying system dynamics and thus is a likely candidate for attempts to extend the theory to handle periodic systems. The technique of modern control design consists of formulating the control requirements as a constrained optimization problem, where the function to be minimized is an expression that trades off system performance with the cost of controller activity. This cost functional is typically a scalar that exhibits quadratic dependence upon both state and control deviations, and the constraint is that the system be governed by the state equations of the plant being controlled. The weighting factors in the cost function can be used to achieve various purposes, such as state-control perturbation tradeoffs, pole placement, output regulation, implicit model following and neighboring-optimal control [Stengel,1981]. An attractive additional benefit is that modern control and state-space techniques are equally capable of including the many degrees of freedom and multiple inputs and outputs present in the helicopter rotor. Like all design methodologies, it is not without its faults. Although the technique does "automatically" compute a feedback scheme that is in some sense "optimal" for the given cost function, a fair amount of

iteration and insight is often necessary in order to specify a mathematical relationship that truly represents the design objectives of the controls engineer [Widnall,1968; Stein,1979].

Of the literature in the controls field relating to periodic control, most concerns the periodic operation of a time-invariant nonlinear system to maximize some measure of performance [Marzollo,1972]. The two most notable examples of this are chemical process control [Fjeld,1969; Rinaldi,1970] and aircraft cruising flight extension [Evans,1980; Gilbert,1982; Speyer and Evans,1981]. In this instance, a technique is developed to determine the necessary conditions under which control of a process can be improved if it is operated under oscillatory conditions instead of at a steady-state. For these problems, the performance function is maximized over one period, with the period left as a free parameter and the states of the process forced to be equal at the completion of one cycle.

Closer to the problem at hand are biological system control problems (since they operate cyclically with a fixed period) [Emanuel and Mulholland,1976], but often these are characterized by state variables that are constrained to be non-negative, such as species populations, or to having

performance criteria that are non-quadratic in the state deviations. Other examples, such as [Wang,1983], address the control of a time-periodic system using state-dependent inputs. Examples of pole-placement techniques for linear periodic systems can be found [Kern,1980; Wiesel and Shelton,1983; Meyers,1982; Wolf,1982], but they are all done without the use of a cost function and as such provide no indication of the effects of various weighting parameters upon the closed-loop dynamics. To the best of the author's knowledge, only [Liebst,1981] addresses the Linear-Quadratic-Regulator (LQR) problem in the context of a periodic coefficient system, but it too falls short in that it gives no indication of system stability or eigenvalue movement with various cost constraints.

1.4 Scope of Current Research

The motivation for this thesis was first encountered during the author's work in [Ham and McKillip,1980], where the wind tunnel model rotor operating under an early feedback controller design exhibited a pronounced parametric excitation at half rotor rotation frequency. Subsequent analysis using Floquet theory showed this result to be predictable, and thus all feedback controller designs were henceforth checked to ensure that they would not possess

similar N/2-per-revolution resonances. For moderate levels of feedback gain and low advance ratios, this approach proved to be adequate for IBC applications involving the control of single-mode response [Ham and Quackenbush,1981; Ham, Behal and McKillip,1983; Biggers,1974].

Applications of the IBC concept to vibration reduction, due to the added complexity of including two out-of-plane modes of response, necessitated the use of state-variable techniques in the controller design. Since this application had a low forward-speed flight condition as its design point, the effects of periodicity were once again neglected in the feedback design phase. The benefits of a simplification to a linear time-invariant form were somewhat overshadowed by the requirement within modern control theory to have all state variables of the problem available for measurement. Since this was quite impossible, attention was then focused on how to best make amends for this lack of information.

Research into observer theory showed that in order to best estimate these states given the measurements available, one must construct a dynamic model of the process to be observed, and drive the model with weighted errors between the expected output and the actual measured output of the system [Bryson and Ho,1975; Kwakernaak and Sivan,1972]. This

then requires one to build a dynamic element, (often electronic) that has the same order as that of the physical system, often a rather severe constraint. Given a suitable selection of effectively noise-free measurements, however, it is possible to construct a lower-order approximation to this observer [Luenberger, 1966]. If one merely wishes to feedback a particular linear combination of these state variables, even further reduction of system complexity may be possible [Melsa and Jones,1970].

Use of these "minimal-order" observers in early IBC vibration controller designs resulted in systems with poor performance. After other competing designs were generated via this same technique, it was discovered that the observer's gains were highly sensitive to variations in the plant parameters. This sensitivity was due not only to variations in actual coefficients, but also to the assumed model structure, stemming from the use of blade-mounted accelerometers as sensors for feedback control.

For most physical systems represented in state-variable notation, pure acceleration is not a state-variable in itself, but instead is a linear combination of the displacement and velocity states of the plant as well as any control or disturbance inputs. Since the accelerometer

measurements are assumed to be relatively noise-free, any unmodelled effects or disturbance dynamics such as tunnel turbulence are propogated directly into the estimation error, and as such could conceivably force the rotor blade to exhibit erratic behavior. This effect could easily be compounded by the neglected periodic variation of the coefficients in the math model of the rotor dynamics. Thus a strong need exists for some guidelines concerning what level of approximation is sufficient for adequate feedback controller design of such a complex system.

The chapters in this thesis fill this gap in knowledge and experience in designing modern control systems for linearly periodic systems through a methodical series of investigations culminating in the periodic control of a model helicopter rotor in forward flight. First, the equations of motion for a single helicopter rotor blade in forward flight are presented in chapter 2, along with a description of the mathematical nature of linear periodic coefficient systems. Chapter 3 presents modern control theory in the context of periodically varying systems, with some numerical results concerning trends in closed-loop pole locations with changes in the cost function. An extension is made in the theory to handle implicit-model-following controller design for periodic systems, and an efficient computational technique

for calculating the feedback and feedforward gains is outlined.

In chapter 4, the system identification problem for linear periodic systems is treated in two parts. First, a novel technique for estimating rotor states using position and acceleration measurements is described. The method is unique in that it contains no periodically varying elements in its observer structure. Second, a least-squares procedure for extracting the periodic system coefficients is explained. The regression uses the state estimates of the observer in its computations. Chapter 5 is devoted to describing the hardware used in the various experiments conducted in the thesis. The analog computer board that simulates the out-of-plane rotor flapping dynamics is diagrammed, and then the actual model helicopter rotor system is described.

Chapter 6 contains experimental results. These encompass work done on the analog simulation concerning state estimation, parameter identification and closed-loop control, as well as data from the actual rotor at high advance ratios. Parameter identification trials and closed-loop controller results are detailed for the wind tunnel test data, and comparisons both with theory and with the results from the simulation tests are made. Conclusions from the research are

drawn in chapter 7, and recommendations for areas of further work are given.

2. EQUATIONS OF MOTION AND PERIODIC SYSTEM MATHEMATICS

2.1 Introduction

In this chapter the equations of motion describing the rigid out-of-plane flapping dynamics of a single articulated rotor blade in forward flight are derived. The asymmetrical nature of the tangential flow field will be shown to give rise to damping, stiffness and control terms that are periodic in blade azimuth angle. To simplify the analysis, a quasi-steady approximation has been used, with no allowances for the effects of compressibility, stall, or blade tip losses in the calculation of the aerodynamic forces present. Only one mode is considered, since: (1) consideration of additional elastic out-of-plane modes would only cloud the picture of the effect of various control designs; (2) the model rotor blade to be tested is in itself very stiff, having a nondimensional bending stiffness near seven times rotor rotation frequency, approximately twice the ratio of a full-size blade; (3) in-plane motion, while not having a high natural frequency, is rather small in magnitude and is not of major importance for an articulated rotor; and (4) effects of torsional flexibility are discounted, since the IBC concept requires broadband control of blade pitch from the outset.

Following a description of the plant dynamics to be controlled, an outline of the available mathematical tools to deal with such peculiar systems is given. This includes a formulation in state-variable notation [DeRusso, Roy and Close,1965] which has proved to be very convenient for handling multi-dimensional control and systems problems. Floquet theory is introduced along with the importance of the state transition matrix for one fundamental period, and computational techniques for obtaining this matrix and thereby determining system stability are presented.

2.2 Derivation of the Rotor Flapping Equations

Several methods exist for arriving at the equations describing the flap motion of an articulated blade in forward flight [Sissingh,1970; Johnson,1980], but perhaps the easiest and most direct is simply to invoke D'Alembert's Principle and consider the moments about the flapping hinge at the hub, as sketched in figure 2.1. In figure 2.1.a can be seen an instantaneous view of the rotor blade as it would appear looking down the shaft from the top of the rotor. Figures 2.1.b and 2.1.c show projections of the side and end view, respectfully. Since the flapping hinge cannot sustain a torque about its axis, the sum of the moments about this point will equal zero. These moments are due to: (1) the centrifugal forces acting radially from the shaft; (2) the inertial reaction of each infinitesimal mass to flapping motion acceleration; and (3) the distributed lifting airloads along the blade span. If one invokes the small-angle assumption that cosines of angles are equivalent to unity and sines of angles are approximately equal to the radian measure of the angles themselves, one arrives at the expression:

$$\int_{\xi}^{R} \ddot{\beta}\,(r-\xi)^2\, m\, dr \;+\; \int_{\xi}^{R} \beta\Omega^2\, m\, r\,(r-\xi)\, dr \;=\; \int_{\xi}^{R} (r-\xi)\frac{dT}{dr}\, dr \qquad (2.2.1)$$

where:

m	is the spanwise distributed blade mass
β	is the flapping angle
Ω	is the rotation frequency
r	is the distance measured from the shaft
R	is the total rotor radius
$\hat{e}$	is the hinge offset divided by rotor radius
$\frac{dT}{dr}$	is the spanwise lift distribution

The spanwise lift distribution is calculated by considering the local flow about a two-dimensional section at an arbitrary radius as in figure 2.1.c. For the quasi-steady case, this is just the product of the dynamic pressure and the chord times the lift coefficient, which itself is just the product of the lift curve slope times local angle of attack. Thus one has:

$$\frac{dT}{dr} = 1/2 * \rho * U^2 * c * a * [\theta - \phi] \qquad (2.2.2)$$

where:

ρ	is the air density
U	is the local flow velocity magnitude
c	is the chord
a	is the 2D lift curve slope
θ	is the pitch angle of the blade
ϕ	is the angle between the local velocity and a plane perpendicular to the shaft

If one again invokes the small angle assumption, the local flow angle ϕ is approximately equal to its tangent. Also, the magnitude of the local velocity can be approximated by the tangential velocity for most of the rotor. Incorporating both of these approximations gives:

$$\frac{dT}{dr} = 1/2 * \rho * a * c * U_T * [U_T * \theta - U_P] \qquad (2.2.3)$$

where:

U_T = $\Omega r + \mu * \Omega R * \sin(\psi)$
(the tangential velocity)

U_P = $r\dot{\beta} + \mu * \Omega R * \cos(\psi) * \beta + \lambda * \Omega R$
(the perpendicular velocity)

μ = $V * \cos(\alpha) / R$
(nondimensional forward flight speed)

λ = $V * \sin(\alpha) / R$
(nondimensional inflow velocity)

ΩR = tip velocity of the rotor

V = forward flight speed

α = shaft tilt into the wind, positive forward

Substitution of (2.2.3) into (2.2.1) will result in a proliferation of symbols, which can be reduced by non-dimensionalization according to the following steps. First, (2.2.1) is divided by the blade inertia about the flapping hinge. Second, the aerodynamic parameters are lumped together into a unit-less quantity called a Lock number. Third, the span is nondimensionalized by rotor radius and the flap natural frequency by rotor rotation frequency. If the inflow effects are neglected for now, the result is:

$$\frac{\ddot{\beta}}{\Omega^2} + M_{\dot{\beta}/\Omega} \frac{\dot{\beta}}{\Omega} + M_\beta \beta = M_\theta \theta \qquad (2.2.4)$$

where the coefficients are:

ORIGINAL PAGE IS
OF POOR QUALITY

$$M_{\beta/\Omega} = \frac{\gamma}{2} \int (x + \mu \sin\psi) \times \eta(x)\, dx$$

$$M_{\beta} = \{ \nu^2 + \frac{\gamma}{2} (\mu \cos\psi) * \int (x + \mu \sin\psi) \eta(x)\, dx \}$$

$$M_{\theta} = \frac{\gamma}{2} \int (x + \mu \sin\psi)^2 \eta(x)\, dx$$

and the nondimensional flapping mode shape is:

$$\eta(x) = \frac{x - \xi}{1 - \xi}$$

and: ν is the nondimensional flapping frequency

$\gamma = \frac{\rho\, acR^4}{I_1}$ is the Lock number

I_1 is the inertia about the flapping hinge

These integrals must be evaluated with some care in order to accurately treat the direction of the incremental lift force on the blade section. As shown in figure 2.2, the various tangential flow regimes of the rotor blade can be broken down into three areas on the rotor disc. At certain combinations of span, azimuth angle and forward flight speed, the local flow direction at a section will be directed from the trailing edge to the leading edge. For high levels of

ORIGINAL
OF POOR

forward flight speed, it is possible that the full span of the blade is in such a state. These three areas, then, correspond to: (1) normal flow, encountered over azimuth angles such that ($-xi < \mu * \sin(\psi) < \mu$); (2) mixed flow, where part of the span is in normal flow and part is in reversed flow, encountered over the the range of azimuth angles such that ($-1 < \mu * \sin(\psi) < -xi$); and (3) reversed flow, where the full blade span is in reversed flow, valid where ($\mu * \sin(\psi) < -1$). This third category can obviously only exist for rotors operating at advance ratios greater than unity. The integration limits on these integrals are then:

(1): $\int_{}^{1} (\ )\, dx$ --- for normal flow,

(2): $\int_{-\mu\sin\psi}^{1} (\ )\, dx - \int_{}^{-\mu\sin\psi} (\ )\, dx$, or

$\int_{}^{1} (\ )\, dx - 2 \int_{}^{-\mu\sin\psi} (\ )\, dx$ --- for mixed flow, and

(3): $-\int_{}^{1} (\ )\, dx$ --- for fully reversed flow.

The results of performing such integrations are given in figure 2.3, where the effect of an offset flapping hinge is included in the evaluations. Plots of these three moment coefficients can be seen in figure 2.4a, 2.4b and 2.4c as a

function of advance ratio.

A few important aspects can be seen in these three time histories of the flapping equation coefficients. Most apparent is the increase of higher harmonic content in each of the coefficients with increasing advance ratio. This is due to the fact that all the periodic terms in the coefficients enter the expression as products of advance ratio and sines or cosines of azimuth angle. As advance ratio increases, these terms dominate the coefficient's character. Second, the flap damping term never changes sign, although its value does become quite small for certain regions near the boundary between regions (2) and (3) on the retreating side. This makes sense since the local velocity due to any flapping motion would produce section angle of attack changes, generating in-phase lift forces that would oppose the motion (for the quasi-static case). And finally, the control moment due to changes in pitch angle can be seen to pass through zero on the retreating side for high advance ratios. This is due to the lift in the normal regime on the outboard span of the blade exactly cancelling the lift in the reversed flow region on the inboard section. These first two observations will help the evaluation of the parameter identification results that follow in a later chapter, and the last effect will be seen to produce singularities for

certain types of controller designs.

2.3 Mathematics of Periodic Linear Systems

2.3.1 Introduction

In this section, the somewhat peculiar nature of systems of linear differential equations having periodic coefficients will be described. Much of the material presented will be drawn directly from [Dugundji and Wendell, 1983] and [Johnson, 1980, ch.8], but the motivation for its inclusion here is to make the thesis self-contained and the notation consistent.

Analyses of periodic coefficient systems are very often approximate due to the considerable added complexity of having to deal with time-varying parameters. These techniques range from perturbation-type methods, where the periodicity is assumed to be of small size relative to the mean parameter values, to harmonic-balance and multimode methods (called "multiblade" for helicopter problems), where a truncated Fourier expansion is substituted into the governing equations in order to determine its free coefficients. The techniques that follow in this section are "exact", in that the approximations present are in the problem formulation and not in their mathematical solution. This is not to say that periodic linear systems are exactly

solvable -- the expressions given below are exact, but in virtually all cases they must be evaluated numerically on a computer, a process which is never exact due to numerical truncation effects.

2.3.2 State Variables and the Transition Matrix

Modern control techniques are fundamentally used with systems described in state-variable notation. The primary advantage of such a system is in economy of representation -- extremely complex linear (and nonlinear) lumped-parameter systems with multiple inputs and outputs can be described with just two matrix-vector equations. The selection of states describing a system, however, is not unique, and can be chosen for computational convenience or physical significance. In most engineering applications for rotorcraft, these states are the displacements and velocities of the modal degrees of freedom under analysis. For a linear system, the n states $x(t)$ can be related to the m inputs $u(t)$ and the l outputs $y(t)$ according to:

$$\dot{x}(t) = A(t)\,x(t) + B(t)\,u(t) \qquad (2.3.1)$$

$$y(t) = C(t)\,x(t) + D(t)\,u(t) \qquad (2.3.2)$$

If just the homogeneous terms of (2.3.1) are retained, a

set of solutions can be obtained for any particular initial condition on x(t) by direct integration of the equations of motion. If n such solutions are obtained for the n initial conditions characterized by having all zeroes except for a 1 in the i-th location, one can combine them column-wise to form the state transition matrix (STM) for this homogeneous system. This matrix relates the homogeneous solution at some time t to the solution at a previous time t0 according to:

$$x(t) = \Phi(t,t0)\, x(t0) \qquad (2.3.3)$$

and since it is composed of solutions to (2.3.1), the state transition matrix must obey the same equation:

$$\dot{\Phi}(t,t0) = A(t)\, \Phi(t,t0) \qquad (2.3.4)$$

Other properties of the STM include:

$$\Phi(t2,t1)\, \Phi(t1,t0) = \Phi(t2,t0) \qquad (2.3.5)$$

$$\Phi(t,t) = I = \Phi(t,t0)\, \Phi(t0,t) \qquad (2.3.6)$$

$$\Phi(t,t0)^{-1} = \Phi(t0,t) \qquad (2.3.7)$$

For the time-invariant case, the STM is not dependent explicitly on the two time parameters, but instead on the time interval (t-t0). If one performs a Taylor-series expansion about t0, one can show that:

$$\Phi(t-t0) = \exp\{ A(t-t0) \} \qquad (2.3.8)$$

where the matrix exponential is defined according to the infinite series:

$$\exp\{ At \} = I + At + (1/2!)\, A^2 t^2 + \ldots + (1/n!)\, A^n t^n + \ldots \qquad (2.3.9)$$

or,

$$\Phi(t,t0) = \sum_{j=0}^{\inf} A^j \frac{(t-t0)^j}{j!} \qquad (2.3.10)$$

For the general time-varying case, a similar but more complex relationship exists for the STM, as shown in [Blair, 1971]:

$$\Phi(t,t0) = \sum_{j=0}^{\inf} [A(t) - DI]^{(j)} I \frac{(t-t0)^j}{j!} \qquad (2.3.11)$$

where D is the operator notation for d( )/dt and the parenthetical superscript (j) denotes the recursive but non-commutative operation of the nxn matrix operator [A(t) - DI]. For example,

$$\begin{aligned} [A(t) - DI]^2 &= [A(t) - DI]\,[A(t) - DI] \\ &= A^2(t) - A(t)DI - DA(t) + D^2 I \\ &= A^2(t) - \dot{A}(t) \end{aligned}$$

since DI = 0. Alternate methods to generate the STM for time-varying systems are direct integration of (2.3.3), or a stepwise approximation by breaking the time interval under consideration into several discrete steps, and forming the product:

$$\Phi(t,t0) \simeq \Phi[tn,t(n-1)] \times \Phi[t(n-1),t(n-2)] \times \ldots \times \Phi[t1,t0] \qquad (2.3.12)$$

where the STM $\Phi[tj,t(j-1)]$ is the result of holding the system matrix constant from time t(j-1) to t(j).

Periodic systems are special cases of these time-varying systems, in that the coefficients are cyclic functions of time:

$$A(t+T) = A(t);\ B(t+T) = B(t), \text{ etc. with } T = \text{period}$$

Floquet's theorem states the <u>form</u> that the STM takes for periodic systems, but not the analytic solution:

$$\Phi(t,t0) = R(t)\ \exp\{\ Q^*(t-t0)\ \}\ R^{-1}(t0) \qquad (2.3.13)$$

where R(t) is a periodic matrix with period T, and Q is a constant matrix. This can be proved by noting that $\Phi(t+T,t0)$ is also a solution to (2.3.3), and letting $\Phi(t0+T,t0) = M$, giving:

$$\Phi(t+T,t0) = \Phi(t+T,t0+T)\ M \qquad (2.3.14)$$

The matrix M is given various names throughout the

literature, but we will call it the Floquet transition matrix (FTM). If we now set M = exp{ QT }, we obtain from (2.3.14):

$$\Phi(t+T,t0) = \Phi(t,t0)\ M \qquad (2.3.15)$$

since $\Phi(t+T,t0+T) = \Phi(t,t0)$. Now if we define:

$$R(t) = \Phi(t,t0)\ \exp\{ -Qt \} \qquad (2.3.16)$$

we obtain:

$$\begin{aligned} R(t+T) &= \Phi(t+T,t0)\ \exp\{ -Q(T+t) \} \\ &= \Phi(t,t0)\ \exp\{ QT \}\ \exp\{ -Q(T+t) \} \\ &= \Phi(t,t0)\ \exp\{ -Qt \} = R(t) \end{aligned}$$

and thus R(t) is periodic in T.

2.3.3 Eigenvalues and Eigenvectors of Periodic Linear Systems

Just as the dynamics of time-invariant systems of equations are governed by the homogeneous system's eigenvalues, the properties of a periodic linear system are directly influenced by the eigenvalues of the Floquet transition matrix. To see this, one need only employ a result from the Cayley-Hamilton theorem for matrices in order to show that any analytic function of a matrix is related to a transformation of the result of applying that same function to the matrix eigenvalues, or:

$$f\{ A \} = X\ f\{ E \}\ X^{-1} \qquad (2.3.17)$$

In order to interpret these results, one must remember that the actual physical response of a system governed by real coefficients must also be real. Hence it is the product of the eigenvectors and the exponentiated eigenvalues and not the eigenvalues themselves that determines the system output. Addition of a multiple of the fundamental frequency to an eigenvalue of Y corresponds to multiplying that mode by exp{ -i2pi(n)t/T }. This is fully consistent with the results developed, since Floquet theory only requires that the mode shape be periodic, and there is no specification as to how the periodicity is apportioned between the eigenvalue and the eigenvector.

The only question left begging is how to determine what multiple of the fundamental must be added to the eigenvectors of Y. This decision can be made readily if the system becomes time-invariant at some limit, such as the helicopter rotor does in hover. For this case, the location of the time-invariant eigenvalues of the rotor can be found readily, and the eigenvalues of the periodic system can be constrained to vary in a continuous fashion from the hover roots with changes in advance ratio. An automated technique, from [Johnson, 1980], is to require the mean value of the eigenvector to have the largest magnitude; then the harmonic of largest magnitude in the eigenvector corresponding to the

where A is a matrix with X as its matrix of eigenvectors and E as its matrix of characteristic values, or eigenvalues. Thus, for the time-invariant case, the STM is:

$$\Phi(t,t0) = X \exp\{ E(t-t0) \} X^{-1} \qquad (2.3.18)$$

For this system to be stable, the homogeneous solutions should either remain at a steady value or decrease with time. In order for this to happen, the matrix exponential should not be an increasing function, which implies that none of the eigenvalues in E have positive real parts.

For periodically varying systems, the STM was shown to be:

$$\Phi(t,t0) = R(t) \exp\{ Q(t-t0) \} R^{-1}(t0) \quad (2.3.13)$$

and if we use S and Y as the eigenvector and eigenvalue matrices of Q, we can then write:

$$\Phi(t,t0) = R(t) S \exp\{ Y(t-t0) \} S^{-1} R^{-1}(t0) \quad (2.3.19)$$

So, since the product R(t)S is periodic in time, the stability of the system is again determined by the eigenvalues of Y, with positive real parts in any elements of Y producing unbounded solutions.

For time-invariant systems, standard methods are

available to compute the eigenvalues of A and thus determine the system's stability. Unfortunately for periodic linear systems, no similar technique exists to determine Y given A(t). However, from (2.3.15) we have a relationship for the Q matrix in terms of the FTM:

$$M = \exp\{ QT \} = S \exp\{ YT \} S^{-1} \qquad (2.3.20)$$

so one can write:

$$Y = \frac{1}{T} \mathrm{Log}\{ S^{-1} M S \} = \frac{1}{T} \mathrm{Log}\{ Z \} \qquad (2.3.21)$$

where Z is the diagonal eigenvalue matrix of M and S is its eigenvector matrix (the same as for Q). In order to evaluate the stability of a periodic linear system, then, it is necessary to first obtain the FTM (M) through any means available, typically via integration of the homogeneous equations over one period. The system is declared stable if the real parts of the eigenvalues in Y are all non-positive.

Since the eigenvalues of Y are related to those of Z through the complex logarithm, it is clear that this same stability criterion is met if the eigenvalues of Z all have magnitude less than unity. This becomes even more obvious if one considers the behavior of the STM over several periods. In this case, since the STM at any time is related to the STM

over one period according to:

$$\Phi(t+nT,t0) = \Phi(t,t0)\ M^{n} \qquad (2.3.22)$$

$$\text{so,}\quad \Phi(t+nT,t0) = \Phi(t,t0)\ S\ Z^{n}\ S^{-1} \qquad (2.3.23)$$

and any eigenvalue of magnitude greater than one will cause the STM to grow unbounded with time.

But perhaps the most peculiar behavior of periodic linear systems is due to the nature of the complex logarithm. Since the logarithm value is dependent upon the branch over which it is defined, the eigenvalues of Y can have a multiple of (2pi/T) added to their imaginary part without affecting the system stability:

$$y = \frac{1}{T}\ [\ \ln|z| + i\ \angle(z)\ ]\ +\ n\ \frac{2pi}{T}\ i \qquad (2.3.24)$$

The eigenvalues of Z can take on three possible values, since M is a real matrix: they can be part of a complex conjugate pair, yielding a complex conjugate pair in Y; they can be positive real, yielding a root of Y at some integer multiple of the fundamental frequency [(n)2pi/T]; or, they can be negative real, yielding a root at some multiple of the half of the fundamental frequency [(n+.5)2pi/T]. This implies that it is entirely possible to have eigenvalues of Y which are complex but have no corresponding conjugate.

In order to interpret these results, one must remember that the actual physical response of a system governed by real coefficients must also be real. Hence it is the product of the eigenvectors and the exponentiated eigenvalues and not the eigenvalues themselves that determines the system output. Addition of a multiple of the fundamental frequency to an eigenvalue of Y corresponds to multiplying that mode by exp{ -i2pi(n)t/T }. This is fully consistent with the results developed, since Floquet theory only requires that the mode shape be periodic, and there is no specification as to how the periodicity is apportioned between the eigenvalue and the eigenvector.

The only question left begging is how to determine what multiple of the fundamental must be added to the eigenvectors of Y. This decision can be made readily if the system becomes time-invariant at some limit, such as the helicopter rotor does in hover. For this case, the location of the time-invariant eigenvalues of the rotor can be found readily, and the eigenvalues of the periodic system can be constrained to vary in a continuous fashion from the hover roots with changes in advance ratio. An automated technique, from [Johnson, 1980], is to require the mean value of the eigenvector to have the largest magnitude; then the harmonic of largest magnitude in the eigenvector corresponding to the

principal value of the eigenvalue gives the frequency n2pi/T.

Finally, it should be mentioned that it is possible to consider the periodic system in terms of modal coordinates, by transforming the equations of motion using the substitution $R(t)S\ v(t) = x(t)$. Upon substitution into (2.3.1), one obtains:

$$\dot{v}(t) = Y\, v(t) + [\, R(t)S \,]^{-1} B(t)\, u(t)$$
$$y(t) = C(t)\, R(t)S\, v(t) + D(t)\, u(t) \quad (2.3.25)$$

and the homogeneous equations are now amenable to standard analysis techniques for time-invariant systems. Note, however, that one is still left with a periodic control and output matrix, and thus standard time-invariant optimal control techniques are still not applicable for this modified form.

3. PERIODIC CONTROL THEORY

3.1 Motivation for the LQR Approach

The control laws designed for the I.B.C. rotor in this thesis are all formulated as a solution to a calculus-of-variations problem, in accordance with the techniques of so-called "modern" control system design. This formulation consists of expressing the controller design objectives as the time integral of quadratic functions of both state variable perturbations and control expenditures, with the state variables constrained to obey a specified set of dynamical equations. This particular method of controller design became popular with the advent of the widespread use of digital computers, allowing a numerical solution to rather complex problems to be obtained within a reasonable amount of time.

These "modern" approaches enjoy some advantages over traditional frequency-domain (or, "classical") control design techniques due to their ability to handle a wider variety of design problems. State-variable formulations of the system dynamics permits one to formulate the optimization problem as a vector-matrix equation and thus allow treatment of almost arbitrarily-large (but finite) order systems, having several

inputs and outputs. A time-domain representation of the plant dynamics makes it possible to treat time-variable systems, something not generally available to the analyst using frequency-domain Laplace variable concepts. And finally, given a predetermined quadratic performance criterion, the feedback gains for all of the state variables are computed uniquely. Since the issue of requiring all the state variables be measurable is intimately related to the area of system identification, we will defer discussion of this latter topic until a later chapter.

This need for a predetermined measure of performance within modern controller design is sometimes one of the technique's toughest requirements. The dynamics of the closed-loop system is totally dependent upon the mathematical representation of the quadratic performance index, such that an inappropriate choice of weighting parameters will most assuredly result in a controller with poor performance. The designer is thus required to express his control objectives in terms of an analytic scalar function of the system's state and control variables, thereby reducing all issues concerning speed of response and amount of control effort expended to a single number. Such a representation of design objectives is not often easily obtained, and it is in this area where much of the iteration of a control law design takes place.

General guidelines exist for how one might initially approach construction of a performance function, the most common being the weighting of each state's squared deviation by the squared inverse of its maximum allowable value [Bryson and Ho,1975]. Other techniques are also available, such as penalizing state rates to limit system bandwidth, but these as well as more complex methods [Stein, 1979] are all for time-invariant systems. There is a definite lack of (and in our case, a clear need for) guidelines in the selection of the terms within the cost function for periodically time varying linear-quadratic control systems. Our approach to this problem will be to attempt to gain some insight into the various effects present in such a selection by considering single degree of freedom systems with time-varying parameters.

3.2 Derivation of the Gain Equations

Formulation of the optimization problem for modern control has been done in countless texts and technical reports for the past twenty years. Instead of presenting the reader with yet another example of vector calculus manipulations, we will include an extremely curt set of equations representing the fundamental relationships, with the main motivation being one of standardization of notation. This is necessary in order to put the extensions to the theory that are developed later in the chapter into the proper perspective. For the complete derivation of the control problem the reader is referred to [Kwakernaak and Sivan,1972] or, [Bryson and Ho,1975].

Given the system:

$$\dot{x}(t) = A(t)\,x(t) + B(t)\,u(t) \qquad (3.2.1)$$

with the performance index (a.k.a. cost function):

$$J = 1/2 \int_0^{\infty} [\, x'(t)Q(t)x(t) + 2x'(t)M(t)u(t) + u'(t)R(t)u(t) \,]\, dt \qquad (3.2.2)$$

the optimal control law is a linear feedback of the state variables according to:

$$u(t) = -R(t)^{-1} [\, B'(t)P(t) + M'(t) \,]\, x(t) \qquad (3.2.3)$$

where the matrix P(t) is the solution to the matrix Riccati equation:

$$\dot{P} = -(A - BR^{-1}M')'P - P(A - BR^{-1}M') + P(BR^{-1}B')P + (-Q + MR^{-1}M') \qquad (3.2.4)$$

It can be shown that the matrix P(t), often called the cost matrix, is related to the optimal cost to control through:

$$J(t) = x'(t)\,P(t)\,x(t), \quad P(tf) = Pfinal$$

with P(tf) representing the cost matrix at the final time; for the cases considered here Pfinal is unimportant as it is assumed zero. Note that we have omitted the explicit dependence on time from most of the matrices.

This equation is obtained after one adds the governing system dynamic equations as a constraint to the cost function using a Lagrange multiplier vector l(t), and then minimizes the combined expression with respect to the control. This procedure produces two coupled first-order linear differential equations in the state vector and the multiplier (or, adjoint) state vector:

$$\begin{bmatrix} \dot{x} \\ l \end{bmatrix} = \begin{bmatrix} (A - BR^{-1}M')' & (-BR^{-1}B') \\ (-Q + MR^{-1}M') & -(A - BR^{-1}M')' \end{bmatrix} \begin{bmatrix} x \\ l \end{bmatrix} \qquad (3.2.5)$$

The solution to this set of equations is complicated by the

fact that it is a two-point boundary-value problem, with initial conditions given for the state vector and final conditions specified for the adjoint state vector. One technique around this problem is to combine the two equations through the cost matrix according to:

$$l(t) = P(t)\, x(t) \qquad (3.2.6)$$

and the above Riccati equation is generated. Though the resulting matrix equation is nonlinear, P(t) is only specified at the final time (in our case, infinite) in the cost function integral, and thus can be solved through integration.

3.3 Solution of the Matrix Riccati Equation

3.3.1 The Time-Invariant Case

The above nonlinear matrix differential equation has no analytical solution except for a very few special cases. For the general case, one must resort to integrating the Riccati equation backwards in time to obtain the feedback gains for the optimal closed-loop system. Since the upper limit in the cost function for the problem considered here is infinite, however, it can be shown that for most well-posed control problems [Kwakernaak and Sivan,1972] that after a sufficient integration time these feedback gains will approach a steady-state value for time-invariant systems, and thus the rate of change of the cost matrix will become zero.

In this instance, it then becomes possible to replace the terminal condition on the adjoint state vector with the initial condition:

$$\lambda(0) = \bar{P}\, x(0) \qquad (3.3.1)$$

and then consider the solution to the Ricatti equation as resulting from a combination of the solution of the original coupled set of first-order linear differential equations in the state and adjoint state variables. Since the cost matrix is constant, it becomes possible to diagonalize this system

using its eigenvectors, and thus yield a "spectral" solution for the steady-state cost matrix. Details of this procedure are given in [Kwakernaak and Sivan, p.243]. The main requirement of this technique is the use of an accurate eigen-system extraction algorithm.

3.3.2 The Time-Varying Case

Just like the time-invariant case, no standard analytic solution to the Riccati equation exists for the case of a system governed by time-varying dynamics. This is even true for the extremely simple special case of a general scalar time-varying system described by a first-order differential equation. However, since we are interested in a small subset of these time-varying systems -- namely, those that are linear but have plant parameters that vary periodically -- one is not restricted to only using straightforward numerical integration of the Riccati equation.

The behavior of the backward integration of the cost matrix reveals, for sufficiently long integration intervals, an asymptotic approach to a periodic steady-state value for linearly periodic systems. Because of this, it becomes possible to incorporate the results of Floquet theory and impose constraints upon the form of the solution to equation

(3.2.5). These conditions show, as was discussed in section 2.3 on linear periodic systems, that once the homogeneous solution to this linear equation is obtained over one period, it is known for all time. Based upon this result, [Nishimura, 1972] develops a hybrid scheme whereby one integrates the coupled system of state and adjoint state variables over one period, and then uses the eigenvalue/eigenvector content of this result to reconstruct the steady cyclic behavior of the optimal feedback gain matrix. This then allows one to generate the steady periodic (albeit numerical) solution to the Riccati equation after only at most two periods of integration passes of equation (3.2.5). A descriptiont of the algorithm, along with the extensions for handling implicit-model-following designs, is given in a later section.

Of some interest concerning special cases of periodic control problems is [Wu, 1980], where the theorem that all time-varying systems are reducible to a solvable form is proved. It is shown that for certain restriced classes of time-varying linear systems, a direct analytic solution is possible, and that this "solvability" is not an inherent property of a particular system, but is only related to how that system is represented in equation form. The solution technique consists of first transforming the system to a

time-invariant representation, and then using standard techniques for time-invariant systems of equations. Since a linear system is invariant under a non-singular (and possibly time-varying) state variable transformation, the conclusion is then reached that all one needs to do to solve a linear periodic system is to discover the appropriate state transformation so as to achieve the time-invariant reformulation. This transformation is, however, just the "modal" transformation for periodic systems as described in chapter 2, and is non-unique and therefore not directly computable.

Thus, to compute the optimal closed-loop gains in a linear-quadratic control design for a periodic system, one must integrate the equations numerically, and Nishimura's hybrid method appears to be the best technique available in terms of speed and accuracy. In order to generate guidelines for selecting cost function parameters in LQR design for linearly-periodic systems, we will now consider trends established by performing numerical experiments upon some simplified examples of linearly periodic systems.

3.4 Numerical Results

3.4.1 Scalar System Case

The same computer program that solved for the periodic "optimal" gains for a given system was also capable of computing the closed-loop system's eigenstructure. This capability made it possible to observe the effect of various cost functions both on closed-loop pole locations and on the periodic eigenvectors. Outputs of the program included eigenvalues of the Floquet Transition Matrix (FTM) and their associated complex logarithm. In order to properly interpret the values of these "poles", some discussion is necessary.

As was pointed out in chapter 2, the FTM represents the state transition matrix of a periodic system over one cycle. If one represents the system in modal form, the new dynamics matrix is just a diagonal matrix of the complex logarithms of the eigenvalues of the FTM (see equation (2.3.25)). These elements are roughly equivalent to what would be the Laplace-domain poles for a time-invariant system (the s-plane poles). The difference here is that the modal variables are periodic functions of time. Similarly, if this system is now discretized with a time-step of one fundamental period, the discrete-time dynamics matrix is a diagonal matrix with the

elements being these same eigenvalues of the FTM. Thus, the controls engineer new to the field of periodic systems cannot help but draw parallels between discrete-time systems and the properties of the FTM poles. The same unit circle criterion for stability applies for the "Floquet poles" on the complex plane as for discrete system poles on the z-plane. Also, poles near the origin on the Floquet plane indicate fast (although periodic) modes are present in the system, just as they would be for the discrete-time counterpart. Even the ambiguity concerning the appropriate branch cut for a particular periodic mode can be thought of as a form of aliasing. Oscillatory modes with a natural frequency greater than the fundamental frequency of the periodicity (such as a flapping mode for a rotor with either an offset hinge or semi-rigid hub) will produce poles in the Floquet plane that exhibit "frequency folding" due to the sampling (discretizing) rate being slower than twice their fundamental oscillation.

The purpose of this section is to provide some guidelines through example as to how various choices of cost function in the problem statement influence the movement of poles, and the nature of their associated eigenvectors, in the closed-loop system. Such correlation is possible for time-invariant systems [Kwakernaak and Sivan,1972],

especially single-input systems, but nothing is available for periodic systems. The reasons for this lack of knowledge become clear upon attempting to deduce such a relationship analytically for even the simplest case -- a first-order dynamic system. Whether one attempts to compute the feedback gain through solution of a nonlinear, scalar, periodic Riccati equation or a linear, second-order set of adjoint equations (as in Nishimura's approach), the result is the same: no general analytic solution exists for the gain function (and hence the closed-loop pole).

As an initial step, a first-order system of the form:

$$\dot{x}(t) = a(t)\, x(t) + b(t)\, u(t) \qquad (3.4.1)$$

where: $a(t) = -1. + 1.*\cos(t)$
$b(t) = 1.$

was considered, with the cost function consisting of quadratic penalties on the state and control deviations, but no cross-cost penalty on products of control and state. The state transition matrix for a scalar periodic system is an analytic function:

$$\phi(t,t0) = \exp\{\int_{t0}^{t} a(t)\, dt\} \qquad (3.4.2)$$

and thus the FTM for a scalar system is directly computable as the exponential of the product of the constant part of

a(t) and the fundamental period. Thus the Floquet-plane pole for this open-loop system will be at exp{ -2*pi } and the Laplace-plane pole at -1. If we set the initial time t0 at the origin, the transition "matrix" is:

$$\phi(t,0) = \exp\{ -t \}*\exp\{ \sin(t) \} \quad (3.4.3)$$

and the periodic eigenvector can be seen to be exp{ sin(t) }.

To get a feel for the effects of periodicity on the pole locations, the penalty weight was increased on the state deviations from zero (open-loop) both for the system of (3.4.1) and for a similar scalar system with the periodicity removed. The following behavior in the poles was observed (with Wuu=1.0):

Wxx	F-plane pole	L-plane pole	Time-invariant L-plane pole
0.	1.868e-03	-1.0	-1.0
.01	1.777e-03	-1.008	-1.005
0.1	1.180e-03	-1.073	-1.049
1.0	8.128e-05	-1.499	-1.414
3.0	2.000e-06	-2.089	-2.000

It can be seen that the closed-loop Laplace-plane poles of the periodic system exhibit the same trend toward infinity as their time-invariant counterpart, but the rate appears to be faster for the same level of state penalty. Figure 3.1 shows the periodic gain function associated with the case of Wxx = 3.0 and its associated spectrum. In figure 3.2 the

corresponding periodic eigenvector for this case and for the open-loop case are plotted together.

Several items from this very simple case are of interest. First, since the periodicity appears only in the dynamics "matrix" and not in the control term, it is possible to cancel the periodicity of this system completely using a gain of the form:

$$k(t) = k0 + \cos(t) \qquad (3.4.4)$$

where k0 is chosen to give the system any closed-loop response time desired. Since this is not the optimum choice, one may infer that the control penalty for such a design would be too great. Second, by merely placing weights on the actual state perturbations and control effort, the periodicity of the closed-loop system was reduced, as evidenced by the reduction of periodicity of the eigenvector. This has intuitive appeal, since a periodic system forced by a single frequency would produce a response (although often negligible) at an infinite number of frequencies related to sums and differences of integer multiples of the fundamental and the excitation frequencies. The time-invariant system, however, would exhibit only a response at the excitation frequency, and thus would concievably produce a lower "cost" for the same disturbance.

Finally, the increase in the closed-loop modal time constant over the constant-coefficient case might be explained by considering the equivalent modal form for (3.4.1) as in (2.3.25). Substituting the mode x(t) = exp{ -sin(t) }*v(t) into the equations yields:

$$\dot{v}(t) = [\ -1\ ]*v(t) + \exp\{\ -\sin(t)\ \}*u(t) \qquad (3.4.5)$$

The cost function is transformed as well:

$$J = (1/2)\int_0^{\infty}\{\ v\ [\ \exp\{\ -\sin(t)\ \}*Wxx*\exp\{\ -\sin(t)\ \}]\ v + u*Wuu*u\ \}\ dt \qquad (3.4.6)$$

so that one has constant-coefficient dynamics, but a periodic control term and state cost. If one now considers only the constant values in the above two expressions, it is clear that there is an increase in modal state penalty, as well as an increase in the control term (called "control power"). Thus, one could argue that the effective cost of control has been made "cheaper" due to both of these effects, giving rise to a faster time constant.

So, even for this almost trivial example, the interaction between speed of response and level of periodicity are by no means obvious. However, it appears in the limit as control cost becomes negligible, the periodic system exhibits closed-loop behavior similar to its

constant-coefficient counterpart: namely, the Laplace-plane pole approaches infinity and the periodicity is reduced. Similar effects for certain weighting functions will be shown for higher-order systems considered in the next section.

3.4.2 Higher Order Systems

Since the eventual application of the design aspects of this thesis was the IBC helicopter rotor, and since relatively simple periodic coefficient structures do not necessarily imply a simple controller function, it was felt that economy of effort could be served by using the IBC rotor dynamics as an example of a higher order system. This choice had other advantages as well. The influence of periodicity can be observed by merely altering the advance ratio within the equations; at hover, the flapping dynamics are described by a second order constant-coefficient equation. Forward flight progressively increases the harmonic content in the spring, damping and control terms. Thus, comparison with the hover poles for a particular cost function is a convenient technique for inferring the effect of periodicity. However, it should be noted that for periodic systems other than the helicopter rotor, the detailed variations due to periodic coefficients are likely to be markedly different -- we are only trying to illustrate <u>global</u> effects here.

In order to interpret the implication of various closed-loop pole locations on blade dynamics, it may first be helpful to review the nature of the unaugmented rotor flapping behavior as advance ratio increases. As mentioned previously, the equation describing the rigid out-of-plane motion of the blade becomes time-invariant at hover. Due to the strong centrifugal stiffening effects of rotation, the undamped natural frequency of this second-order system is close to that of the rotation frequency. For articulated blade with a hinge offset, or for hingeless rotors, this frequency is slightly greater than unity when nondimensionalized by rotation frequency. Damping for this motion, in the absence of any external mechanical devices, is due to aerodynamic effects, namely local angle of attack changes along the span due to flapping motion. The damping coefficient value can be seen (equation (2.2.4)) to be directly proportional to the Lock number. Most helicopters in use today have blades with Lock numbers ranging anywhere from around 5 to 10, depending upon the particular hub geometry, and thus have less than critical damping. This means that the hover poles are a pair of complex conjugates in the Laplace-plane (or, for that matter, the Floquet-plane as well).

As forward flight speed increases, however, the periodicity enters in such a fashion to initiate a shift in these poles toward the real axis for both Floquet and Laplace complex planes. In most cases, however, they never make it, and instead lock onto the line representing +j or -j in the Laplace-plane. As advance ratio increases still further, these poles cease to be complex conjugates (for the Laplace-plane case), and one becomes more stable along this line while the other becomes less stable. This odd behavior, characteristic of periodic systems, can be described as having the system instability lock onto a particular frequency. Such pole movement seems perfectly acceptable when viewed in the Floquet-plane, as the roots are seen to coalesce on the real axis prior to splitting and moving away from each other. A sketch of this migration can be seen in figure 3.3 for a typical rotor.

Three different forms of direct state weighting were used in the design studies to be described here. These correspond to (1) penalties on flapping position deviations only, (2) penalties on flapping rate deviations only, and (3) equal penalties on both flapping position and flapping rate. For the rotor equations of motion expressed as:

$$\beta'' + A1(\psi)*\beta' + A0(\psi)*\beta = B0(\psi)*\theta \quad (3.4.7)$$

where primed quantities represent derivatives with respect to azimuth angle, we have in state variable form:

$$\frac{d}{d\psi}\begin{bmatrix}\beta\\ \beta'\end{bmatrix} = \begin{bmatrix}0 & 1\\ -A0 & -A1\end{bmatrix}\begin{bmatrix}\beta\\ \beta'\end{bmatrix} + \begin{bmatrix}0\\ B0\end{bmatrix}\theta \qquad (3.4.8)$$

These three cases then correspond to weighting matrices having the forms:

$$(1)\ Wxx = \begin{vmatrix} x & 0\\ 0 & 0\end{vmatrix};\ Wxu = \begin{vmatrix}0\\ 0\end{vmatrix};\ Wuu = |\,1\,|$$

$$(2)\ Wxx = \begin{vmatrix} 0 & 0\\ 0 & x\end{vmatrix};\ Wxu = \begin{vmatrix}0\\ 0\end{vmatrix};\ Wuu = |\,1\,|$$

$$(3)\ Wxx = \begin{vmatrix} x & 0\\ 0 & x\end{vmatrix};\ Wxu = \begin{vmatrix}0\\ 0\end{vmatrix};\ Wuu = |\,1\,|$$

where the variable x was varied from zero to some large value. These were used as inputs to the gain calculation program for eight different advance ratio cases and five levels of weights. In order to discern the trends present in the results, we will first consider the effects of advance ratio upon a fixed weighting structure, and then look at the effects of an increase in the weighting value for fixed advance ratio.

Figure 3.4a plots the Laplace-plane poles for the position-only weighting structure. The lines of pole movement indicate the locus of constant values of this weighting parameter with increases in advance ratio. The

plotted poles represent an advance ratio increase form zero (hover) to 1.4 in steps of 0.2. Thus, the x=0.0 locus represents the variation of the Laplace poles for the open-loop case (since no penalty on the state produces no regulation action and thus zero feedback gain). This particular locus shows typical behavior for an articulated rotor. As the weighting value is increased, however, quite different trends are present. The locus of Laplace-plane poles appears to undergo a rotation with increasing position penalty. This rotation is stabilizing, in that increases in weighting values produce closed-loop poles with more negative real parts for the same advance ratio. This fact is even more evident in a later figure. Also of interest from the figure is the fact that, for high levels of position-only weights, the response time of the closed-loop system is actually <u>faster</u> for increasing levels of periodicity given the same cost value. This second result corresponds to the observation made on the scalar system: increased levels of periodicity appear to produce "optimal" systems with faster responses given the same levels of cost.

Figures 3.4b and 3.4c show these same constant-cost loci plotted on the upper half of the Floquet-plane (the complex poles in the Floquet-plane always have a complex conjugate since the STM is a real matrix). The same two trends are

equally evident here: the rotation of the loci toward the origin and away from the unit circle is stabilizing, and the poles corresponding to the higher advance ratios move closer to the origin for moderate levels of position weighting, indicating a shorter system response time.

The next weighting function considered was a rate-only penalty on the flapping motion. Figure 3.5a shows the constant-weight loci for increasing advance ratio. Once again, increases in penalty values are stabilizing, since each locus is further to the left on the real axis for increasing rate cost. The character of each locus is quite different, however. Instead of rotating away from the imaginary axis, they keep their general shape and, for high levels of weight and/or advance ratio, exhibit the same "lock-in" behavior seen previously for the unaugmented flapping dynamics. Figures 3.5b and 3.5c show this effect in the Floquet-plane. The stabilizing influence of higher cost values is apparent, but almost all loci show the "lock-in" phenomenon.

The third and final cost structure was an equal penalty on both position and rate deviations. Since this is analogous to a penalty on both potential and kinetic energy, it can be used a a means of limiting closed-loop "bandwidth"

(see [Widnall,1968], p.93). It also serves to bridge the gap between the purely position weighting and purely rate weighting schemes considered. The results for this structure are seen in figure 3.6a, where the Laplace-plane poles are plotted for constant cost values with increasing advance ratio. The shape of the loci is similar to those of figure 3.5a, but their location is further away from the imaginary axis, indicating an increase in stability over the pure rate weighting scheme. The "lock-in" behavior is also delayed a bit longer in this instance, occurring at a higher penalty value for the same range of advance ratios. Figures 3.6b and 3.6c document this result for the Floquet-plane poles.

Perhaps more familiar to the controls engineer are the next set of loci, where the flight condition is fixed (i.e., constant advance ratio) and the weighting parameter is increased from zero, the open-loop case. Figure 3.7a show the Laplace-plane root loci for the three forms of cost function considered for the hover condition. All three of these curves represent constant-coefficient system pole locations, and thus provide a known point of comparison for the effects of system periodicity. Several aspects should be pointed out. First, the position-only weighting generates closed-loop poles for this second order system that approach a Butterworth-type structure, namely, a damping ratio of 0.7

with a frequency that increases with position penalty [Kwakernaak and Sivan,1972]. Second, the rate-only weighting can be seen to drive the system to a reduced frequency and increased damping, such that in the limit the two poles of the system would coalesce on the real axis, and then split. One of these poles would approach the origin and the other would head toward negative infinity. Finally, the bandwidth-weighting structure forces the closed-loop pole to an increased damping level at approximately the same frequency. Floquet-plane equivalents of this behavior are given in figure 3.7b.

At an advance ratio of 0.6 these trends are still present, as is seen in figures 3.8a and 3.8b, but the rate- and bandwidth-weighting curves begin to suffer a stability degradation from the higher periodicity. It should be emphasized, though, that this stability degradation is in the general shape of the loci, and not for the specific value of cost. And finally, figures 3.9a and 3.9b show, on a different scale, the movement of poles for a high advance ratio condition, namely mu=1.4. The open-loop roots that have coalesced on the +j and -j lines on the Laplace-plane are first driven away from this "lock-in" point, and then for large bandwidth- and rate-penalties, return to the same branch line, but at a more stable location.

As a final check on the effects of periodicity, figures 3.10a and 3.10b show the real and imaginary part of one element of the eigenvector matrix for the closed-loop system at an advance ratio of 1.4. The dominant two-per-revolution (2P) behavior present in the open-loop response is suppressed for all cost functions shown, but the response modes that result are still very much periodic. Just as was true for the scalar system, increases in penalty weights influence both the eigenvectors and their response times in a rather complex fashion.

In summary, then, these numerical exercises have produced the following set of "rules of thumb" for periodic system controller design:

(1) the movement of closed-loop poles with increases in penalty weights is similar to that of constant-coefficient systems -- displacement-only penalties produce Butterworth-type responses, rate-only penalties generate loci with the same qualitative damping increases, and the combination of the two appears to limit the modal response time;

(2) increases in levels of periodicity, such as increased forward flight speed in the case of a helicopter rotor, tend to produce <u>faster</u> modal response times for the same numeric values in the cost function -- the level of increase appears

to be a complex function of both the actual values of the penalty weights and the level and type of periodicity. The reasons for this effect are probably due to an increased level of modal "control power" in the examples considered, making the cost of control "cheaper" for the same level of modal acceleration.

(3) optimal control theory using penalties on squared deviations in states and controls forces a periodic system to a closed-loop structure that has a smaller relative level of periodicity. This reduction in periodic nature is not at present predictable, and must be determined through numerical means. The unsatisfactory nature of this last result brought about a search for more attractive design techniques in the selection of a performance index, as is outlined in the next section.

3.5 Model-Following Systems

3.5.1 Introduction

As any helicopter engineer knows, a successful rotor system must be designed and built with careful attention given to its aeroelastic properties. Control over the many natural frequencies present in the rigid and elastic modes must be maintained in order to limit vibration, reduce blade stresses and prolong blade life. This includes the avoidance of resonances at integer multiples of rotor rotation frequency to prevent large modal excitations due to the aerodynamic forcing of the harmonic rotor wake. As was demonstrated in the previous section, standard LQR approaches to penalize excursions in flapping response with diminishing penalties on controller action will result in closed-loop systems with a high bandwidth. This is not particularly desirable, because: (1) there may be interaction effects with other modes not accounted for in the math model that are destabilizing at such high bandwidth (gain) values; (2) the closed-loop natural frequencies may fall close to an integer multiple of rotation frequency and thus promote possible aerodynamic forcing; and (3) high penalties on system periodicity produce large gain values that may be difficult to implement in the controller hardware.

Problems exist even for the other cost functions considered that included some penalty on state rate deviations. While these provide a means of reducing controller bandwidth, they do not offer much promise in specifying the level of periodicity in the closed-loop system. Thus, tight control over a mode would require an excessive amount of iteration in order to generate the desired eigenvector structure.

Because of these drawbacks, a straightforward LQR approach to rotor blade modal control could run into serious difficulty. However, many other cost functions are possible for controller design using modern methods, the most useful for this case probably being model-following. Model-following entails expressing in the cost function a desire for the plant being controlled to possess dynamics similar to some prototype system. This prototype can be either be a physical (often electronic) system, such as for explicit model-following [Tyler,1964], or an implied dynamic structure, as realized through selection of the elements in the weighting matrices [Kreindler and Rothschild,1976; Kriechbaum and Stineman,1972]. The appeal of this technique for periodic system control is twofold. First, the desired pole locations of the closed-loop system can be achieved by incorporating them into the model, and then driving the

system to emulate the model through liberal weighting of the difference between the two in the cost function. Second, control over the level of periodicity can be achieved through the same technique -- proposing a model with as much (or as little) periodicity desired and penalizing the deviations from it.

This latter feature is especially attractive for helicopter rotor control. Since the lift, propulsion and control of the helicopter are all accomplished through the rotor system, increased control over the blade response to pilot commands, flight condition and atmospheric disturbances would provide a better handling vehicle. Pilot stick deflections are essentially magnitude and direction commands on the rotor thrust vector -- any deviation of this resultant force from the desired constitutes degraded performance. Such a deviation might come from a sub- and super-harmonic response of the periodic blade dynamics, translating into a wobbling of the tip-path-plane of the rotor and possible instability at high forward speed. For this reason, then, the periodic nature of the flapping dynamics is considered a nuisance, something to be reduced through feedback control.

The model used as the prototype for this design study (and subsequent test) was that of the hover flapping

dynamics, although this choice is somewhat arbitrary. This particular choice of model has the advantage that: (1) the feedback gains go to zero at hover; (2) the model is a constant-coefficient system, helping to reduce the periodicity of the closed-loop system in forward flight (and augment its stability); (3) the bandwidth of the model is well defined and thus should produce a controller without modal interaction problems; and (4) a stability-augmentation system for a full-scale helicopter would be greatly simplified if the rotor dynamics, due to inner-loop control, were relatively constant throughout the flight envelope.

3.5.2 Implicit-Model-Following with Input Feedforward

As mentioned above, model-following for linear-quadratic regulator design can take two forms, either explicit or implicit. In explicit-model-following, an external analog system is used as a prefilter, or command generator, to provide reference signals for the system being controlled. The cost function is a simple weighted quadratic in the difference between the outputs of this analog system and the actual plant. The resulting controller has not only feedback gains on the state variables of the plant, but also feedforward gains on the states of the analog model. This is an unfortunate (but not very surprising) result, since it

requires the construction of additional hardware for the analog model, as well a means of implementing the feedforward gains.

Implicit-model-following, however, is not so demanding on closed-loop system complexity. By formulating the cost function to penalize the difference between the time derivative of the state vector and the desired model accelerations, a set of weighting matrices is arrived at that are functions only of the plant state and control vectors. This results in a set of gains that are only as numerous as the number of states. For a constant-coefficient plant, this saving in hardware may not be significant; for a periodic system it could be substantial due to the need to program time-varying gains. Because of this reduced hardware requirement, the approach taken in this thesis was to use the implicit-model form.

The model-following approaches described in the previous paragraphs are regulator-type designs, in that no mention was made of including command inputs. These can be incorporated through various means, such as augmenting the state with a vector differential equation whose initial conditions can be altered to produce typical command histories [Anderson and Moore,1971], or by including the command signal explicitly in

the model dynamics [Kriechbaum and Stineman,1972]. Due to our ever-present constraint on system order, we will develop the gain equations for the latter approach.

Given the system:

$$\dot{x}(t) = A(t)\, x(t) + B(t)\, u(t) \qquad (3.5.1)$$

and the model:

$$\dot{x}_m(t) = F\, x(t) + G\, d(t) \qquad (3.5.2)$$

where d(t) represents input commands to the model, consider a cost function penalizing deviations in accelerations according to:

$$J = (1/2) \int \{ (\dot{x} - \dot{x}_m)' Q (\dot{x} - \dot{x}_m) + u' R\, u \}\, dt \qquad (3.5.3)$$

Substitution of (3.5.1) and (3.5.2) into the above integral gives, after some algebra:

$$J = (1/2) \int \{ x' Wxx\, x + u' Wuu\, u + d' Wdd\, d + 2\, x' Wxu\, u - 2\, x' Wxd\, d - 2\, d' Wdu\, u \}\, dt \qquad (3.5.4)$$

where:
$$
\begin{aligned}
Wxx &= (A - F)'Q(A - F) \\
Wuu &= (R + B'QB) \\
Wdd &= G'QG \\
Wxu &= (A - F)'QB \\
Wxd &= (A - F)'QG \\
Wdu &= G'QB
\end{aligned}
$$

Next, the derivation follows the standard steps: append the dynamical equations of the plant to the cost function as a constraint, integrate by parts, and take the first variation in cost with respect to the control, state, and adjoint variable (see [Bryson and Ho,1975] or [Kwakernaak and Sivan,1972]). Variations in the input variable $\underline{d}(t)$ are not allowed because it is external to the system, and can be thought of as an unknown disturbance. This results in three equations relating the input $d(t)$ and the control $u(t)$ to the state $x(t)$ and adjoint state $l(t)$:

$$
\begin{aligned}
\dot{l} &= -Wxx\,x - Wxu\,u + Wxd\,d - A'l \\
u &= Wuu^{-1}\{-Wxu'x - B'l + Wdu'd\} \\
\dot{x} &= A\,x + B\,u
\end{aligned}
\qquad (3.5.6)
$$

and upon substituting for $u(t)$:

$$\begin{bmatrix} \dot{x} \\ \dot{1} \end{bmatrix} = \begin{bmatrix} [\, A - B\, Wuu^{-1}\, Wxu\,]' & [\, -B\, Wuu^{-1}\, B\,]' \\ [\, -Wxx + Wxu\, Wuu^{-1}\, Wxu\,]' & [\, -A' + Wxu\, Wuu^{-1}\, B\,]' \end{bmatrix} \begin{bmatrix} x \\ 1 \end{bmatrix}$$

$$+ \begin{bmatrix} [\, B\, Wuu^{-1}\, Wdu\,]' \\ [\, Wxd - Wxu\, Wuu^{-1}\, Wdu\,]' \end{bmatrix} [\, d\,] \qquad (3.5.7)$$

Comparison with equation (3.2.5) will show that the only difference here is in the extra term due to the model input. As was done for the homogeneous equation of (3.2.5), we will assume the solution for the adjont variable to be a linear function of the state variable, but we'll also include an inhomogeneous part due to the model input:

$$1(t) = P(t)\, x(t) - S(t)\, d(t) \qquad (3.5.8)$$

which upon taking the derivative becomes:

$$\dot{1}(t) = \dot{P}(t)\, x(t) + P(t)\, \dot{x}(t) - \dot{S}(t)\, d(t) \qquad (3.5.9)$$

Since the model input is a measurable but unpredictable quantity, the best estimate of its derivative is zero; therefore it does not appear in equation (3.5.9) [Kriechbaum and Stineman,1972]. Substituting into (3.5.7) gives:

$$\dot{P}x + P[\, A - B\, W_{uu}^{-1} W_{xu}' \,]x + P[\, -B\, W_{uu}^{-1} B' \,]Px - PSd + P[\, B\, W_{uu}^{-1} W_{du}' \,]d - \dot{S}d = [\, -W_{xx} + W_{xu}\, W_{uu}^{-1} W_{xu}' \,]x - [\, A - B\, W_{uu}^{-1} W_{xu}' \,]' Px + [\, A - B\, W_{uu}^{-1} W_{xu}' \,]' Sd + [\, W_{xd} - W_{xu}\, W_{uu}^{-1} W_{du}' \,]d \tag{3.5.10}$$

If the cost were truly at a minimum, then the above equation must be true regardless of the variation in x or the value of d. Thus, we can separate out all the dependence upon these two quantities, giving two separate equations:

$$-\dot{P} = P[\, A - B\, W_{uu}^{-1} W_{xu}' \,] + [\, A - B\, W_{uu}^{-1} W_{xu}' \,]' P - [\, -W_{xx} + W_{xu}\, W_{uu}^{-1} W_{xu}' \,] + P[\, -B\, W_{uu}^{-1} B' \,]P \tag{3.5.11}$$

$$-\dot{S} = [\, A - B\, W_{uu}^{-1} W_{xu}' \,]' S + P[\, -B\, W_{uu}^{-1} B' \,]S - P[\, B\, W_{uu}^{-1} W_{du}' \,] + [\, W_{xd} - W_{xu}\, W_{uu}^{-1} W_{du}' \,] \tag{3.5.12}$$

and the control is then:

$$u = -W_{uu}^{-1} [\, W_{xu}' + B' P \,]x + W_{uu}^{-1} [\, W_{du}' + B' S \,]d \tag{3.5.13}$$

Several observations concerning the form of these equations can be made. First, the Riccati equation for the state cost matrix, (3.5.11), is unchanged from the form of (3.2.4). The only differences are the actual values for the cost matrices. From (3.5.4), one may note that these cost

matrices are independent of G, the input matrix in the model dynamics. Second, equation (3.5.12) for the variation of S, the state and model input cross-cost, is linear and depends explicitly on both the G matrix and the solution to the Riccati equation (3.5.11). And finally, the expression for the optimal control shows a feedback gain for the states that depends on P and a feedforward gain for the model input that depends on S. Only the feedforward gain is influenced by the choice of the model input matrix G.

Since the homogeneous equations were shown to have an efficient "spectral" solution that could be calculated after at most two integration passes of equation (3.2.5) over the fundamental period [Nishimura,1972], it would be very desirable to develop a similar technique for handling the calculation of the feedforward gains. Fortunately, one was found by incorporating a combination of the method of [Nishimura,1972] with the algorithm for initial conditions of [Dugundji and Wendell,1983].

Following the lead of [Nishimura,1972], if one represents equation (3.5.7) in the form:

$$\begin{bmatrix} \dot{x} \\ 1 \end{bmatrix} = \begin{bmatrix} A(t) \end{bmatrix} \begin{bmatrix} x \\ 1 \end{bmatrix} + \left[\begin{array}{c} M(t) \\ \hline N(t) \end{array}\right] \qquad (3.5.14)$$

one can numerically compute this system's (2nx2n) augmented state transition matrix, where n is the dimension of both x(t) and l(t) [Friedmann, Hammond and Woo,1977]. Call this matrix B(t,t0). If one solves for the eigenvalues and eigenvectors of the resulting Floquet transition matrix for this 2n system, and then separates them into stable and unstable modes, the steady-state periodic solution to the Riccati equation of (3.5.11) can be shown to be:

$$P(T) = T21(T)\ T11(T)^{-1}$$

and:

$$P(t+T) = [\ B21(t,0)*T11(T) + B22(t,0)*T21(T)\ ] * [\ B11(t,0)*T11(T) + B12(t,0)*T21(T)\ ]^{-1} \qquad (3.5.15)$$

where the matrices T11 and T21 represent the (2nxn) eigenvectors associated with the stable modes of the FTM.

This is only the solution to the homogeneous part of (3.5.14). One then solves for the (2nxm) <u>particular</u> periodic solution of (3.5.14) using [Dugundji and Wendell,1983]; call the transpose of this (2nxm) time-varying matrix [Xp' | Lp'], where m is the dimension of the model input. Then (with considerable hindsight) one has the solution to the cross-cost matrix S as:

$$S(t) = -Lp(t) + P(t)\ Xp(t) \qquad (3.5.16)$$

Verification of this result can be done by taking the

derivative of (3.5.16), substituting the two equations of (3.5.14) and the Ricatti equation of (3.5.11), and comparing the result with (3.5.12).

This process can be improved upon by combining the solution for the particular form of (3.5.14) with the procedure for determining the (2nx2n) state transition matrix by integrating the augmented matrix:

$$Z(t)_{(2nx(2n+m))} = \left[\begin{array}{c|c} B(t) & \begin{array}{c} X(t) \\ \hline L(t) \end{array} \end{array}\right] \qquad (3.5.17)$$

with the initial conditions:

$$B(0) = I_{(2nx2n)}, \quad X(0) = L(0) = 0_{(nxm)}$$

over a modified form of (3.5.14):

$$\dot{Z}(t) = A(t) * Z(t) + \left[\begin{array}{c|c} 0_{(2nx2n)} & \begin{array}{c} M(t) \\ \hline N(t) \end{array} \end{array}\right] \qquad (3.5.18)$$

Where I represents the identity matrix. After one cycle of integration, one has:

$$Z(T) = \left[\begin{array}{c|c} FTM_{(2nx2n)} & \begin{array}{c} X(T)_{(nxm)} \\ L(T)_{(nxm)} \end{array} \end{array}\right] \qquad (3.5.19)$$

Then from [Dugundji and Wendell,1983] one obtains the initial conditions for the particular solution as:

$$\begin{bmatrix} Xp(0) \\ Lp(0) \end{bmatrix} = \begin{bmatrix} I_{(2nx2n)} - FTM_{(2nx2n)} \end{bmatrix} \begin{bmatrix} X(T) \\ L(T) \end{bmatrix} \qquad (3.5.20)$$

Upon finding the eigenvalues and eigenvectors of the FTM, one need only preform a second integration pass over equation (3.5.18) to solve for the matrices P(t) and S(t). In this way, the number of integration passes can be reduced by one, a considerable saving for high-order periodic systems.

3.5.3 Numerical Results for Implicit-Model-Following

In order to see the effects of a model-following design on a periodic system using a constant-coefficient model, the same scalar example of section 3.4 was used. As the weighting matrix Q was varied, the following behavior in the poles was observed (with R=1.0):

Q	F-plane pole	L-plane pole
0.	1.868e-03	-1.0
.01	1.822e-03	-1.004
0.1	1.552e-03	-1.029
1.0	1.231e-03	-1.066
3.0	1.392e-03	-1.047
10.	1.642e-03	-1.020
100.	1.839e-03	-1.010
(R=0.)	1.867e-03	-1.000

This behavior is typical of model-following designs for periodic plants that posess enough controllability to allow an exact model matching. This can be seen in figure 3.11, where the gain function for the case of no control penalty (R=0.) is plotted. The curve is a perfect cosine function,

which exactly cancels the system's periodicity, as can be seen in figure 3.12, where the open- and closed-loop eigenvector are shown.

For the helicopter rotor operating at a high-advance ratio, however, exact model matching is not always possible. A good example of this can be seen in figure 3.13, where one of the rotor feedback gain functions for an advance ratio of 1.4 is plotted for increasing values of state penalty, Q. Even though the flapping dynamics represent a higher-order system, the fact that the equations are written in a control-canonical form (meaning the states are just the various time derivatives of the displacement) reduces the model-matching cost term in (3.5.3) to a scalar. The most striking feature of this plot is the manner in which the gain values approach singularities on the retreating side of the rotor azimuth. This can be explained by referring to the control power term in the equations of motion in figure 2.4c. At this high advance ratio, the control term can be seen to cross through zero twice on the retreating side. Thus, in order to force the closed-loop system:

$$\dot{x} = [\, A(t) - B(t)\, K(t) \,]\, x + [\, B(t)\, Kff(t) \,]\, d \qquad (3.5.20)$$

to act like a constant-coefficient system, the gain would

have to become infinite to cancel the periodicity of A(t) at that particular azimuth angle.

This result raises the question of controllability for linear periodic systems. [D'Angelo, 1970, ch.4] defines several types of controllability, all of which are rather difficult to assess without substantial computational resources. The strongest level is "uniform controllability", where the state can be driven through impulsive inputs in an infinitesimal time to another desired state at any instant over some specified time interval. Clearly the above example falls short of this ideal, since it is uncontrollable at two specific azimuth locations on the retreating side. All is not lost, however, as these two points are isolated instants and not continuous stretches of time, and thus limit this example to a case of "total controllability". Quite reasonable results can be achieved even for this case, as can be seen by the plot of the real part one of the eigenvectors of the closed-loop system in figure 3.14. Significant reductions are realized in the system's periodicity for moderate levels of model-matching cost and feedback gains.

The closed-loop pole locations for fixed cost and varying advance ratio are shown in figures 3.15a for the Laplace-plane and 3.15b and 3.15c for the Floquet plane. It

is evident that the effect of increasing advance ratio is diminished for larger cost values, as the poles do not shift nearly as much as for previously considered controller designs. This is indeed an attractive feature for helicopter rotor control, and thus this approach was used for the controllers demonstrated in the following sections of this thesis.

4. OBSERVER DESIGN AND PARAMETER IDENTIFICATION

4.1 Introduction to Observer Theory

Most control system engineers, if they have produced a design using modern control theory state-space concepts, have had to wrestle with the following problem upon completion of their choice of a candidate regulator: not all the state variables of the system are available for measurement. The most frequent situation is that just a few are measurable, and even these may be constrained to be measurable only in certain linear combinations. This general situation can be represented by the linear time-varying set of equations:

$$\dot{x}(t) = A(t)\, x(t) + B(t)\, u(t) \qquad (4.1.1)$$

$$y(t) = C(t)\, x(t) + D(t)\, u(t) \qquad (4.1.2)$$

where $x(t)$ is the n-dimensional state vector, $u(t)$ the m-dimensional control vector, and $y(t)$ is the l-dimensional measurement vector. This predicament is not unsolvable within the context of the theory, but the solution is often the most complex element of the controller design process.

One obvious way to generate the estimates of the state variables is to integrate the equations (4.1.1-2) forward in time. This simplistic approach is, in general, doomed to

failure because it requires both an exact representation of the actual system dynamics and the knowledge of the initial conditions of the state variables. Such a technique makes no use of the current value of the measurement and as such becomes susceptible to any and all errors introduced through disturbances acting on the actual system. Furthermore, if the system being modelled is unstable, these errors are likely to grow without bound.

Observer theory incorporates the concept of negative feedback to force the errors in the state estimates to approach zero exponentially with time. This is done by driving a model of the system with an input proportional to the difference between the actual measurements and the predicted values based on the current state vector estimate. That is, we formulate the system (for the continuous-time case) as:

$$\dot{\hat{x}}(t) = A(t)\,\hat{x}(t) + B(t)\,u(t) + K(t)\,[\,y(t) - C(t)\,\hat{x}(t)\,] \qquad (4.1.3)$$

where:

$$y(t) = C(t)\,x(t) \qquad (4.1.4)$$

If we define the estimation error as:

$$e(t) = \hat{x}(t) - x(t) \qquad (4.1.5)$$

then the error is governed by:

$$\dot{e}(t) = [A(t) - K(t)C(t)]\, e(t) \qquad (4.1.6)$$

The choice of this proportionality constant K(t) determines the speed in which these errors are reduced, and can be selected using any of several methods, the most popular being the Kalman Filter. But perhaps the most important result from observer theory is the fact that use of the state estimates instead of the actual states for feedback does not alter the closed-loop stability of the system. The poles of the combined observer-controller are those of the state-feedback controller, plus those of the observer error dynamics. The only consequence of using an observer is often a deterioration of the transient response of the complete closed-loop system. This result is called the "separation principle" and allows one to perform independent designs of the state feedback gains and the observer dynamics.

A Kalman Filter is a technique for producing the best linear estimate of a state vector given the a-priori knowledge of the random processes perturbing the system to be observed, the knowledge of the structure of the noise corrupting the measurements, and the exact model of the plant dynamics relating the various physical quantities. It can be shown that the formulation of the Kalman Filtering problem is "dual" to that of the optimal controller problem, in that the

optimization equations only differ through a sign change, representing a forward propogation of time instead of a reverse one [Kwakernaak and Sivan, 1972, p.364]. The proportional feedback gains on the measurement errors (known as "residuals") are computed as representing the best tradeoff between reduced sensitivity to sensor noise and increased ability to quickly track changes in the state vector.

The requirements for implementing a full Kalman Filter for a complex plant are often too severe in terms of required a-priori knowledge and system order to warrant its use in a feedback controller design. In the context of helicopter rotor control, a full-blown Kalman Filter would necessitate modelling several rotor blade modal degrees of freedom along with the highly complex dynamics of the rotor wake, including any effects of gusts, dynamic inflow, returning tip vortices, and so on. Such a model, even if made reasonably accurate, would be so complex and costly as to render its use in a control design impractical. Thus, techniques to generate a simpler, sub-optimal estimate of the state vector would be very valuable.

One step in this direction is the method attributed to [Luenberger, 1964, 1966]. He showed that, for a

deterministic system with noise-free measurements, it is possible to reconstruct the state of a system using a dynamic element with an order less than that of the full state vector, given certain restrictions on how well the measurements span the state-space. Since there are no considerations of stochastic effects upon mean square state reconstruction error, the feedback gains can be chosen arbitrarily so as to achieve any desired response characteristics. This dynamic element, however, is related to the actual plant equations through a (possibly time-varying) transformation, and thus depends on the knowledge of the parameters of the system being observed. And for some choices of transformations, this relationship can be highly sensitive to small changes in these parameters.

4.2 Observers for Rotor Control

Put in the context of a complex helicopter rotor system, the Luenberger observer simplification is not much of an improvement -- the only real change is in the elimination of a need for noise specifications and a possible reduction in observer hardware. Since the blade dynamics will be changing with flight condition (most notably with forward flight speed), any estimation technique that depends strongly upon accurate knowledge of the process dynamics will have to

change as well. This is even further complicated by the fact that, just like the rotor blade equations of motion, the observer equations will be periodic with blade azimuth angle. The state-variable controller design process has thus produced a requirement not only for periodic state feedback gains, but also for these to be cascaded with a flight condition-dependent periodic dynamic system acting as a state estimator.

Various techniques for solving this difficulty have been proposed by helicopter dynamicists. [DuVal, 1980] has suggested throwing out any plant dynamics and just using the observer gains to form the structure of the estimator. [Fuller, 1981] uses a state transformation technique to reformulate the system to a constant-coefficient set of equations. Both of these techniques concern generating estimates of the lower harmonics of blade flapping motion, and as such are limited to frequencies less than half that of the highest term in the truncated series approximation. Also, by eliminating the interaction between the state variables present in the full rotor dynamics equations, these estimators lack any "feedforward" effects from disturbances or inputs present in a standard Kalman filter. That is, the state estimates will change only through the output error term, and as such must always lag the actual state values.

Since it is exactly these feedforward terms that allow one to invoke the "separation principle" in the controller design, use of these estimators for feedback control must be done only after the total system closed-loop stability is checked.

The solution presented in the following pages to this problem arose out of the need to adequately describe the sensor complement present in the Individual-Blade-Control model rotor system. The two available sensors for out-of-plane blade motion detection are a tip-mounted accelerometer, with its sensitive axis perpendicular to the blade surface, and a strain gauge mounted at the flapping hinge for measuring blade root angle. As can be seen in figure 4.1, this particular choice of location for the accelerometer results in its output being proportional to out-of-plane <u>position</u> as well as acceleration, due to its orientation in a centrifugal force field. If the rotor blade motion is described by an infinite series of time-varying modal displacements, then the ratio of these two effects is determined by the mode shape slope and displacement at the tip for each blade mode considered. That is, if the out-of-plane displacement is:

$$z(t) = \sum_{i=1}^{inf} \eta_i(x)\, g_i(t) \quad , \quad x = r / R \qquad (4.2.1)$$

then the accelerometer senses:

$$\text{accel}(t) = \sum_{i=1}^{\inf} \{ \eta_i(x) \frac{d^2 g(t)}{dt^2} + r\Omega^2 \frac{d\eta_i(x)}{dr} g_i(t) \} \quad (4.2.2)$$

If we restrict ourselves to considering only the first out-of-plane mode of the blade, namely, rigid flapping, then this infinite sum is truncated at the first term, and we have a sensor that gives a signal that is a linear combination of flapping position and acceleration. Looking back at equation (4.1.2), one notices that the standard form for representing a sensor's output is as a linear combination of states and controls, but it is immediately apparent that this has been complicated by using an accelerometer. Since modal acceleration is not a state variable but a time derivative of a state, one must represent the sensor by incorporating the system dynamics in the observation matrices. Thus, for an accelerometer that senses the combination:

$$\text{accel}(t) = H1\, x(t) + H2\, \dot{x}(t) \quad (4.2.3)$$

then this can be reconfigured to be:

$$\text{accel}(t) = H1\, x(t) + H2 \{ A(t)\, x(t) + B(t)\, u(t) \} \quad (4.2.4)$$

or,

$$\text{accel}(t) = \{ H1 + H2\, A(t) \}\, x(t) + \{ H2\, B(t) \}\, u(t) \quad (4.2.5)$$

This is indeed an unfortunate situation. Whereas before we had a sensor that was related to a combination of the state vector and its time derivative, now the representation of the sensor content is directly dependent upon the description of the system dynamics, including all its elements of periodicity and variation with flight condition. An observer or Kalman filter design based upon this set of equations would be complex indeed! Fortunately, there are techniques to circumvent such difficulties, two of which are described in the next section.

4.3 Incorporation of Accelerometers into Observer Design

For a lumped-parameter system, if one knows the lumped mass and inertial properties of a system incorporating an accelerometer sensor, it becomes possible to solve for the applied forces and moments acting on it. These include any control actions or disturbances of the plant, and thus could supply a predictive quality, or "lead", for any observer using an accelerometer in the estimation task. It is with this concept in mind that the following two approaches were developed. The first consists of treating the accelerations as a Brownian motion process, with modal acceleration represented as a state variable in the process dynamics; the second considers the acceleration as a deterministic input

into the system, which can be accurately measured.

To illustrate both of these procedures, we shall consider a very simple example of observing the states of a second-order system using measurements of acceleration and position. Given a system described by:

$$\frac{d}{dt}\begin{bmatrix} x \\ \dot{x} \end{bmatrix} = \begin{bmatrix} 0 & 1 \\ -1 & -1 \end{bmatrix}\begin{bmatrix} x \\ \dot{x} \end{bmatrix} + \begin{bmatrix} 0 \\ 1 \end{bmatrix} u(t) \qquad (4.3.1)$$

$$y(t) = \begin{bmatrix} 1 & 0 \\ -1 & -1 \end{bmatrix}\begin{bmatrix} x \\ \dot{x} \end{bmatrix} + \begin{bmatrix} 0 \\ 1 \end{bmatrix} u(t) \qquad (4.3.2)$$

we shall construct an observer based on the assumed model:

$$\frac{d}{dt}\begin{bmatrix} x \\ \dot{x} \\ \ddot{x} \end{bmatrix} = \begin{bmatrix} 0 & 1 & 0 \\ 0 & 0 & 1 \\ 0 & 0 & 0 \end{bmatrix}\begin{bmatrix} x \\ \dot{x} \\ \ddot{x} \end{bmatrix} + \begin{bmatrix} 0 \\ 0 \\ 1 \end{bmatrix} w(t) \qquad (4.3.3)$$

$$y(t) = \begin{bmatrix} 1 & 0 & 0 \\ 0 & 0 & 1 \end{bmatrix}\begin{bmatrix} x \\ \dot{x} \\ \ddot{x} \end{bmatrix} + \begin{bmatrix} v1(t) \\ v2(t) \end{bmatrix} \qquad (4.3.4)$$

where w(t) represents a zero-mean gaussian process noise, and v1(t) and v2(t) represent zero-mean gaussian sensor noises.

As mentioned in a previous section, an observer for this system model would have the form of equation (4.1.3), with the gains K(t) chosen according to any of several methods. Since the gains for this problem comprise a 3x2 matrix, the selection of specific values for a prespecified set of pole

locations is non-unique. To illustrate one such example, if we place the poles of the observer in a Butterworth pattern at a frequency of approximately five times as fast as the natural frequency of the process being observed (so as to minimize the transient effects when used in closed-loop control), one such set of gains is:

$$K = \begin{bmatrix} 10.0 & -12.0 \\ -10.0 & -24.0 \\ 5.0 & 0.0 \end{bmatrix}$$

producing observer pole locations at (-5.0,0.0j), (-2.5,4.33j) and (-2.5,-4.33j). While this may seem acceptable on the surface, the fact that we have violated the separation principle warrants our checking the response of this observer design against the actual process dynamics.

To do this, we'll extend the notation representing the various dynamic elements present to include the observer as:

$$\dot{\hat{x}}(t) = F\,\hat{x}(t) + K\,[\,y(t) - H\,\hat{x}(t)\,] \qquad (4.3.5)$$

or,

$$\dot{\hat{x}}(t) = [\,F - K\,H\,]\,\hat{x}(t) + K\,y(t) \qquad (4.3.6)$$

but since, from (4.1.3),

$$y(t) = C(t)\,x(t) + D(t)\,u(t) \qquad (4.1.3)$$

then this can be combined into:

$$\dot{\hat{x}}(t) = [\, F - K\,H \,]\, \hat{x}(t) + K\,C(t)\, x(t) + K\,D(t)\, u(t) \qquad (4.3.7)$$

If one combines (4.3.7) with (4.1.1) into an augmented state vector representing the actual state variables and the states of the observer, the result is:

$$\frac{d}{dt}\begin{bmatrix} x \\ \hat{x} \end{bmatrix} = \begin{bmatrix} A(t) & 0 \\ KC(t) & [\, F - KH \,] \end{bmatrix} \begin{bmatrix} x \\ \hat{x} \end{bmatrix} + \begin{bmatrix} B(t) \\ KD(t) \end{bmatrix} u(t) \qquad (4.3.8)$$

Since control inputs are not considered in the assumed plant dynamics for the above observer design, a reasonable measure of performance would appear to be how well the observer output can track changes in state due to sudden control inputs. The tracking ability of the observer would thus also represent how well it would respond to various other disturbances such as gusts and rotor wake effects.

A digital computer simulation of the above combined system was run to compare the actual state vector respose to a step input in control with the estimated values from the third-order observer. In order to provide an adequate test case, an initial condition was imposed upon the two state variables of position and velocity of -1. and -0.5 respectfully, with a unit step input applied at t = 0.0. This is necessary because observer theory shows that if an

exponential observer is given the proper initial conditions, it will track the states perfectly in the absence of external disturbances. Since it is not available directly for measurement, it was felt that the velocity of the system would provide a suitable state for comparisons among the actual system and the estimates of the various observers considered.

Such a comparison can be seen in figure 4.2a and 4.2b, where the output of the third-order observer with the above gain matrix is plotted along with the actual velocity response of the system. The performance of this pole-placement observer design is terrible -- not only does the transient response differ markedly from the actual velocity of the plant, but this particular observer approaches a non-zero steady-state velocity estimate. Investigation of the gain matrix reveals why this is so: since the zero value in the bottom right corner precludes any accelerometer feedback to the acceleration estimate, a bias on the accelerometer output would go unchecked and directly influence the velocity estimate. Because straightforward picking of gain values just to place poles can result in such poor results, an alternate approach to observer design is needed.

In order to improve how the measurements are blended to provide an accurate set of state estimates, the gains for the system (4.3.3) and (4.3.4) were calculated using Kalman Filter techniques, with the measurement noises v1(t) and v2(t) assumed to have equal covariances. After some iteration on the assumed value of the process noise covariance, the following gain matrix was produced:

$$K = \begin{bmatrix} 1.414 & 3.024e\text{-}02 \\ 1.0 & 1.0 \\ 3.024e\text{-}02 & 3.163e{+}01 \end{bmatrix}$$

which results in closed-loop observer poles of (-31.6,0.j), (-0.707,0.707j) and (-0.707,-0.707j). The response of this observer design is shown in figure 4.2c. In this case we have significantly improved the velocity estimate, both in transient capture capability and steady-state response, indicating a much better utilization of the sensor information. This observer design technique could thus probably be used in a state-feedback control design, provided its response times were made reasonably fast with respect to the closed loop regulator time constants.

But even this design can be improved upon. As one can see, we have been considering an observer that is one order higher than that of the actual system being observed. This extra "state" of the observer represents an estimate of the

acceleration of the plant, but since this value would not be used for feedback control purposes (in the designs considered here), generation of this value is somewhat pointless. As an alternative, if one is willing to assume that process noise dominates the stochastic elements present in the system, we can treat the acceleration as a measurable, "deterministic" quantity and use it to drive a system modelled by the equations:

$$\frac{d}{dt}\begin{bmatrix} x \\ \dot{x} \end{bmatrix} = \begin{bmatrix} 0 & 1 \\ 0 & 0 \end{bmatrix}\begin{bmatrix} x \\ \dot{x} \end{bmatrix} + \begin{bmatrix} 0 \\ 1 \end{bmatrix} \text{accel}(t) + \begin{bmatrix} 0 \\ 1 \end{bmatrix} w(t) \qquad (4.3.9)$$

$$y(t) = \begin{bmatrix} 1 & 0 \end{bmatrix}\begin{bmatrix} x \\ \dot{x} \end{bmatrix} + [\,1\,]\, v1(t) \qquad (4.3.10)$$

Trading off the values of the process noise covariance with the position sensor covariance produced a design with a gain matrix of:

$$K = \begin{bmatrix} 14.14 \\ 100.0 \end{bmatrix}$$

and observer poles of (-7.07,7.07j). The tracking performance of this observer design is illustrated in figure 4.2d, where the velocity estimate is almost indistinguishable from the actual system response. This observer structure would also appear to be a good candidate for use in a feedback controller design. The advantage of this approach

is a reduction in observer hardware without a deterioration in performance.

4.4 Observing the states of a time-varying plant

Since the ultimate purpose of these observer designs is to generate state estimates of a time-varying rotor system, it seems most appropriate to test them against the actual values present in such a complex environment. This validation procedure, however, is complicated by the fact that the M.I.T. Individual-Blade-Control model rotor system has no means of measuring flapping rate -- if it did, the need for an observer would then not exist! Instead, an analog simulation of the full out-of-plane rigid flapping equations of motion was built up from operational amplifiers and integrated circuits, as outlined in chapter 5, to serve as a test bed for both observer design and controller implementation. This simulation includes the effects of reversed flow and provides as output several voltages representing all the rotor states, controls, sensor outputs, and periodically-varying equation coefficients present in the linearized small-displacement flapping equation of motion.

The second-order observer designed in the previous section was also built from analog hardware and connected to

the "sensor" outputs of the analog simulation. These "sensor" signals represent the outputs from the flap strain gauge and the tip accelerometer. Since the observer was designed on the assumption that the acceleration was directly measurable, the centrifugal component of flapping displacement had to be subtracted out of the simulated tip accelerometer signal prior to incorporation into the observer structure. This by no means presents any difficulty, as the portion of the tip accelerometer signal multiplying flapping displacement is time-invariant, being neither a function of azimuth nor flight condition.

Just as was done previously for the digital computer simulation trials, the flapping rate signal was selected as the means of comparison for evaluating the observer's tracking performance. In order to provide adequate testing of transient conditions, a square-wave was fed into the pitch signal of the analog simulation, and the resulting flap rate and flap rate estimate were observed. These signals, along with the once-per-revolution timing pulse, are plotted in figure 4.3, representing a rotor operating at an advance ratio of 1.14. The results are similar for all other advance ratios and all other types of external forcing functions: the flapping rate signal is essentially perfectly reconstructed. There is no doubt that use of this quantity in a

state-feedback controller would produce satisfactory results, as it tracks even small detailed fluctuations in state due to the pitch forcing.

This most fortunate result has interesting implications. Since a time-invariant observer incorporating acceleration measurements is capable of adequately observing the state of a complex, time-varying plant, one then wonders if similar techniques are equally applicable to nonlinear or even nonlinear and time-varying systems as well. Of equal interest is how to estimate additional modal degrees of freedom using the same type of sensor complement, and how to attribute the measurement residuals to the various modes.

This latter question appears to be solvable using the second method outlined above, that of forcing a "double-integral" plant with a modal acceleration and correcting its output with a position measurement. Since all that is really needed for such an application is an accurate measurement of the particular modal acceleration and displacement, one does not even need to simultaneously estimate the dynamics of the lower-order modes. This can be best seen if one considers the modal content of each of the sensors.

For a system of, say, two modes instead of one, each accelerometer will measure some linear combination of the modal accererations that will depend upon its location on the structure. Thus, if two accelerometers are located at different points on the structure, their outputs can be combined so as to solve for each modal acceleration, provided their outputs do not also contain modal position information as well, such as in equation (4.2.2). This same argument holds for requiring two position sensors in order to solve for the two modal displacements. For the case of the Individual-Blade-Control rotor, since the accelerometers contain modal displacement information as well, one can add two additional accelerometers to the previous complement of a tip accelerometer and root angle transducer, and still solve for the two modal accelerations and displacements uniquely.

Once one has the individual modal acceleration and displacement information, one need merely design an observer such as that of (3.3.9-10), with a bandwidth picked to be sufficiently faster than the mode's natural frequency. Unlike a conventional Kalman Filter, there is no need to estimate the lower modal states, and thus the observer need only be of order two for any mode desired. However, we have reduced the complexity of the Kalman Filter approach, with all its possible time-variation and higher order, at the

expense of additional sensors. For some plants, this may not be justifiable, but for helicopter rotor control, the advantages appear to outweigh the additional cost of more sensors.

4.5 Periodic System Parameter Identification

Even with perfect measurements of the system state variables, any controller design based on modern techniques would be doomed to failure if the mathematical model for the plant being controlled were grossly in error. This applies equally for periodically time-varying systems as well as for time-invariant ones. Fortunately, given the accurate state variable estimation results of the previous section, extracting the periodic coefficients of the flapping equation (or for that matter, any reasonably uncoupled modal response) can be reduced to a basic least-squares procedure. The technique described below is equally applicable to any other type of time-varying dynamics, provided that the time variation of the coefficients can be described using weighted linear combinations of orthogonal time functions.

Given the flapping equation of the rotor in the rotating frame as:

$$\beta'' + A1(\psi)*\beta' + A0(\psi)*\beta = B0(\psi)*\theta \qquad (4.5.1)$$

where the primes indicate differentiation with respect to azimuth angle, the periodic coefficients A1, A0 and B0 can be represented as an infinite sum of trigonometric functions of azimuth according to:

$$A1(\psi) = A10 + \sum_{n=1}^{inf} \{ A1cn*\cos(n\psi) + A1sn*\sin(n\psi) \}$$

$$A0(\psi) = A00 + \sum_{n=1}^{inf} \{ A0cn*\cos(n\psi) + A0sn*\sin(n\psi) \}$$

$$B0(\psi) = B00 + \sum_{n=1}^{inf} \{ B0cn*\cos(n\psi) + B0sn*\sin(n\psi) \} \quad (4.5.2)$$

If these expressions are substituted into equation (4.5.1) and the resulting products of state variables and coefficient harmonics are expanded, one obtains (after solving for the acceleration):

$$\beta'' = [\beta' + \beta'*\cos(\psi) + \beta'*\sin(\psi) + \beta'*\cos(2\psi) + \beta'*\sin(2\psi) + \beta'*\cos(3\psi) + \ldots + \beta + \beta*\cos(\psi) + \beta*\sin(\psi) + \beta*\cos(2\psi) + \beta*\sin(2\psi) + \ldots + \theta + \theta*\cos(\psi) + \theta*\sin(\psi) + \theta*\cos(2\psi) + \theta*\sin(2\psi) + \theta*\cos(3\psi) + \ldots] *$$
$$[-A10\ -A1c1\ -A1s1\ -A1c2\ -A1s2\ -A1c3\ \ldots\ -A00\ -A0c1\ -A0s1\ -A0c2\ -A0s2\ \ldots\ B00\ B0c1\ B0s1\ B0c2\ \ldots\ ]^T \quad (4.5.3)$$

This equation is linear in the parameters representing the harmonics of the periodic coefficients. Since the observer structure outlined in the previous section provides accurate estimates of the states and modal acceleration, if we measure the control input (as we must) we can treat these harmonics as the unknowns in our problem. This then gives us a linear

equation in as many unknowns as we care to estimate, corresponding to the number of harmonics desired to represent the periodic coefficients.

Since this equation is valid over any azimuth angle, substitution of the rotor states, control input and accelerations into (4.5.3) for many different azimuth locations will provide as many or more equations than unknowns that are needed to solve for these coefficients uniquely. Due to the complex nature of the rotor wake, a least-squares approach was used in order to reduce the variance in these estimates due to process noise. If one rewrites (4.5.3) in vector form and solves for the error between the measured acceleration and that predicted from the coefficient values, one has:

$$E = Y - [\, dY/dA \,] * A \qquad (4.5.4)$$

where: E is a (mx1) vector of prediction errors
Y is a (mx1) vector of measured accelerations
[dY/dA] is a (mxn) matrix of products of states and controls with sines and cosines
A is a (nx1) vector of harmonics of coefficients
m is the number of data points (azimuth locations) considered
n is the number of harmonics to estimate

and to minimize the sum-squared error in the estimate, one takes the first derivative of the square of (4.5.4) and equates it to zero. This results in the traditional "normal equations":

$$A = \{ [dY/dA]^T [dY/dA] \}^{-1} * [dY/dA] * Y \qquad (4.5.5)$$

In order to reduce the effects of unmodelled accelerations or sensor noise, many data points should be used. This will cause the data-dimension (m) of the vector Y and of the matrix [dY/dA] to grow to an unacceptable size in terms of storage requirements unless the following steps are taken. Since the dimension m gets "absorbed" in the inner products of [dY/dA] with itself and in [dY/dA] with Y, one can treat these two products as "buffers" of dimension (nxn) and (nx1), and sum each new data point vector into them according to:

$$A = U^{-1} * V \; ; \quad U = \sum_{i=1}^{m} [dY_i/dA] [dY_i/dA]^T$$

$$V = \sum_{i=1}^{m} [dY_i/dA] Y_i \qquad (4.5.6)$$

where i represents a single azimuth angle. It should be noted that U is formed by summing <u>outer</u> products of sensitivity vectors. In this way the largest storage dimension is just n, the number of coefficient unknowns.

To test this approach, a computer program was written that would solve for the periodic coefficients given the desired number of harmonics and the data files of rotor

state, acceleration and control input. The analog simulation described in chapter 5 was once again used to generate time histories for such testing purposes, and the results can be seen in figures 4.4a, 4.4b and 4.4c. The analog model was excited using a swept-sinewave source on the pitch simulation channel, and the outputs representing flap and tip accelerometer signal were fed into the second-order observer to generate flapping acceleration and rate estimates. These signals as well as the actual coefficient voltages were fed into the PDP-11/03 computer, digitized, and stored as data files. The estimated coefficients compare quite favorably with the actual measured values, indicating the validity of this technique.

5. EXPERIMENTAL APPARATUS

5.1 Analog Simulation

In order to both test concepts and validate controller designs, it was felt necessary to construct an electronic circuit that would produce signals much like that of the Individual Blade Control rotor in the wind tunnel. This circuit card was designed to have coefficients that were periodic functions of time similar to those of the actual model. During the early stages of design it was found that by incorporating several voltage multiplication integrated circuits (IC's) it would indeed be possible to simulate the single flapping mode equations. Through a series of comparitor IC's described below, it was even possible to include the effects of reversed flow in the coefficients.

Construction of the simulation was done on a single plug-in card that was compatible with the instrumentation rack used in the actual rotor signal processing. This was initially intended to allow its use as a dynamic element within a full-blown Kalman filter state estimator, although this later proved to be unnecessary. The rack mounting provided the card's supply voltages, and all other voltages representing rotor states and coefficients were brought to a

central terminal strip at the front of the instrument cabinet. A photograph of the simulation card can be seen in figure 5.1

The layout of the circuit, shown in block_ diagram form in figure 5.2, was done in four segments: timing generation, coefficient computation, coefficient selection, and blade flapping simulation. This division was used in order to reduce the parts count of the simulation as much as possible. As was explained in chapter 2, the rotor blade passes through at least two and possibly three different regions of tangential airflow as it rotates about the shaft. The aerodynamic moments created about the flapping hinge for these cases of normal, mixed, and reversed flow can be expressed analytically, although each coefficient formula is only valid for that particular region. In order to accurately express this periodic variation of coefficients analytically for the entire azimuth, many harmonics would have to be retained. This would create the need for an unacceptably large number of IC's, and thus the design incorporated an analog switching network to select the appropriate equation coefficients for the current azimuth angle of the simulation.

Inspection of the coefficient equations in chapter 2

reveals that, for the case of no hinge offset, each region's variation with azimuth angle is constrained to polynomials in the product of advance ratio and the sine of the azimuth angle. Thus, given an input sinusoid with amplitude proportional to advance ratio, one may readily generate the higher terms of the polynomial using analog multiply IC's. Weighted values of these products of sinusoids were then combined using standard operational amplifiers to produce voltages that corresponded to the expressions valid for each flow region. These were fed simultaneously to a set of analog multiplexers that would select whichever of the three voltages (three for each of three coefficients) was appropriate at the particular azimuth angle of the simulation.

Timing for the circuit was accomplished using a commercially available function generator IC, capable of oscillating at a frequency set by external passive components. Outputs of this IC included a fixed-amplitude sine wave and square wave. Since a cosine wave was also needed for the coefficient generation (in the aerodynamic flapping spring term), a constant-amplitude phase lead network was built to shift the sine wave signal by 90 degrees. As such a network's phase shift is not independent of frequency, it became necessary to fix the oscillator

frequency to a specific value. This was set to 5 Hertz in order to match the rotation speed of the actual model rotor.

The oscillator's sine wave was input to an amplifier to vary its amplitude according to an "advance ratio" set by a dial potentiometer on the front panel. Since the transition between different flow states of the blade (and hence its coefficient expressions) is directly dependent upon this value, this was also used as a control voltage for input to the comparitor IC's that generated the select voltages that drove the multiplexers. This same amplified sinusoid was used for the polonomial term generation as described earlier.

Finally, the blade dynamics were simulated using standard op-amps as with most analog computers, but the coefficients for the system were taken from the outputs of the multiplexers. These were fed into another set of analog multiply IC's in order to permit time-varying dynamics. The integrators in the simulation were scaled to keep these coefficient voltages to values well within those of the power supply. Also, the voltages representing the flap angle and flap acceleration were combined to simulate the blade tip accelerometer signal. This voltage, along with the voltages representing the rotor blade flap angle, flap velocity, flap acceleration, pitch angle, coefficient values, sine and

cosine waves and the square wave timing signal, were all brought to a terminal strip on the front panel. This arrangement allowed rapid evaluation of candidate control laws as well as verification of the response of the modal state estimator.

5.2 Model Rotor Hardware and Instrumentation

The Individual Blade Control model rotor used at M.I.T. is a four foot diameter single-bladed rotor with two opposing counterweights. The blade flapping hinge is offset slightly from the shaft centerline and attached to a fully articulated hub incorporating a spherical bearing arrangement, permitting flap, lag and pitch degrees of freedom to have coincident axes. A steel flexure attached to this hub allows measurement of blade flap and pitch angle through a set of strain gauges mounted on its surface. Mounted within the blade structure at the tip is a miniature accelerometer, with its sensitive axis oriented perpendicular to the blade surface. This location permits measurement of both flapping displacement as well as flapping acceleration, as described in an earlier chapter. Blade pitch control is achieved through a series of pushrods and gears driven by a shaft mounted DC motor, with a servo loop closure formed around the pitch angle strain gauge and the motor's integral tachometer

signal.

The model rotor hub geometry and pitch actuator were unchanged from that used for a previous gust-response test [Ham and McKillip, 1980]. For completeness, the pertinent blade inertial and geometric properties are presented in figure 5.3. However, since the rotor no longer needed to align with external gust generators, a new housing was constructed for the slipring assembly at the end of the shaft that permitted a vertical shaft orientation. This eliminatedd spurious once-per-revolution gravity effects on the tip accelerometer sensor allowing operation at lower rotation speeds on an existing rotor test stand within the M.I.T. acoustic wind tunnel. Figure 5.4 shows the single-bladed model rotor and rotor stand, along with a simulated fuselage forebody attatched to the upstream side.

While the rotor hardware was unchanged from the gust alleviation tests, the instrumentation complement for acquiring, displaying and processing the wind tunnel data was vastly improved. Figure 5.5 details the signal paths from the rotor sensors to the amplifiers, signal conditioners and data recorders used in the experiment. Central to the experiment was the signal conditioning rack. This unit contained the pitch and flap strain gauge differential

amplifiers, the tip accelerometer amplifier, the servo motor current amplifier and power supply along with the servo feedback controller card, the instrumentation amplifier power supply, and a set of timing circuitry capable of measuring rotor rotation and supplying a squarewave at rotation frequency and another squarewave at an integer multiple of rotation frequency.

Attached to this rack were an FM tape recorder for saving analog voltage data; a Nicolet 660B dual-channel spectrum analyzer for transfer function, power spectrum and quick-look data analysis; a set of oscilloscopes for rotor sensor monitoring; and a PDP-11/03 minicomputer for digital data collection and storage. This same computer was used to generate the synchronized periodic feedback control, and because of the time-critical nature of this task, the computer data collection for closed-loop tests was done off-line using the signals collected on the FM tape recorder.

A typical experiment run consisted of the following set of procedures. First the pitch servo was energized and the rotor brought up to rotation speed using the hydraulic drive system mounted in the tunnel. Then the wind tunnel speed was increased while the rotor collective pitch was adjusted to minimize the flapping response of the blade. A

swept-sinewave source was fed into the blade pitch command summing junction, and a set of open-loop analog data was stored on the four-channel FM tape recorder, consisting of the 1/rev timing squarevave, the excitation signal, the flapping gauge signal, and the tip accelerometer voltage. These last two signals were also simultaneously fed into the analog observer, whose outputs were in turn brought to the 8-channel anti-aliasing filter box. After a record of sufficient length was captured, a program was run on the computer to compute the feedback control law based on the state estimates from the observer. The control command was output through a digital-to-analog converter board to the pitch servo summing junction, and used a precomputed set of feedback gains stored in memory. A digital controller was used as the computation speed required for the multiplication operations was well within the capability of the minicomputer. A listing of the computer control program for the PDP-11/03 is given in an appendix.

The same four voltages were then stored on the tape recorder, and the spectra of the pitch and flap channels were monitored to observe the effect of controller action on the system. Upon tunnel and rotor shut-down, the cables were swapped and the tape recorder was played back into the signal conditioning rack to generate the timing pulses for the

analog-to-digital converter board. These same signals were fed into the observer circuitry, and the whole complement of sensor and state estimate data was fed through an eight-channel low-pass anti-aliasing filter box and into the computer. The data files resulting from the digitized data were used for subsequent analysis and parameter identification experiments, the results of which appear in the next chapter.

6. EXPERIMENTAL RESULTS

6.1 Introduction

Classical representations of system dynamics, such as transfer functions, cannot easily be used to describe systems with periodic coefficients. Familiar concepts such as phase and gain margin are not applicable since these systems exhibit responses at several frequencies to a single excitation frequency. Because of this, a higher level of sophistication is necessary to quantify the character of a periodic plant. In chapter 4, a unique direct parametric representation was shown to be possible, due to the relative ease of reconstruction of the missing state variables. This same technique will be used in this chapter. By comparing the identified periodic coefficients for open- and closed-loop time response tests on the experimental apparatus, we will be able to judge the effect of a particular control law on system performance.

Prior to actual wind tunnel tests of the rotor model, a series of control laws were tested on the analog simulation. All the closed-loop controller designs were of model-following structure, with the model possessing time-invariant dynamics. Thus, the closer the identified

coefficients approached a constant value, the more the closed-loop system behaved like the desired model. The next two sections of this chapter illustrate exactly this behavior for both the simulation and the actual rotor.

6.2 Analog Simulation Results

The test procedure for the analog simulation was very similar to that for the wind tunnel model as described in chapter 5. First, a swept-sinewave excitation was fed into the pitch channel of the simulation, and this signal as well as the simulated flap channel and tip accelerometer channel were stored on an FM tape recorder. After a sufficient amount of data was collected, these signals were played back as input to the observer. These signals, as well as the observer's estimates of simulated flap rate and acceleration, were then brought to the 8-channel anti-aliasing filter box, digitized and stored in a data file in the computer. After several of these files were collected, the coefficient regression routine was run on them, and the fitted values as well as statistical goodness-of-fit parameters were printed on a hard-copy terminal. Then the digital controller was turned on and the entire process repeated. A plot of a typical data file for use in the coefficient identification process can be seen in figure 6.1. It should perhaps be

noted that the regression only uses four of these channels directly: the excitation signal, and the flap angle, flap rate and flap acceleration signals..

In order to provide a suitably harsh test environment, the simulation was run at an effective "advance ratio" of 1.4, corresponding to the highest advance ratio to be experienced by the model in the wind tunnel. This test condition provided the highest level of periodicity present in the system to be controlled, and hence the largest gains and greatest controller effort required. Inspection of figures 6.2a, 6.2b and 6.2c reveal that this simulation operating point posed no problem for the controller, as the periodicity can be seen to be reduced for the control power, spring and damping terms of the system.

Closer inspection of these figures shows that in some cases the mean levels of the parameters were reduced. This is not a destabilizing effect of periodic control, but instead a consequence of the particular model chosen for the performance function; a model with higher damping would have produced higher damping levels in the closed-loop system. The limiting factor in model-following ability appears to be associated with the controllability issue addressed earlier. Systems that do not posess full controllability over all

azimuth locations cannot be made to match a model perfectly.

As a final check of the reduction of periodicity in the system, a single frequency excitation was fed into the simulation for both the open- and closed-loop cases. The resulting input and output power spectra are shown in figures 6.3a and 6.3b. Not only is the subharmonic just below the fundamental (at 5Hz) reduced, but responses near twice the fundamental and at very low frequencies are eliminated entirely. This would indeed be a desirable property for the out-of-plane flapping dynamics of the rotor.

6.3 Wind Tunnel Model Results

Given the successful demonstration of the control concept on the analog simulation, tests were run on the actual rotor in the wind tunnel. Open-loop excitation runs were performed first to extract the system coefficients on which to base the control design. Initial efforts to estimate these periodic parameters were hampered by the presence of extraneous fluctuations and strong levels of periodicity in the transducer signals. Due to the controlled and benign nature of the analog simulation, no special measures were found necessary to identify the parameters for that situation. For the rotor data, however, two additional

features had to be incorporated in the parameter estimation scheme: inclusion of additional "forcing" terms, and a change in sampling speed.

The need for additional terms in the identified model can be best understood by considering the effect of a bias present in any of the pitch, flap, flap rate or flap acceleration signals of equation (4.5.1). These biases would get multiplied by the periodic coefficients and show up as spurious harmonics present in the flapping acceleration estimate. By combining the effects of all these biases, one can account for their contribution to the estimation error quite easily. If (4.5.3) is extended to include the terms:

$$\ldots + 1 + \cos(\psi) + \sin(\psi) + \cos(2\psi) + \sin(2\psi) + \cos(3\psi) + \ldots] * [\ f0\ f1c\ f1s\ f2c\ f2s\ f3c\ \ldots\ ]$$

then these free coefficients can be solved for at the same time as the periodic parameters using the same technique. Incorporation of these additional terms into the math model also accounts for responses due to any higher harmonic rotor wake effects.

Even though the non-dimensional first out-of-plane bending frequency was at seven times rotor rotation speed, the tip accelerometer was corrupted by a significant amount of vibration energy. This tended to force the initial

parameter estimates to have a larger higher harmonic content than was predicted by the quasi-steady theory. In order to eliminate this effect, the FM tape recorder was played back at a higher speed through the anti-aliasing filters, and the data was sampled at 32 samples per revolution, half its normal rate. This effectively doubled the number of rotor cycles present in any given data file, and significantly improved the quality of the identified parameters. It should be pointed out that the time constants of the observer had to be appropriately reduced in order to allow it to track the higher frequencies present.

Results of the parameter estimation routine are plotted in figures 6.4a, 6.4b and 6.4c for open- and closed-loop cases at an advance ratio of 1.4. Even for this severe case of reverse flow over the rotor, the periodicity of the system can be seen to be reduced. All the coefficients exhibit tendencies to approach a constant value with the addition of closed-loop control. The level of reduction is not as dramatic as for the analog simulation due to the model blade's low Lock number (requiring a higher gain value) and the particular choice of model-following cost. However, these results show that periodic control of rotor blade dynamics in the rotating frame is definitely possible even for rather extreme flight conditions.

7. CONCLUSIONS AND RECOMMENDATIONS

7.1 Conclusions from the Research

This study has been concerned with the modal control of an individual helicopter rotor blade in the high forward-flight speed regime. This operating condition poses a unique control problem in that the perturbation equations of motion are linear with coefficients that vary periodically with time. The design of a control law based on extensions to modern multivariable systhesis techniques was aided by a novel approach to the reconstruction of the missing system state variables. The controller was tested on both an electronic analog simulation of the out-of-plane flapping dynamics and on an actual model rotor in a wind tunnel. Results of these experiments indicate that periodic control of helicopter rotor blades in the rotating frame is possible using a modest amount of computational hardware. The ability to reduce the level of periodicity within the system has direct applications for stability enhancement and handling qualities improvement of modern helicopters having individual-blade-control.

Several contributions to the expanding field of periodic system dynamics have been made as a consequence of this

investigation:

(1) Sensitivity studies have been shown for Linear-Quadratic-Regulator control designs for both simple and complex periodic systems. While these have been numerical in nature, trends in the movement of closed-loop poles and variations in eigenvector structure have been identified for various types of cost function selection. Such information is important to the controls engineer in an initial approach to controlling a periodic system.

(2) Implicit-model-following control design techniques were extended to handle periodic time-varying systems. An efficient spectral method of calculating these gains was also derived, enabling rapid iteration over many candidate control laws in a short time. Implicit-model-following is a valuable tool for systems that do not benefit from their inherent periodicity, such as rotor blade flapping behavior.

(3) A novel method of incorporating an accelerometer for observing the state variables of a time-varying linear system was developed. The observer has the attractive property of having constant coefficients in its structure and not requiring an accurate model of the plant dynamics. It does require, however, an accurate

description of the sensor dynamics (if present) and modal content over the bandwidth of its response.

(4) A simple technique to estimate the parameters of a linear periodic system using the aforementioned modal observer was described. The harmonic representation of the plant coefficients permits a linear-in-the-parameters formulation of the estimation problem, with its corresponding efficient one-step solution of a set of linear simultaneous equations.

(5) A practical periodic controller was demonstrated for two systems: the first a periodically varying electronic analog computer, and the second a wind tunnel model helicopter rotor system. The controller was shown to be of rather simplified form, suitable for microprocessor implementation.

7.2 Recommendations for Further Investigations

Results from this thesis have suggested several interesting applications and extensions of the above developments in the areas of periodic systems, rotorcraft dynamics, and control and estimation of time varying plants:

Most input-output response investigations of linear periodic systems require a numerical integration of the

equations of motion to determine system stability and transient behavior. This is a time-consuming process that does not yield trend information until after many different cases have been studied. No equivalent to time-invariant frequency response techniques yet exists for a non-parametric analysis of periodic systems. However, since any linear periodic system can be thought of as a collection of transfer functions for each sub- and super-harmonic type of response [Johnson,1980], it appears possible that a technique could be developed to estimate these transfer functions from response data using Fast-Fourier-Transform analysis of the spectral content of the input and output signals. This approach was not pursued in this investigation since the methodology for developing a control law from this information does not exist. However, such a procedure would be valuable in quick processing of data from periodic systems.

An alternative to the above procedure might be the use of nonstationary spectral analysis techniques (as is used for digital speech processing) to estimate a periodically varying transfer function for periodic systems. This might permit standard classical design techniques to be used for each analysis interval and the results combined in a periodically varying control law. This is similar to the case of a perfect-model-following design, as was demonstrated for the

scalar example in chapter 3.

The encouraging results of chapter 4 suggest possible applications of accelerometer-based observers to estimate states of non-linear and alternate time-varying systems. Since the modal content of acceleration sensors is often given in kinematical relations, it appears that such a use would be equally successful. The benefit of using this technique, however, would only exist for systems where computation complexity was more costly than sensor installation.

An additional benefit of this observer structure might be its ease of incorporation into adaptive control systems. Since all of the modal states and accelerations are avaliable for processing, it may be possible to accurately determine the system coefficients on-line using a minimum amount of data. This type of identification scheme would need to have a response time sufficiently faster than both the observer and the plant being controlled. The problem of generating feedback gains for such a complex structure would be more complex, however, due to the necessity of ensuring stability over its full operating range.

Finally, use of accelerometer-based observers for parameter estimation of rotor systems appears to be easily extendable to handle estimation of external forcing functions.

The residual in the acceleration estimate can be attributed to unmodelled aerodynamic loading as well as neglected higher modes of response and sensor bias. Should an additional transducer be available (such as a hot-wire probe, for example), the methods of section 4.5 could be used to determine the correlation between various external effects (e.g. fuselage upwash or blade-vortex interaction) and rotor blade modal responses.

REFERENCES

Anderson, B. D. and Moore, J. B. Linear Optimal Control. Prentice-Hall, Englewood Cliffs, N.J., 1971.

Biggers, J. C., "Some Approximations to the Flapping Stability of Helicopter Rotors", NASA SP-352, Proc. Specialists Meeting on Rotorcraft Dynamics, Moffet Field, California, February, 1974.

Blair, W. B., "Series Solution to the General Linear Time Varying System", IEEE Transactions on Automatic Control, V. AC-16, n. 2, 1971, pp. 210-211.

Bryson, A. E., Jr. and Ho, Y. Applied Optimal Control. John Wiley and Sons, New York, 1975.

D'Angelo, H. Linear Time-Varying Systems: Analysis and Synthesis. Allyn and Bacon, Boston, 1970.

Dasarathy, B. V. and Srinivasan, P., "A New Approach to the Study of Systems with Periodically Varying Parameters", Int. J. of Control, V.8, n.3, 1968, pp. 265-267.

DeRusso, P. M., Roy, R. J. and Close, C. M. State Variables for Engineers. Wiley, New York, 1965, pp. 372-375.

Dragan, V. and Halanay, A., "Suboptimal Stabilization of Linear Systems with Several Time Scales", Int. J. of Control, V.36, n.1, 1983, pp.109-126.

Dugundji, J. and Wendell, J. H., "Some Analysis Methods for Rotating Systems with Periodic Coefficients", AIAA Journal, V. 21, n.6, 1983, pp.890-897.

DuVal, R., "Use of Multiblade Sensors for On-Line Rotor Tip-Path-Plane Estimation", Journal of the AHS, V.25, n.4, 1980, pp.13-21.

Emanuel, W. R. and Mulholland, R. J., "Linear Periodic Control with Applications to Environmental Systems", Int. J. of Control, V.24, n.6, 1976, pp. 807-820.

Evans, R. T., "Optimal Periodic Control Theory", Frank J. Seiler Research Laboratory TR-80-0024, USAF Academy, Colorado, 1980.

Fjeld, M., "Optimal Control of Multi-Variable Periodic Processes", Automatica, V.5, n.4, 1969, pp. 497-506.

Friedmann, P., Hammond, C. E. and Woo, T., "Efficient Numerical Treatment of Periodic Systems with Application to Stability Problems", Int. J. for Numerical Methods in Engineering, V.11, 1977, pp. 1117-1136.

Fuller, J., "Rotor State Estimation for Rotorcraft", Proc. AHS National Specialists Meeting on Helicopter Vibration, Hartford, Connecticut, November 1981.

Gaonkar, G. H., Sinha Prasad, D. S. and Sastry, D., "On Computing Floquet Transition Matrices of Rotorcraft", J. of the AHS, V.26, n.3, 1981, pp. 56-61.

Gessow, A. and Meyers, G. C., Jr. Aerodynamics of the Helicopter. Ungar Publishing Co., New York, 1967.

Gilbert, E. G., "System Optimization by Periodic Control", Air Force Office of Scientific Research TR-82-0575, Bolling AFB, D. C., 1982.

Guinn, K. F., "Individual Blade Control Independent of a Swash Plate", Journal of the AHS, V.27, n.3, July 1982.

Ham, N. D., "A Simple System for Helicopter Individual-Blade-Control Using Modal Decompisition", Vertica, V.4, n.1, 1980.

Ham, N. D., "Helicopter Individual-Blade-Control and Its Applications", Proc. Ninth European Rotorcraft Forum, Stresa, Italy, September 1983.

Ham, N. D., Behal, B. L. and McKillip, R. M., Jr., "Helicopter Lag Damping Augmentation Through Individual-Blade-Control", Vertica, V.7, n.4, 1983.

Ham, N. D. and McKillip, R. M., Jr., "A Simple System for Helicopter Individual-Blade-Control and Its Application to Gust Alleviation", Proc. Thirty-Sixth AHS National Forum, May 1980.

Ham, N. D. and Quackenbush, T. R., "A Simple System for Helicopter Individual-Blade-Control and Its Application to Stall-Induced Vibration Alleviation", Proc. AHS National Specialists Meeting on Helicopter Vibration, Hartford, Connecticut, November 1981.

Haug, A. Theoretical Solid-State Physics, Vol. I. Pergamon, Oxford, 1972, pp. 59-62.

Hohenemser, K. H. and Yin, S., "Some Applications of the Method of Multiblade Coordinates", J. of the AHS, V.17, n.3, 1972, pp. 3-12.

Johnson, W., "A Peturbation Solution of Rotor Flapping Stability", NASA TM-X-62165, July 1972.

Johnson, W. Helicopter Theory. Princeton University Press, Princeton, New Jersey, 1980.

Johnson, W., "Self-Tuning Regulators for Multicyclic Control of Helicopter Vibration", NASA TP-1996, March 1982.

Junkins, J. L. An Introduction to Optimal Estimation of Dynamical Systems. Sijthoff and Noordhoff, The Netherlands, 1978, pp. 142-143.

Kern, G., "Linear Closed-Loop Control in Linear Periodic Systems with Application to Spin-Stabilized Bodies", Int. J. of Control, V.31, n.5, 1980, pp. 905-916.

Kreindler, E. and Rothschild, D., "Model-Following in Linear-Quadratic Optimization", AIAA Journal, V.14, n.7, July 1976, pp. 835-842.

Kretz, M., "Research in Multicyclic and Active Control of Rotary Wings", Vertica, V.1, n.2, 1976.

Kriechbaum, G. and Stineman, R., "Design of Desirable Airplane Handling Qualities via Optimal Control", AIAA Journal of Aircraft, V.9, n.5, 1972, pp.365-369.

Kwakernaak, H. and Sivan, R. Linear Optimal Control Systems. Wiley-Interscience, New York, 1972.

Leibst, B. S., "A Pitch Control System for Large Scale Wind Turbines", Ph.D. Thesis, Department of Aeronautics and Astronautics, M.I.T., Cambridge, Massachusetts, 1981.

Luenberger, D. G., "Observers for Multivariable Systems", IEEE Transactions on Automatic Control, V. AC-11, n. 2, 1966, pp. 190-197.

Magnus, W. and Winkler, S. Hill's Equation. Dover, New York, 1979.

Marzollo, A., ed. Periodic Optimization, vols. I and II. International Centre for Mechanical Sciences, Course no. 135, held at the Department of Automation and Information,

Udine, Italy, 1972. Springer-Verlag, New York, 1972.

Meirovitch, L. Methods of Analytical Dynamics. McGraw-Hill, New York, 1970, ch. 9.

Melsa, J. L. and Jones, S. K. Computer Programs for Computational Assistance in the Study of Linear Control Theory. McGraw-Hill, New York, 1970.

Molusis, J. A., Hammond, C. E. and Cline, J. H., "A Unified Approach to the Optimal Design of Adaptive and Gain Scheduled Controllers to Achieve Minimum Helicopter Rotor Vibration", Proc. Thirty-Seventh AHS Annual National Forum, May 1981.

Myers, G. E., "Active Control of Linear Periodic System with Two Unstable Modes", M.S. Thesis, Air Force Institute of Technology, Wright-Patterson AFB, Ohio, 1982.

Nafeh, A. H. Introduction to Peturbation Techniques. Johr Wiley and Sons, New York, 1981.

Nafeh, A. H. and Mook, D. T. Nonlinear Oscillations. John Wiley and Sons, New York, 1979, ch. 5.

Nishimura, T., "Spectral Factorization in Periodically Time-Varying Systems and Application to Navigation Systems", AIAA J. of Spacecraft and Rockets, V.9, n.7, 1972, pp. 540-546.

Peters, D. A. and Hohenemser, K. H., "Application of the Floquet Transition Matrix to Problems of Lifting Rotor Stability", J. of the AHS, V.16, n.2, 1971, pp. 25-33.

Peters, D. A. and Ormiston, R. A., "Flapping Response Characteristics of Hingeless Rotor Blades by a Generalized Harmonic Balance Method", NASA TN-D-7856, February 1975.

Rahnema, M. "Alleviation of Helicopter Fuselage-Induced Rotor Unsteady Loads Through Deterministic Variation of the Individual Blade Pitch", NASA CR-166234, 1981.

Ramnath, R. V., "A New Approach to the Design of Time-Varying Control Systems with Application to the Space Shuttle Boost", Fifth IFAC Symposium on Automatic Control in Space, Genova, Italy, June 1973.

Rinaldi, S., "High-Frequency Periodic Processes", IEEE Transactions on Automatic Control, V.AC-15, n.6, 1970, pp.671-673.

Shaw, J. and Albion, N., "Active Control of Rotor Blade Pitch for Vibration Reduction: A Wind Tunnel Demonstration", Vertica, V.4, n.1, 1980.

Speyer, J. L. and Evans, R. T., "A Sufficiency Condition for Optimal Periodic Processes", Proc. 1981 Joint Automatic Control Conf., Charlottesville, Virginia, June 1981.

Stein, G., "Generalized Quadratic Weights for Asymptotic Regulator Properties", IEEE Trans. on Automatic Control, V.AC-24, n.4, 1979, pp. 559-566.

Stengel, R. F., "An Introduction to Stochastic Optimal Control Theory", AGARD AG-251, Theory and Applications of Modern Control Techniques in Aerospace, July 1981.

Taylor, R. B., Zwicke, P. E., Gold., P. and Miao, W., "Analytical Design and Evaluation of an Active Control System for Helicopter Vibration and Gust Response Alleviation", NASA CR-152377, July 1980.

Tyler, J., Jr., "The Characteristics of Model-Following Systems as Synthesized by Optimal Control", IEEE Trans. on Automatic Control, V.AC-9, n.4, 1964, pp.485-498.

Vepa, R. and Balasubramanian, T. S., "Numerical Treatment of Helicopter Rotor Stability Problems", Proc. of the ASME Aerospace Conf., San Francisco, California, August 1980.

Wang, P. K. C., "Feedback Control of Parametric Instabilities", Int. J. of Control, V.37, n.4, 1983, pp. 755-773.

Wendell, J. H., "Simplified Aeroelastic Modeling of Horizontal Axis Wind Turbines", Ph.D. Thesis, Department of Aeronautics and Astronautics, M.I.T., Cambridge, Massachusetts, 1982.

Wiesel, W. and Shelton, W., "Modal Control of an Unstable Periodic Orbit", J. of the Astronautical Sciences, V.31, n.1, 1983, pp. 63-76.

Widnall, W. S. Applications of Optimal Control Theory to Computer Controller Design. M.I.T. Press, Cambridge, Massachusetts, 1968.

Wolf, C. S., "Pole Placement for Time Periodic Systems", M.S. Thesis, Air Force Institute of Technology, Wright-Patterson AFB, Ohio, 1982.

Wood, E. R., "Higher Harmonic Control for the Jet Smooth Ride", Vertiflite, V.29, n.4, 1983, pp. 28-32.

Wu, M., "Solutions of Certain Classes of Linear Time-Varying Systems", Int. J. of Control, V.31, n.1, 1980, pp. 11-20.

Zwicke, P. E., "Helicopter Gust Alleviation: An Optimal Sampled-Data Approach", Proc. Thirty-Sixth AHS National Forum, May 1980.

ORIGINAL PAGE IS
OF POOR QUALITY

Fig. 2.1: Rotor blade force diagram in forward flight

Fig. 2.1a: Top view

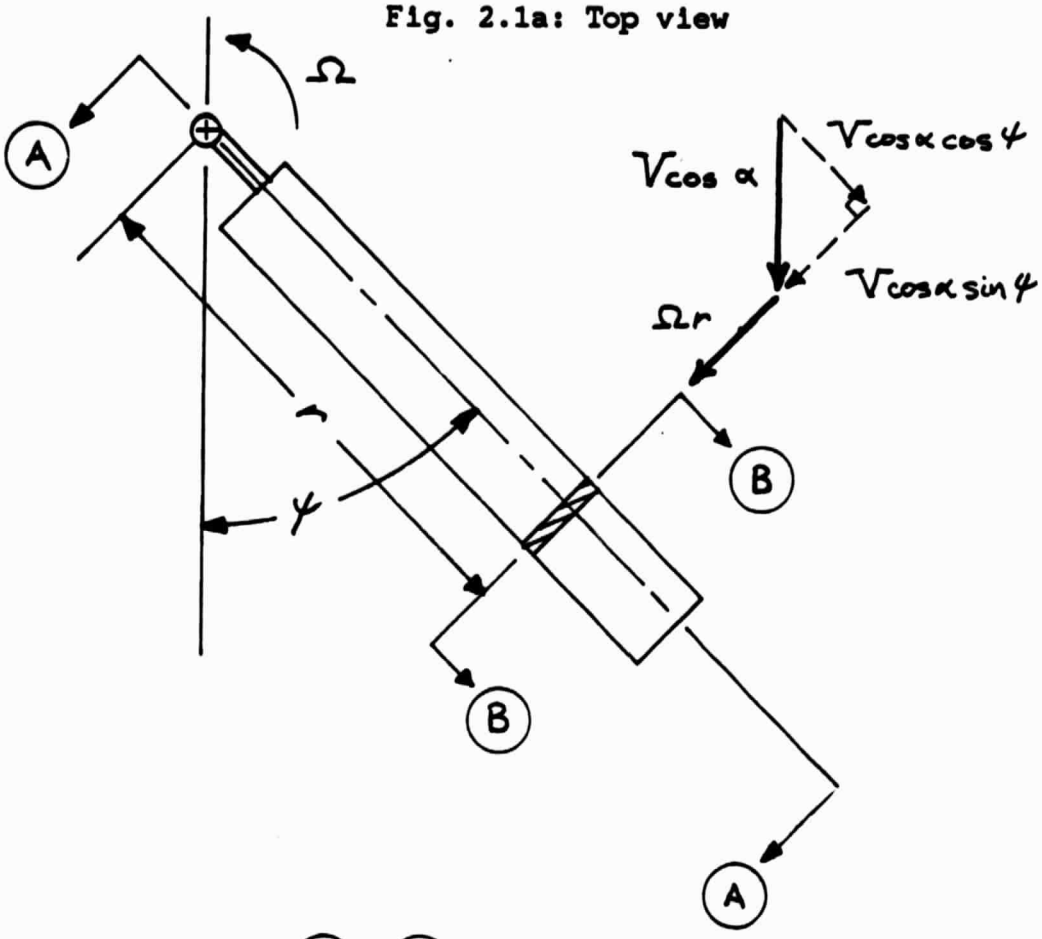

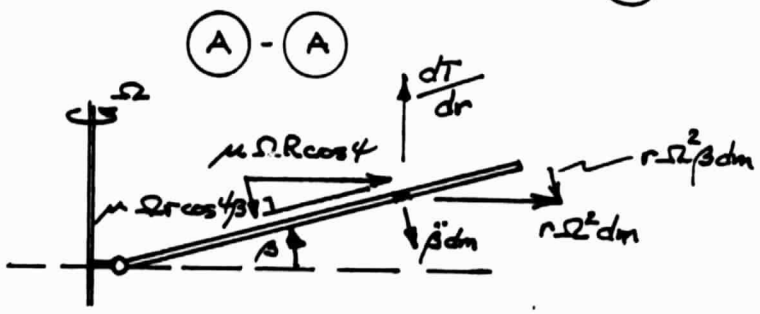

Fig. 2.1b: Side view

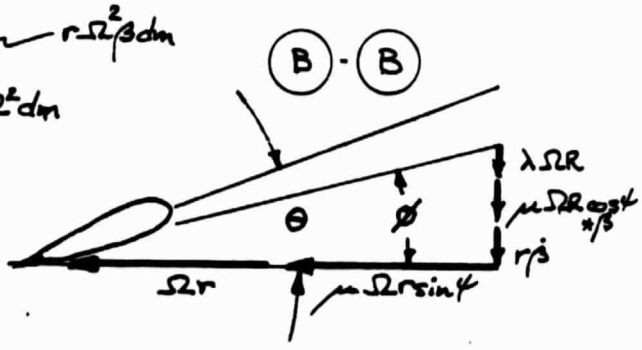

Fig. 2.1c: End view

ORIGINAL PAGE IS
OF POOR QUALITY

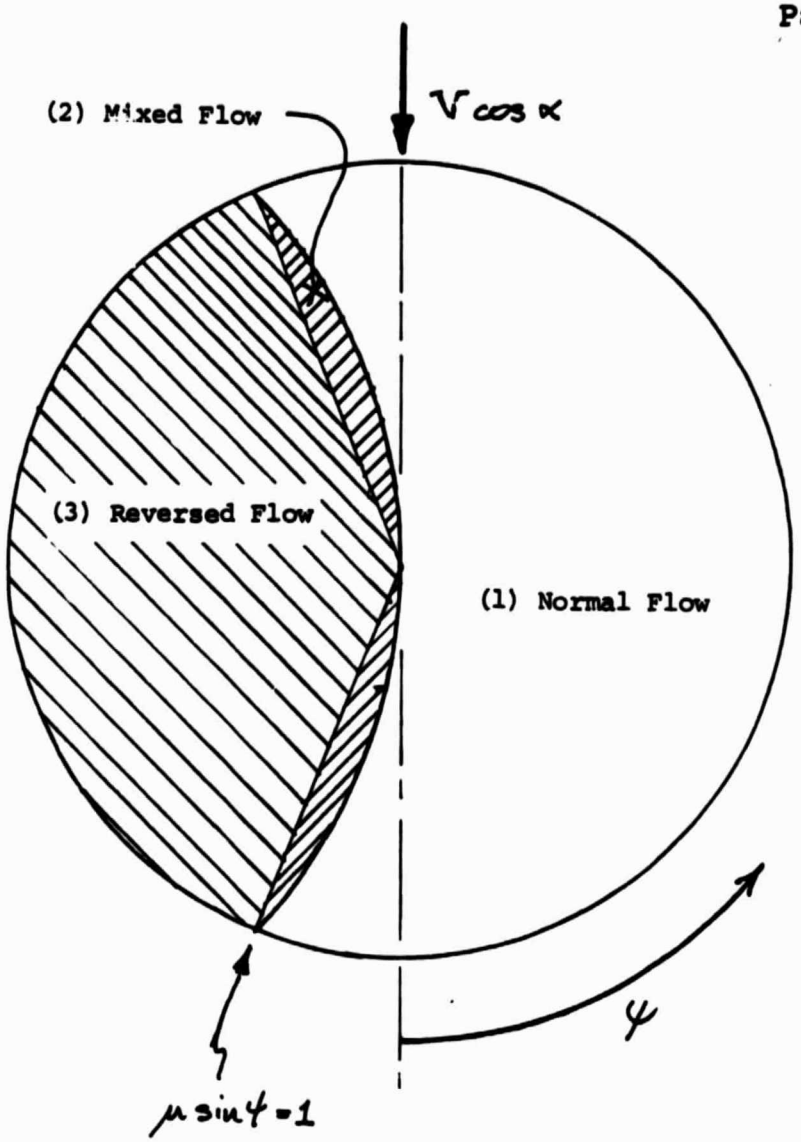

Fig. 2.2: Rotor flow regimes in high speed forward flight

ORIGINAL PAGE IS
OF POOR QUALITY

The flapping equation is:

$$\frac{\ddot{\beta}}{\Omega^2} + M_{\dot{\beta}/\Omega}\frac{\dot{\beta}}{\Omega} + M_\beta \beta = M_\theta \theta$$

where the coefficients are:

$$M_{\dot{\beta}/\Omega} = (1): \gamma\left[\frac{1}{8} - \frac{1}{24}(\xi + \xi^2 + \xi^3) + \mu\sin(\psi)\left(\frac{1}{6} - \frac{1}{2}(\xi + \xi^2)\right)\right]$$

$$(2): \quad [\,(1)\,] + \gamma\left(\frac{1}{1-\xi}\right)\left[\frac{1}{12}(\mu\sin(\psi) - \xi)(\mu\sin(\psi) + \xi)^3\right]$$

$$(3): \quad -[\,(1)\,]$$

$$M_\beta = (1): \nu^2 + \gamma\mu\cos(\psi)\left[\frac{1}{6}\left(1 + \frac{1}{2}\xi\right)(1 - \xi) + \mu\sin(\psi)\frac{1}{4}(1 - 2\xi)(1 + \xi)\right]$$

$$(2): \quad [\,(1)\,] - \gamma\left(\frac{1}{1-\xi}\right)\mu\cos(\psi)\left[\frac{1}{6}(\mu\sin(\psi) + \xi)^3\right]$$

$$(3): \quad -[\,(1)\,]$$

$$M_\theta = (1): \quad \gamma\left[\frac{1}{8} - \frac{1}{24}(\xi + \xi^2 + \xi^3) + \mu\sin(\psi)\left[\frac{1}{3} - \frac{1}{6}(\xi + \xi^2)\right] + (\mu\sin(\psi))^2\left(\frac{1}{4} - \frac{1}{4}\xi\right)\right]$$

$$(2): \quad [\,(1)\,] - \gamma\left(\frac{1}{1-\xi}\right)\frac{1}{12}(\mu\sin(\psi) + \xi)^4$$

$$(3): \quad -[\,(1)\,]$$

Fig. 2.3: Single blade flapping moment coefficients

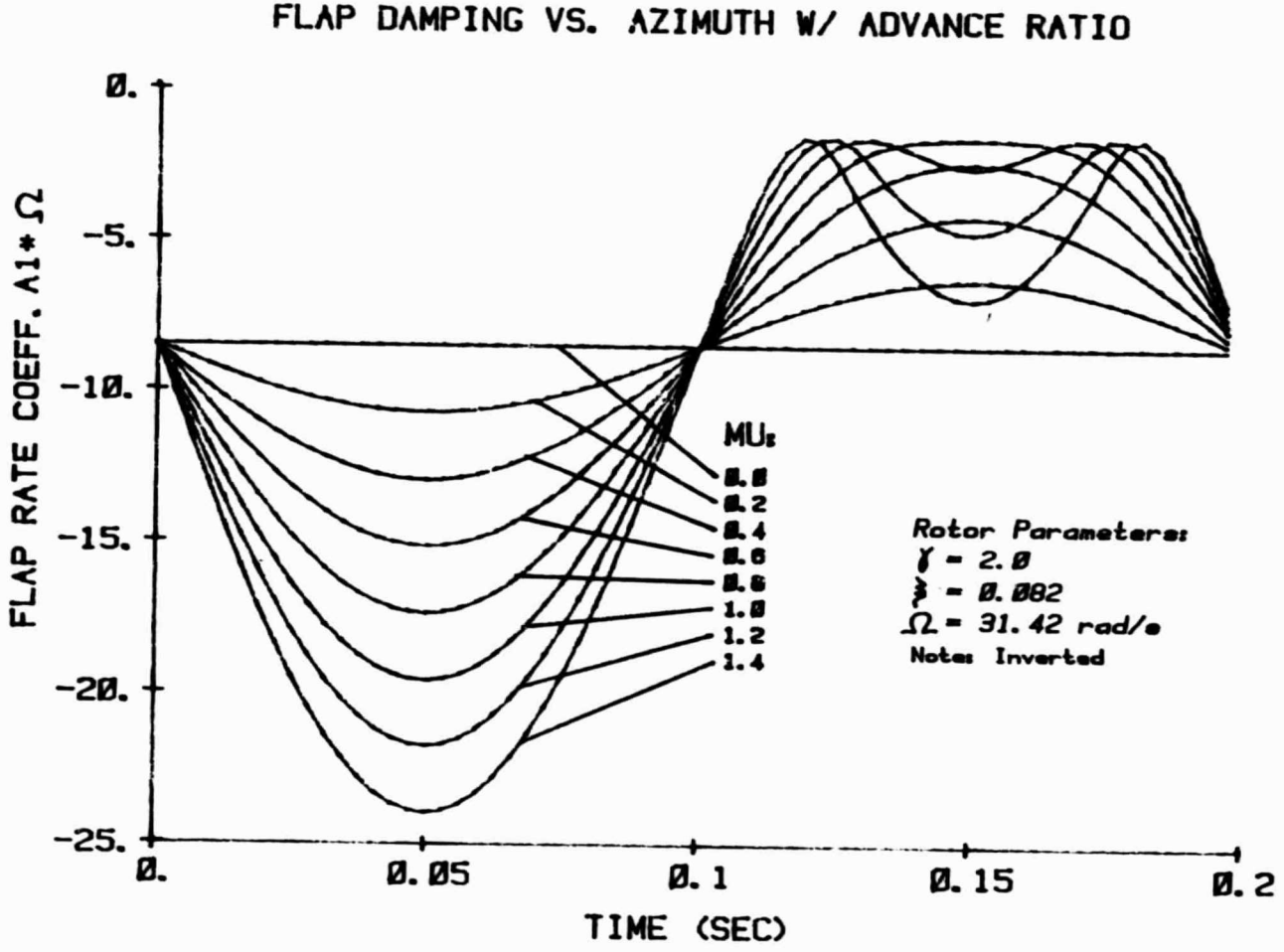

Fig. 2.4a: Flap damping (inverted) versus time for Ω = 5 Hz

ORIGINAL PAGE IS
OF POOR QUALITY

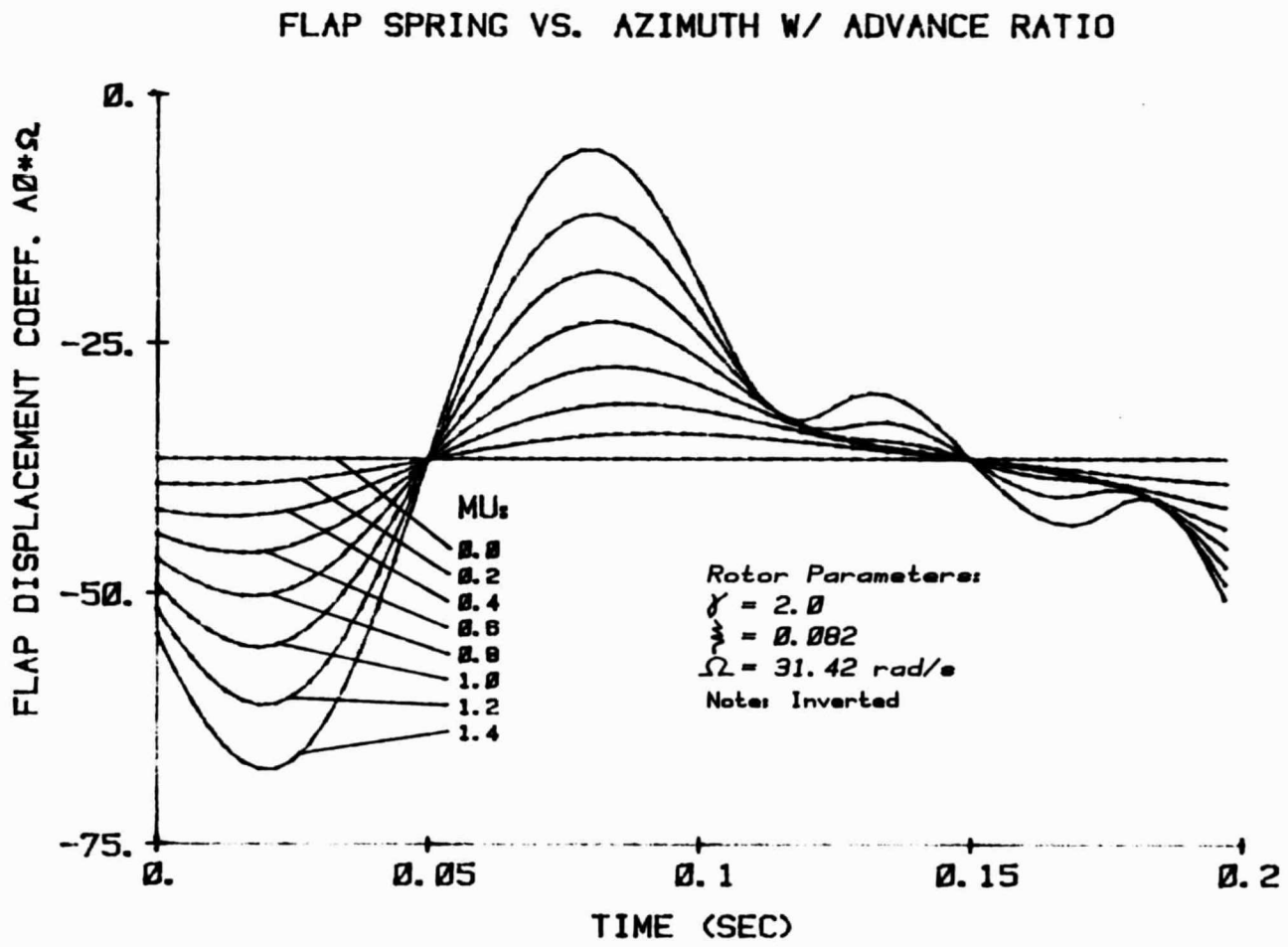

Fig. 2.4b: Flap spring (inverted) versus time for $\Omega = 5$ Hz

ORIGINAL PAGE IS
OF POOR QUALITY

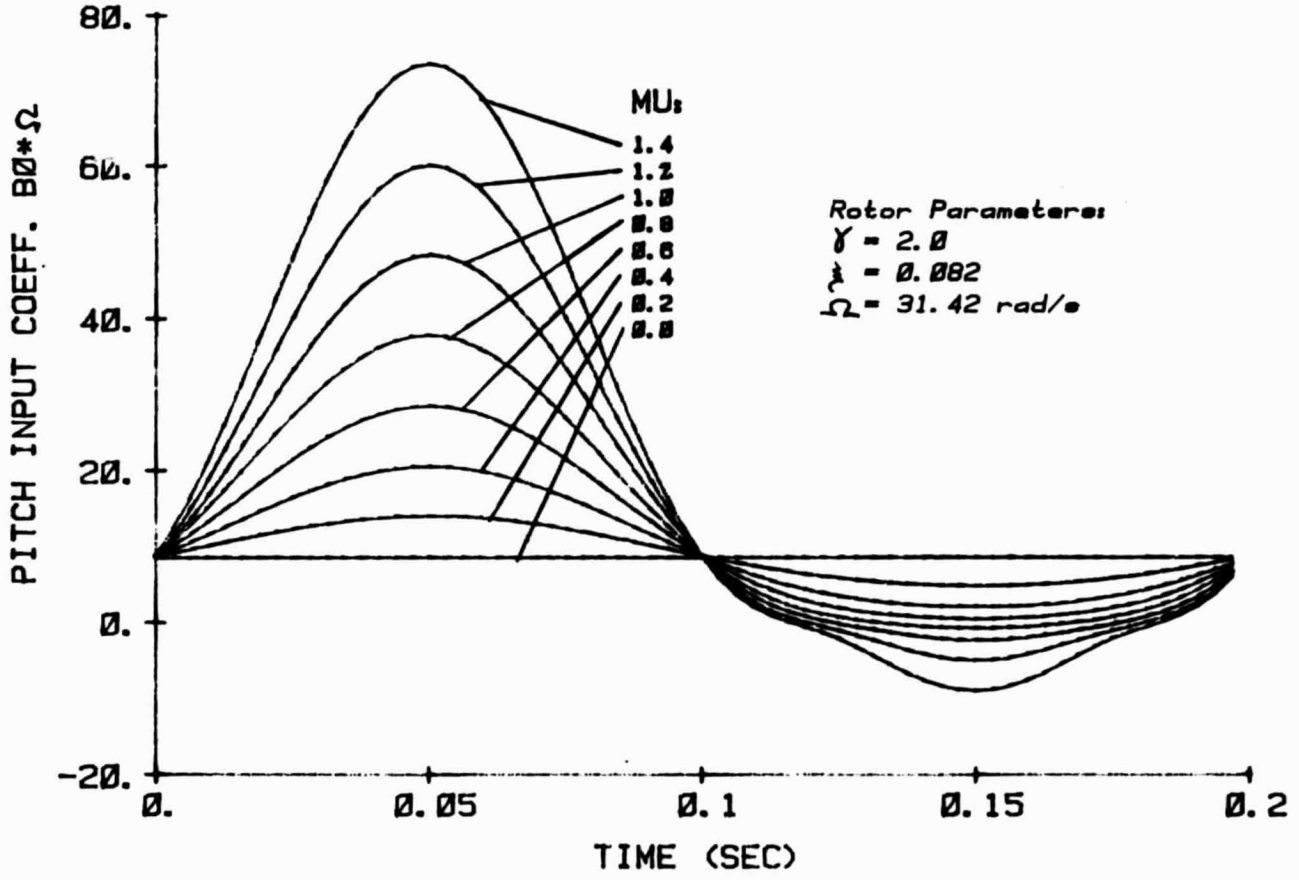

Fig. 2.4c: Pitch control power versus time for Ω = 5 Hz

ORIGINAL PAGE IS
OF POOR QUALITY

ORIGINAL PAGE IS
OF POOR QUALITY

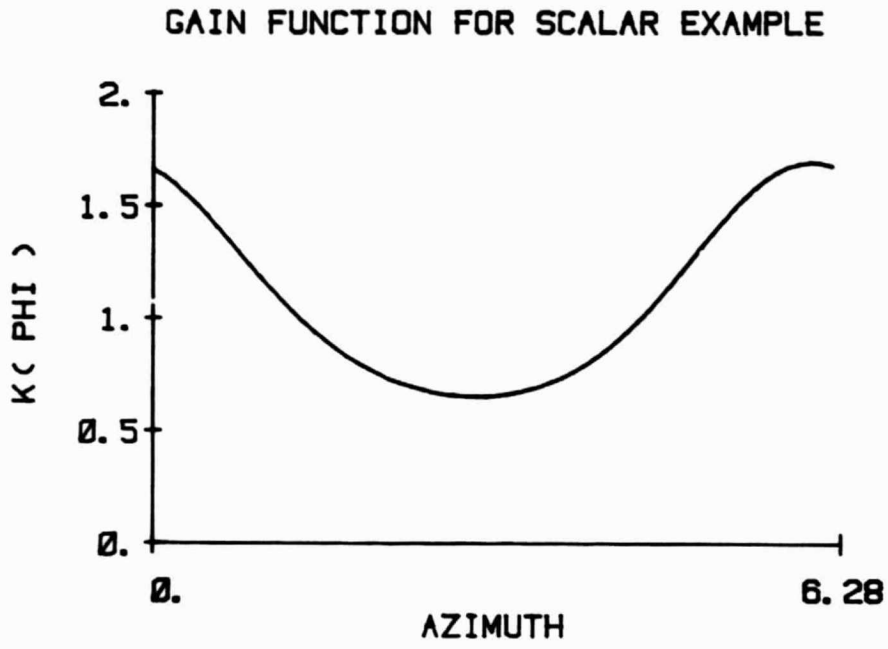

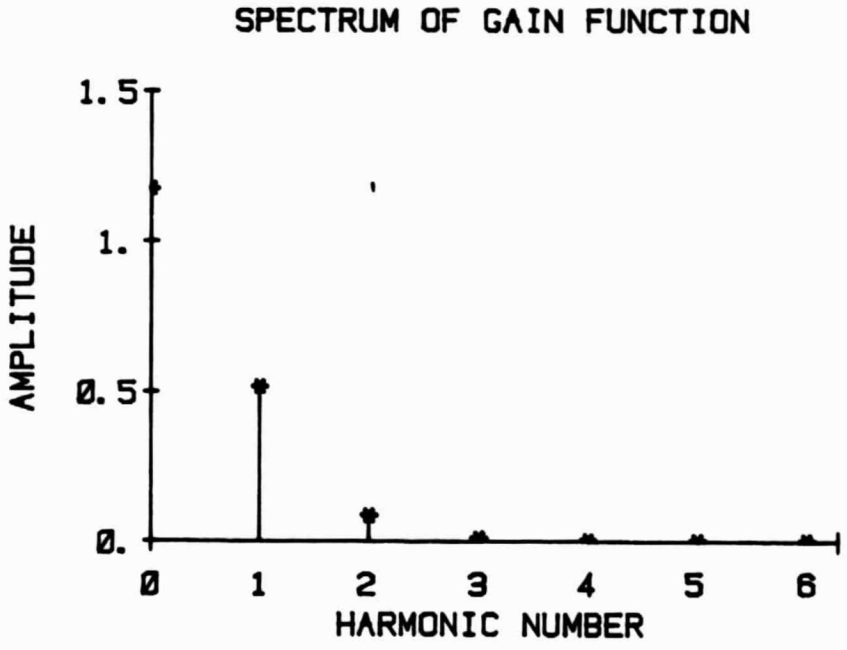

Fig. 3.1: Feedback gain for scalar example

ORIGINAL PAGE IS
OF POOR QUALITY

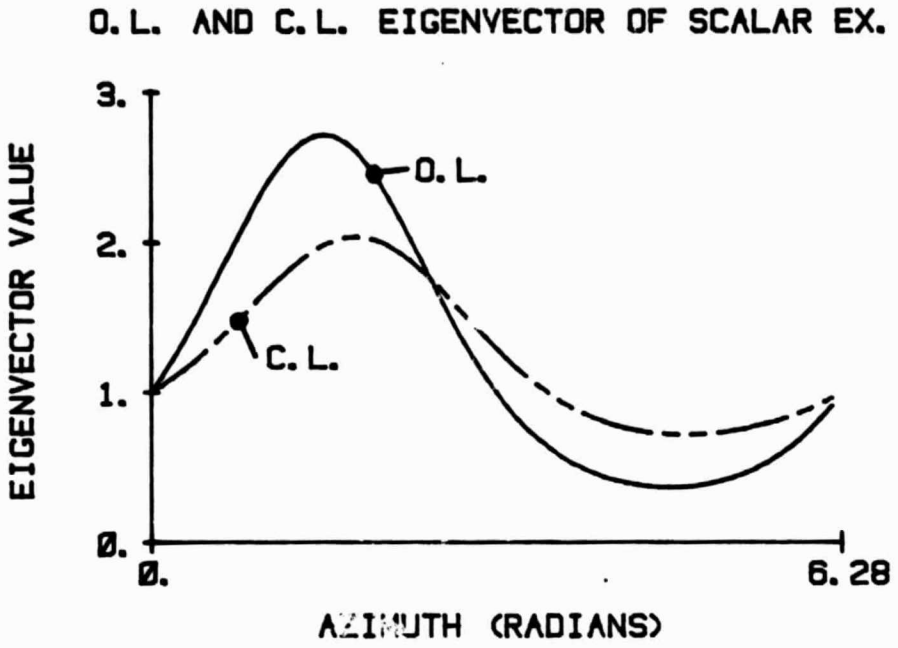

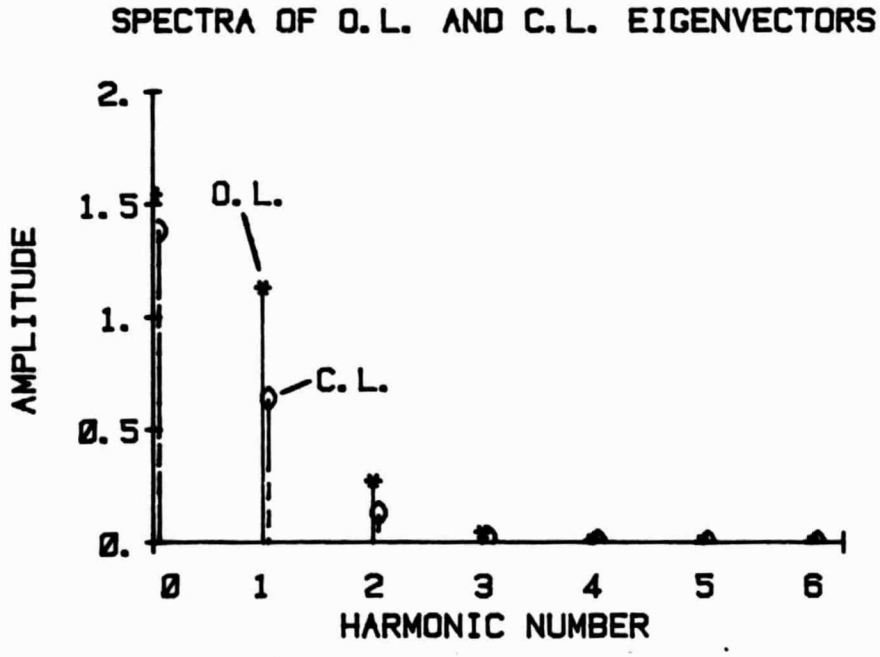

Fig. 3.2: Eigenvector of scalar example

ORIGINAL PAGE IS
OF POOR QUALITY

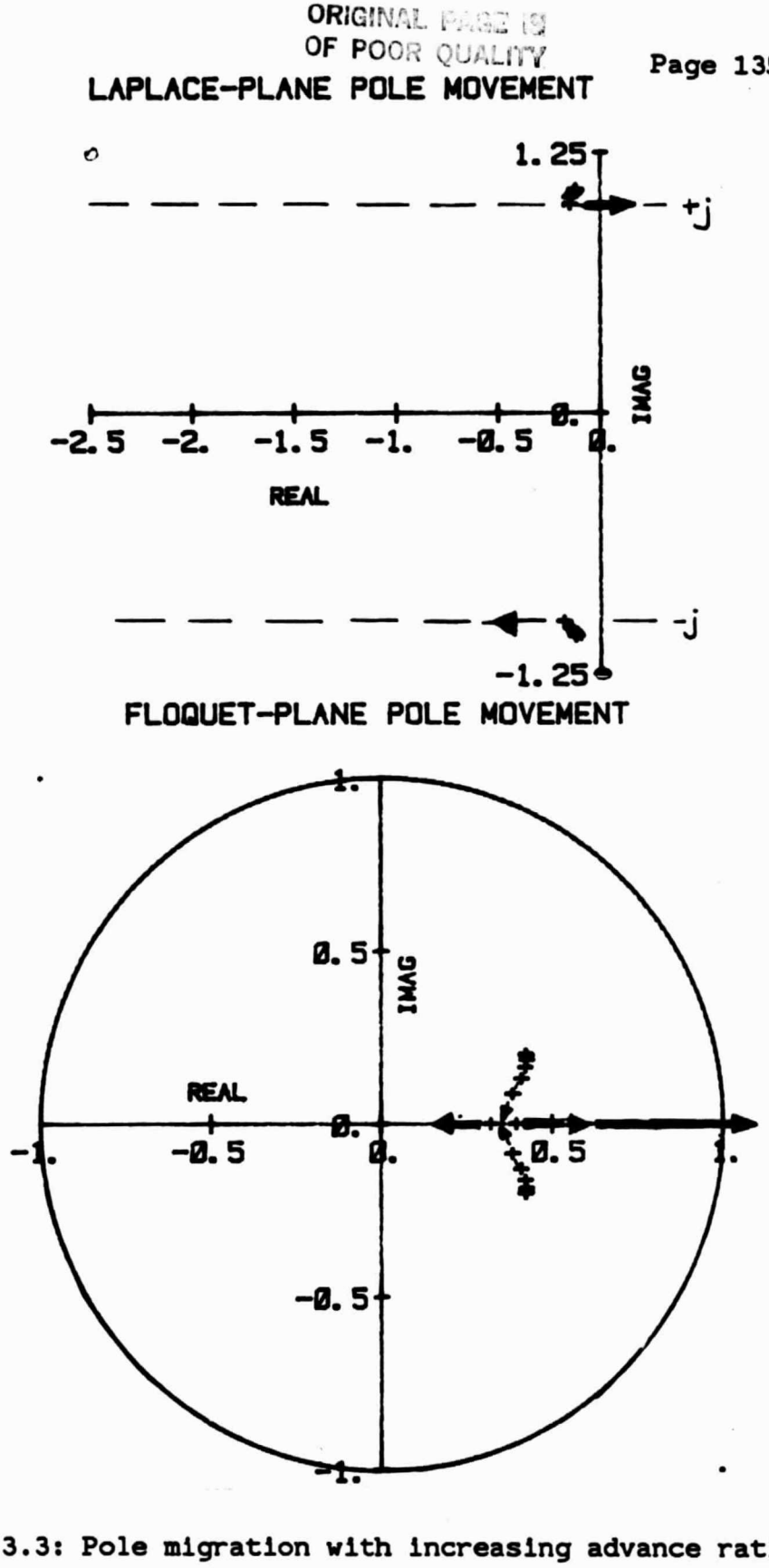

Fig. 3.3: Pole migration with increasing advance ratio

ORIGINAL PAGE IS
OF POOR QUALITY

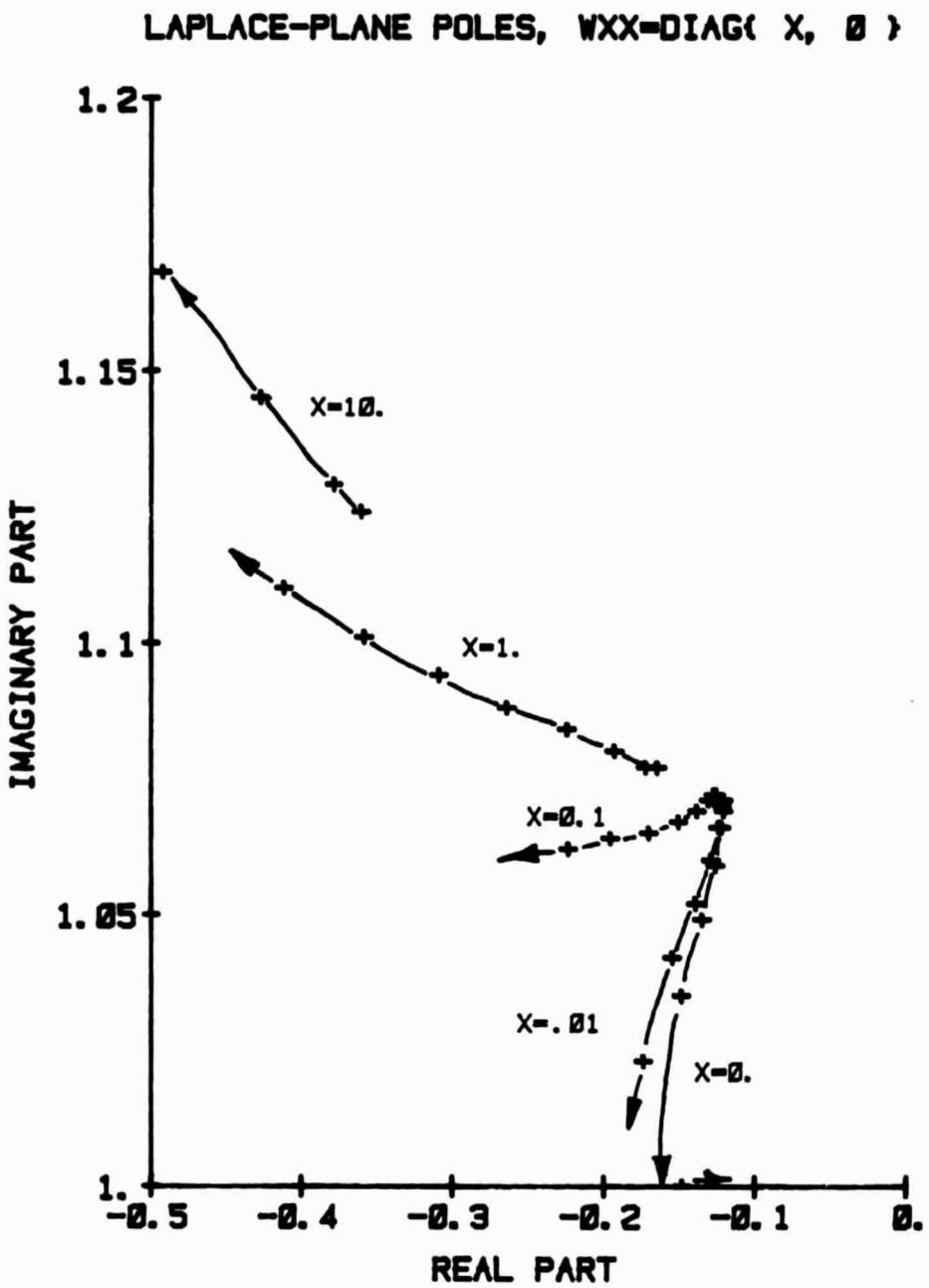

Fig. 3.4a: Laplace-plane poles, position-only weighting

ORIGINAL PAGE IS
OF POOR QUALITY

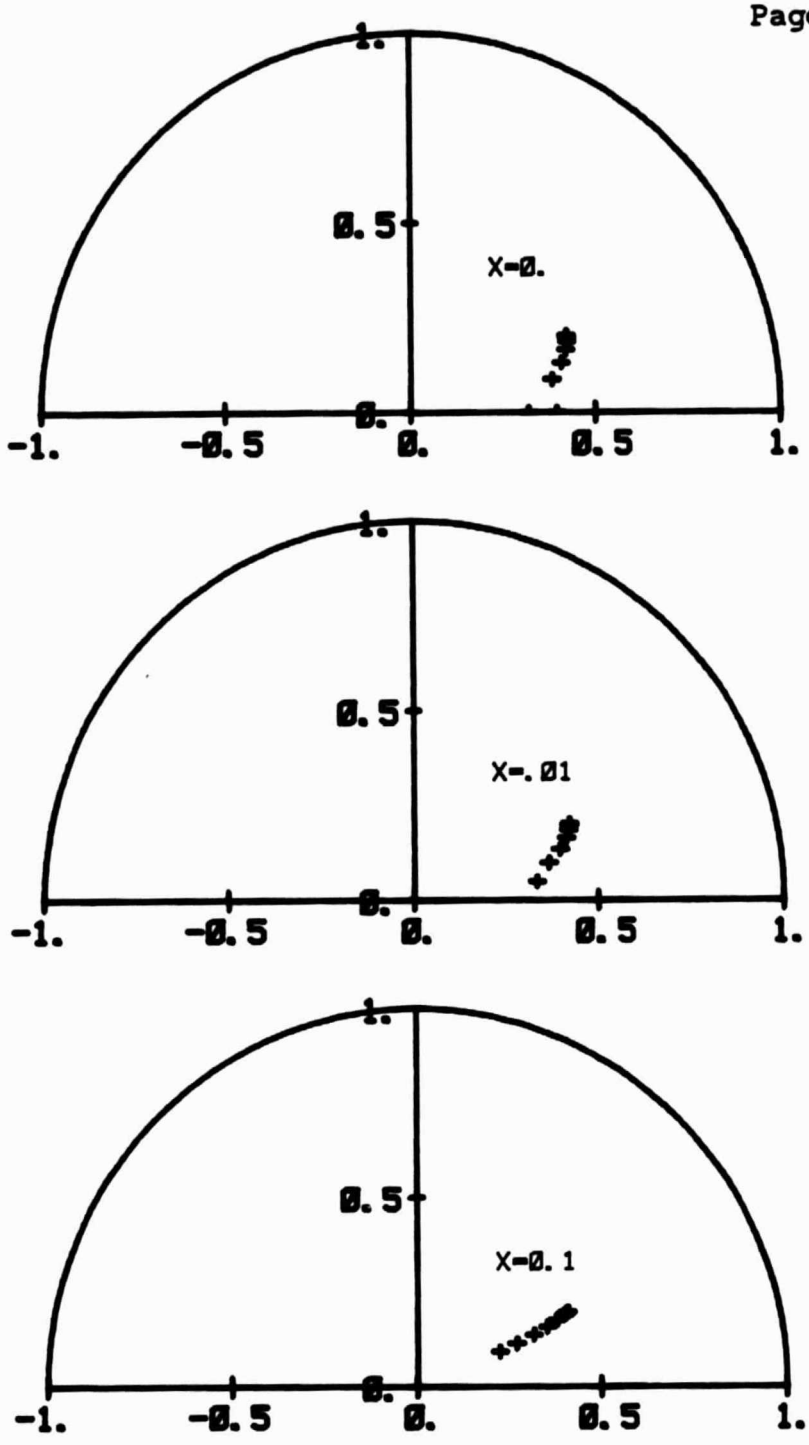

Fig. 3.4b: Floquet-plane poles, position-only weighting

ORIGINAL PAGE IS
OF POOR QUALITY

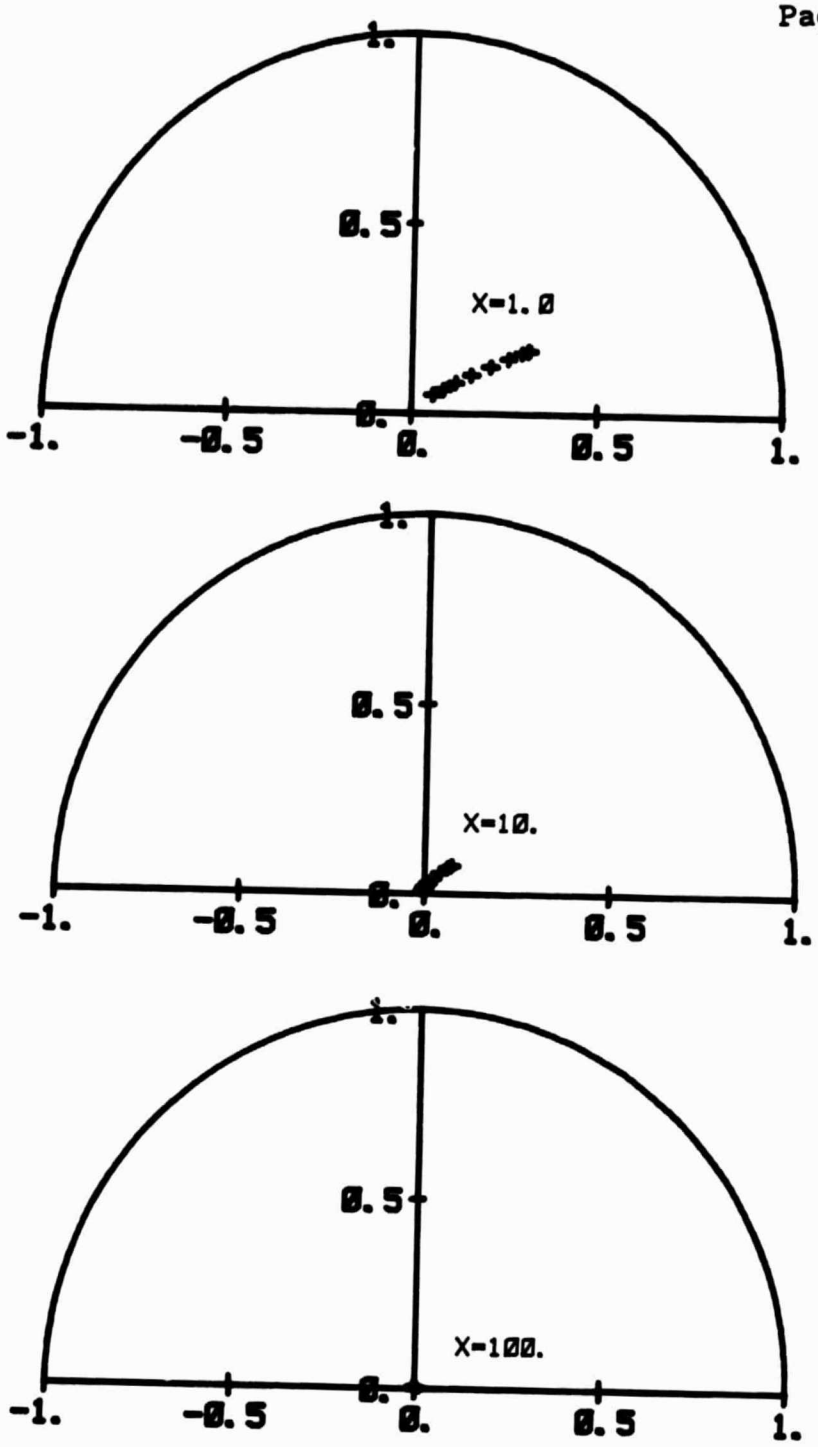

Fig. 3.4c: Floquet-plane poles, position-only weighting

ORIGINAL PAGE IS
OF POOR QUALITY

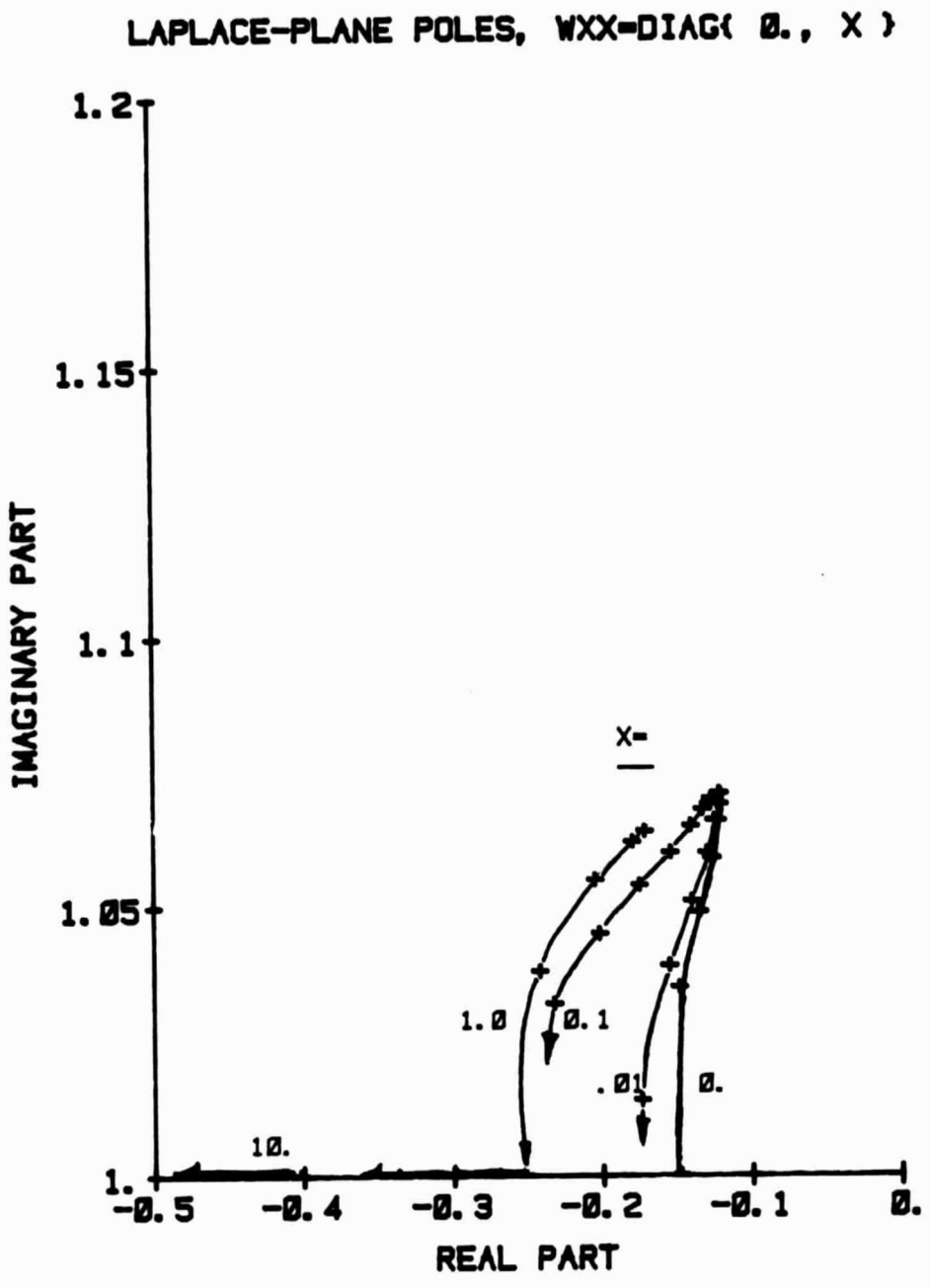

Fig. 3.5a: Laplace-plane poles, rate-only weighting

ORIGINAL PAGE IS
OF POOR QUALITY

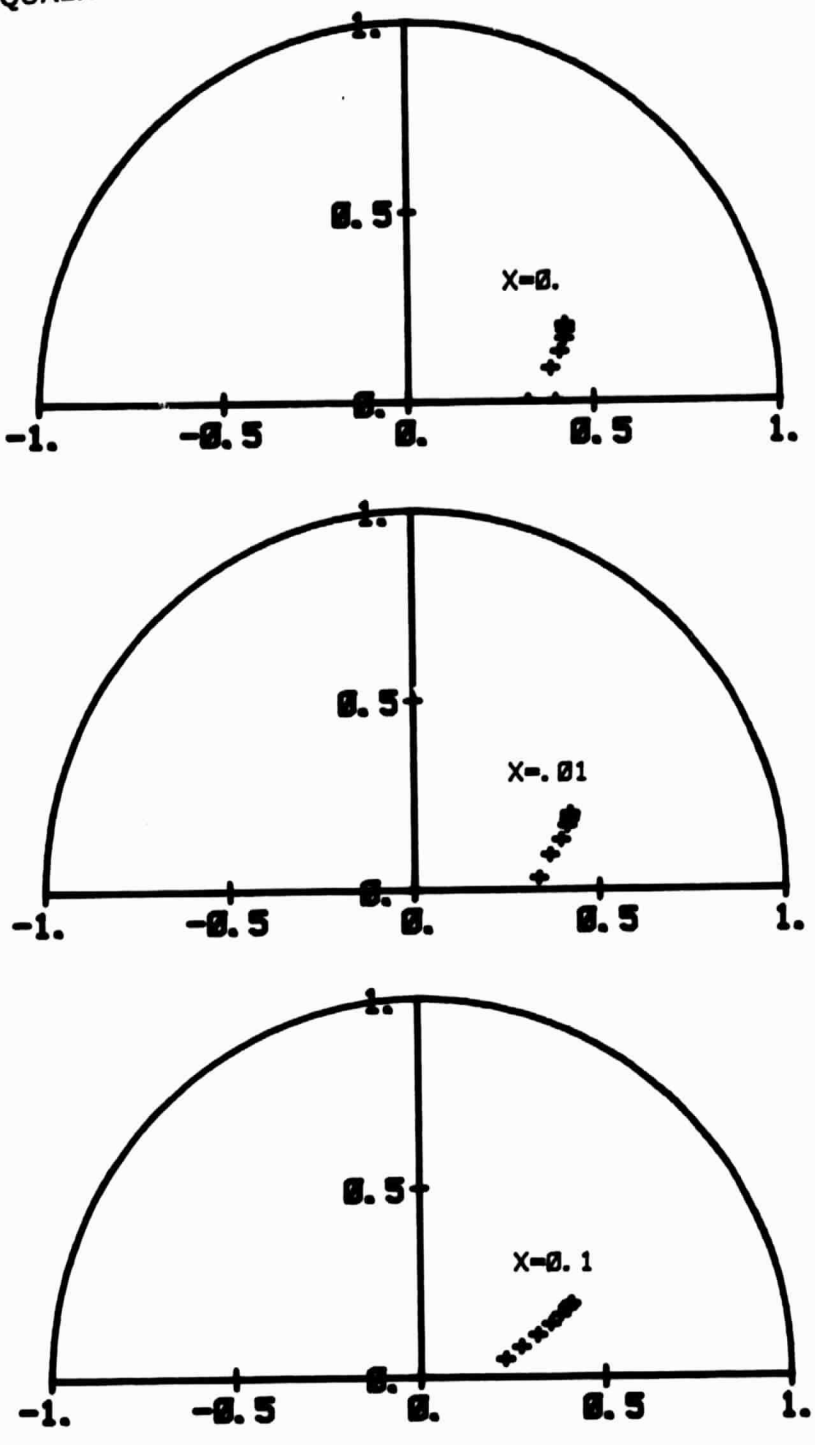

Fig. 3.5b: Floquet-plane poles, rate-only weighting

ORIGINAL PAGE IS
OF POOR QUALITY

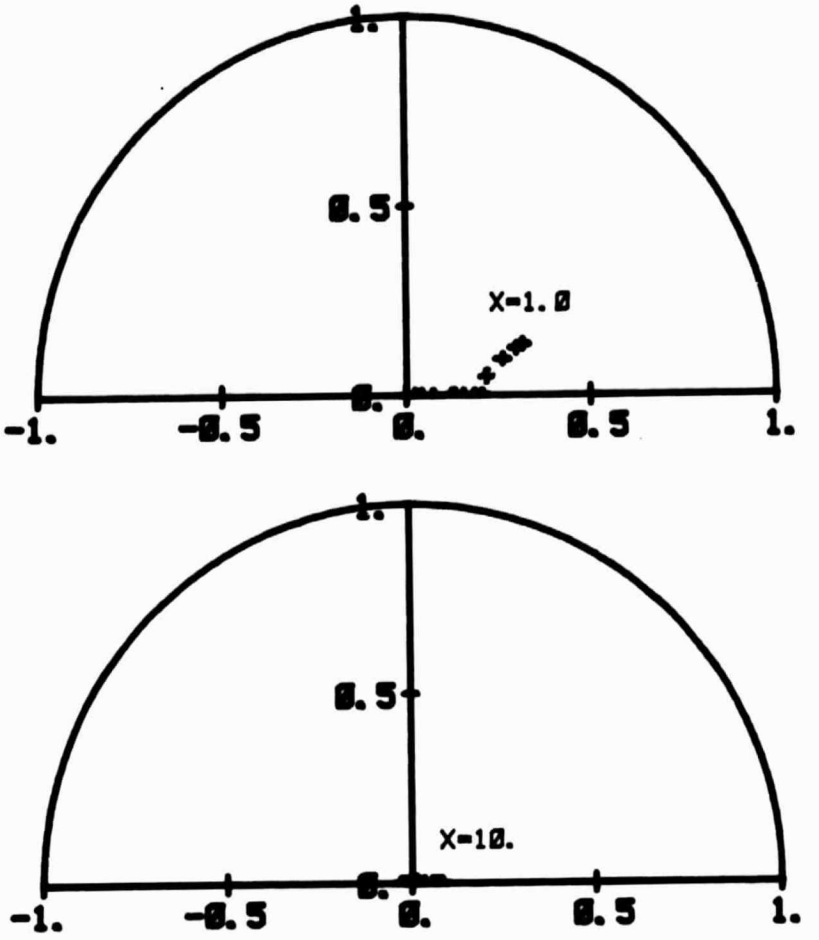

Fig. 3.5c: Floquet-plane poles, rate-only weighting

ORIGINAL PAGE IS
OF POOR QUALITY

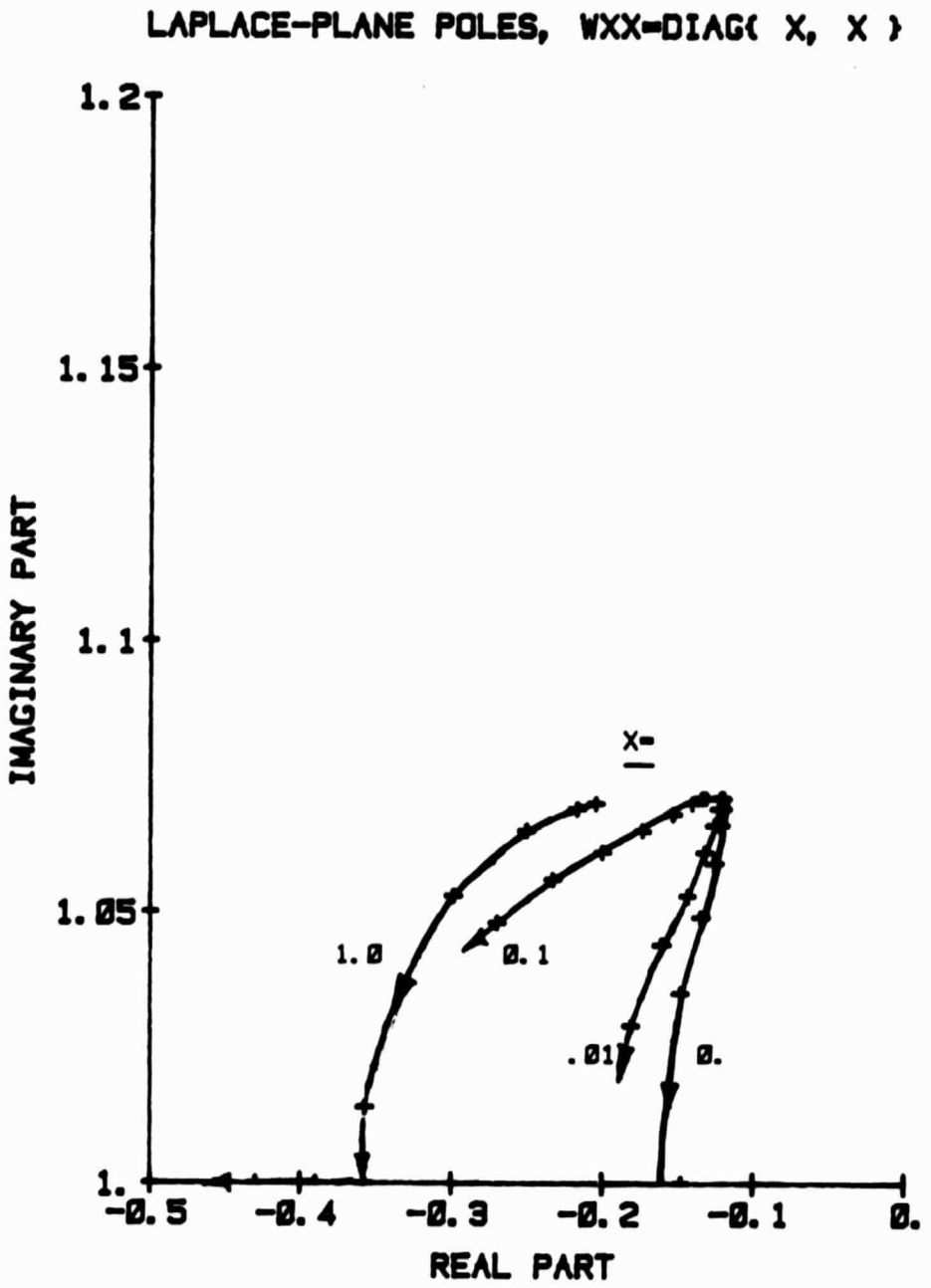

Fig. 3.6a: Laplace-plane poles, position+rate weighting

ORIGINAL PAGE IS
OF POOR QUALITY

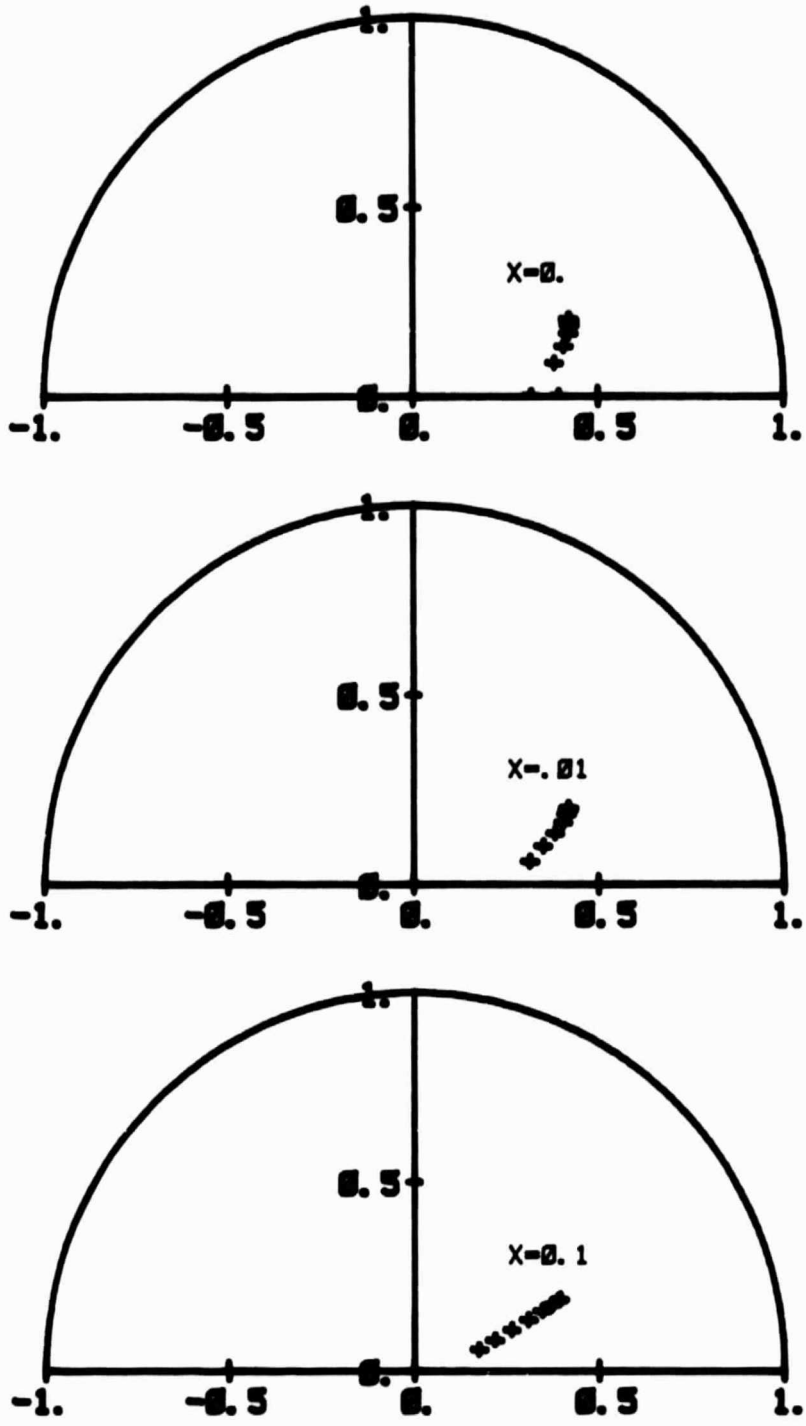

Fig. 3.6b: Floquet-plane poles, position+rate weighting

ORIGINAL PAGE IS
OF POOR QUALITY

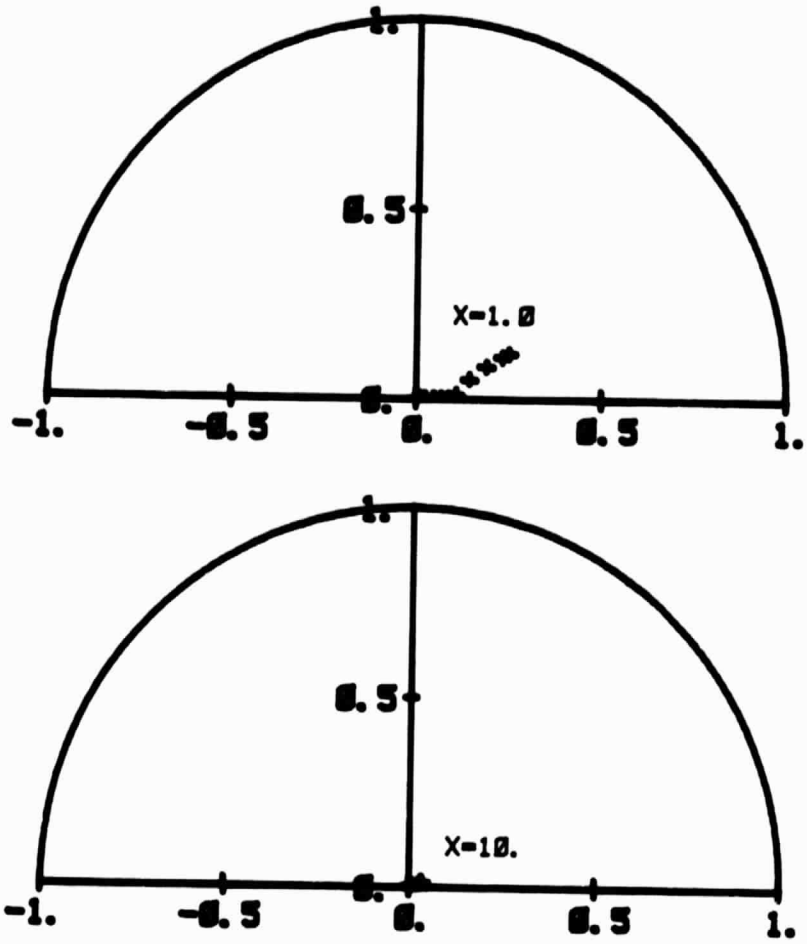

Fig. 3.6c: Floquet-plane poles, position+rate weighting

ORIGINAL PAGE IS
OF POOR QUALITY

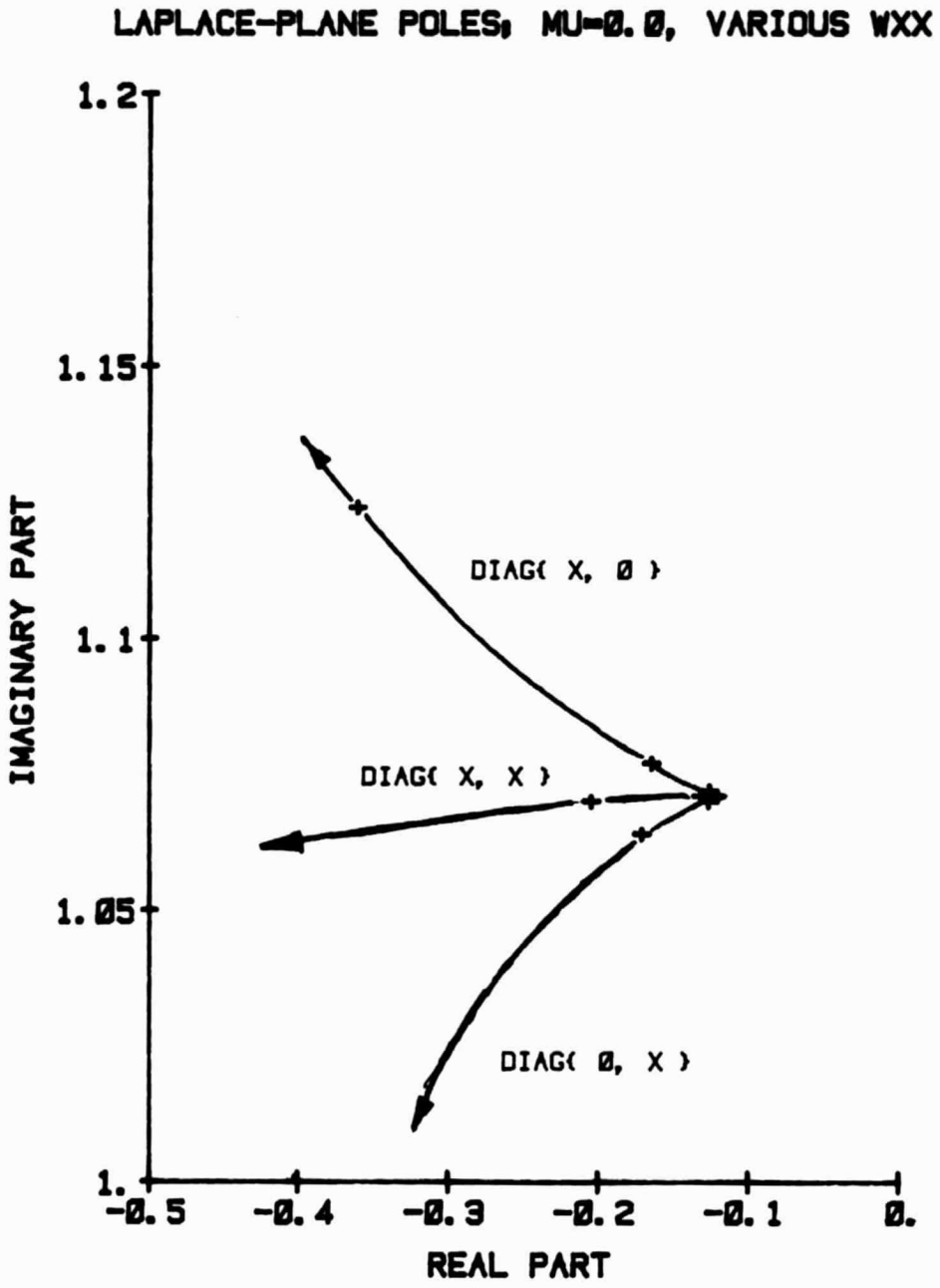

Fig. 3.7a: Laplace-plane poles, hover, various weightings

ORIGINAL PAGE IS
OF POOR QUALITY

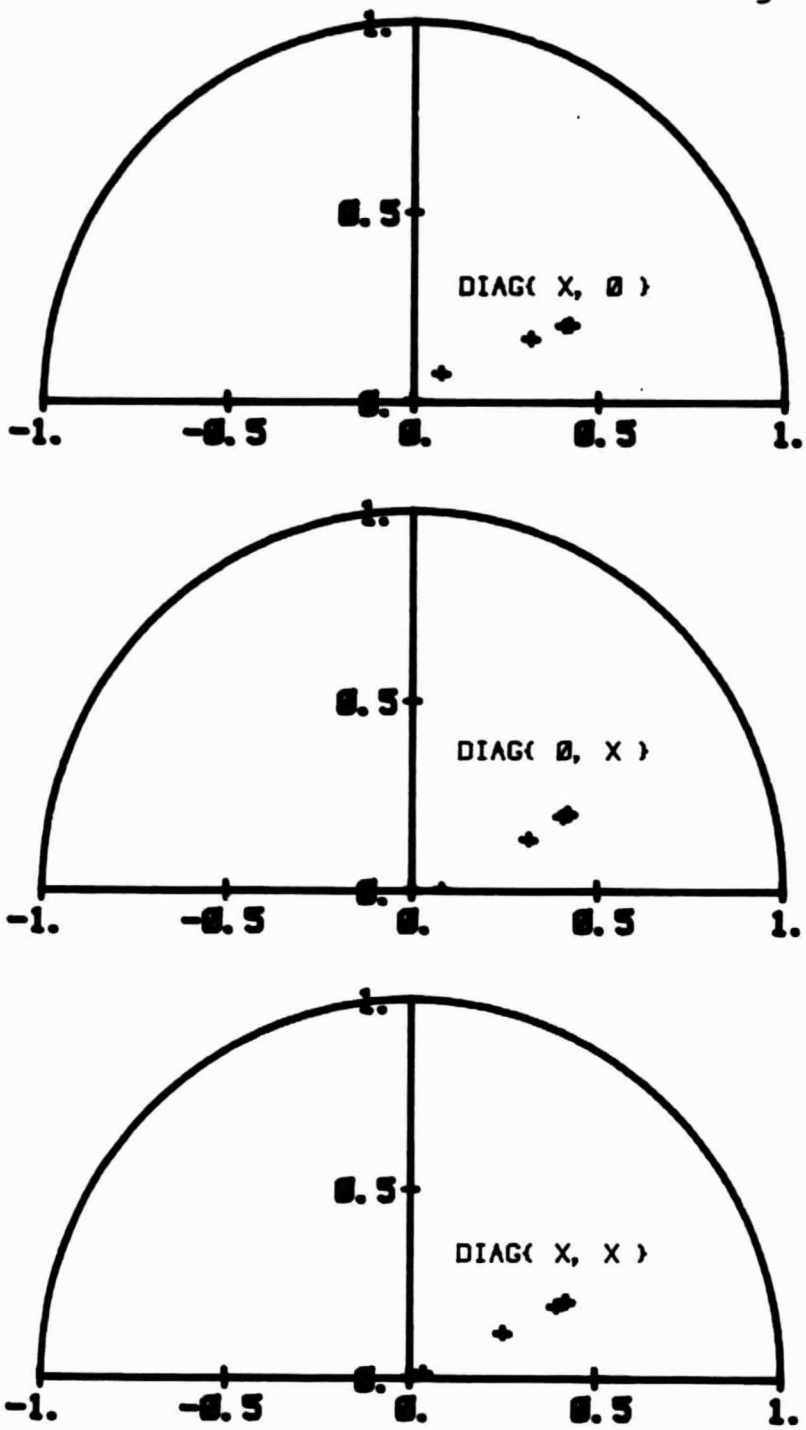

Fig. 3.7b: Floquet-plane poles, hover, various weightings

ORIGINAL PAGE IS
OF POOR QUALITY

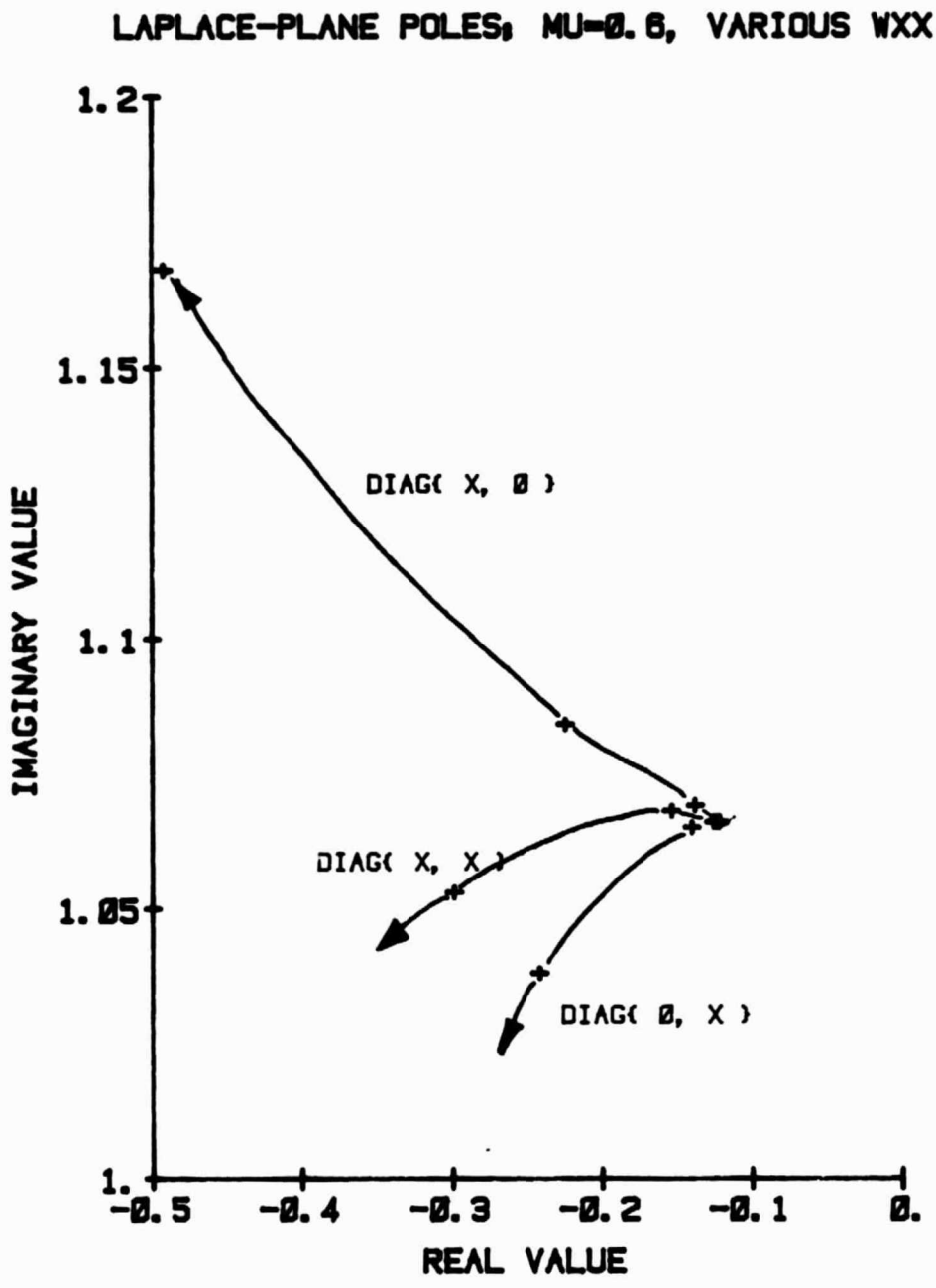

Fig. 3.8a: Laplace-plane poles, mu=0.6, various weightings

ORIGINAL PAGE IS
OF POOR QUALITY

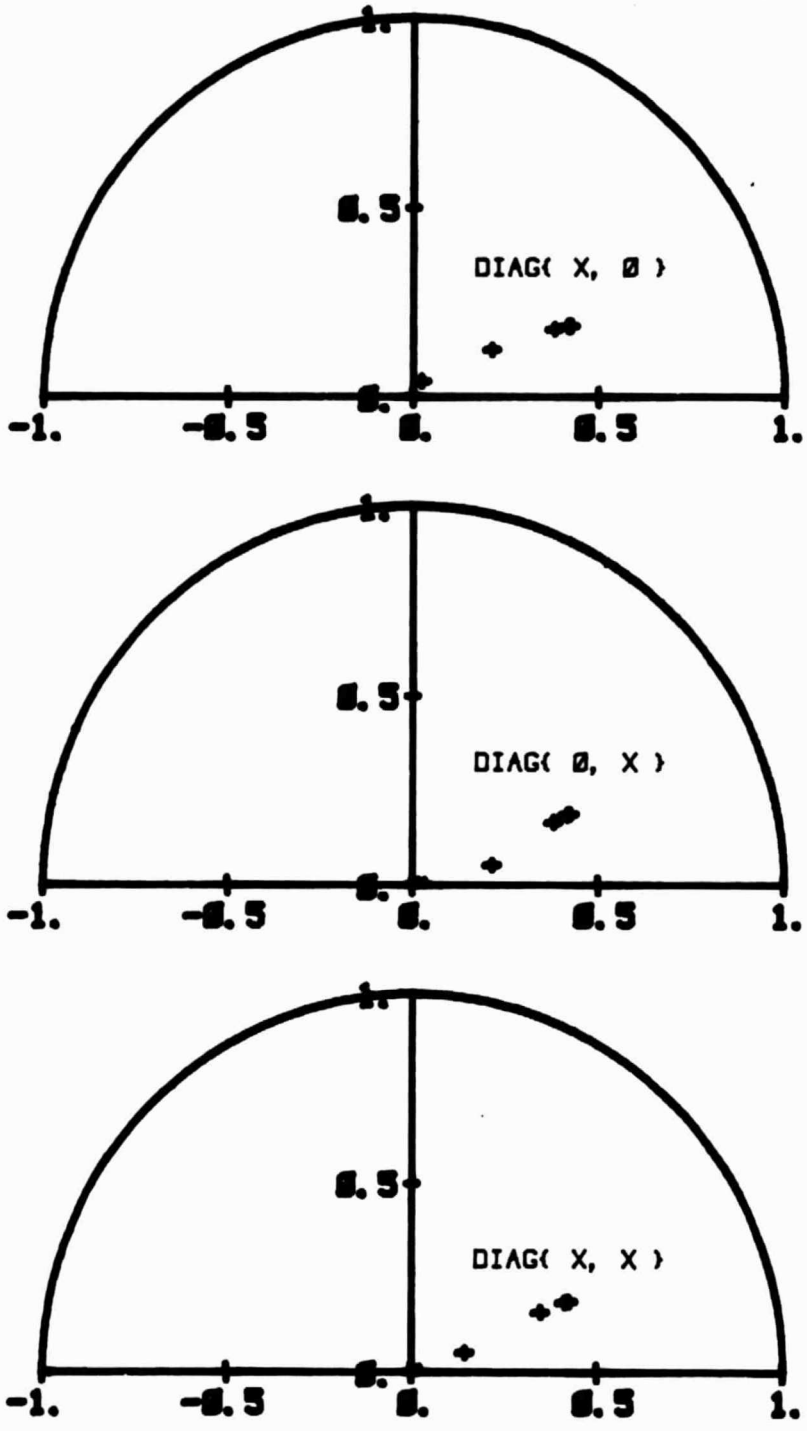

Fig. 3.8b: Floquet-plane poles, mu=0.6, various weightings

ORIGINAL PAGE
OF POOR QUALITY

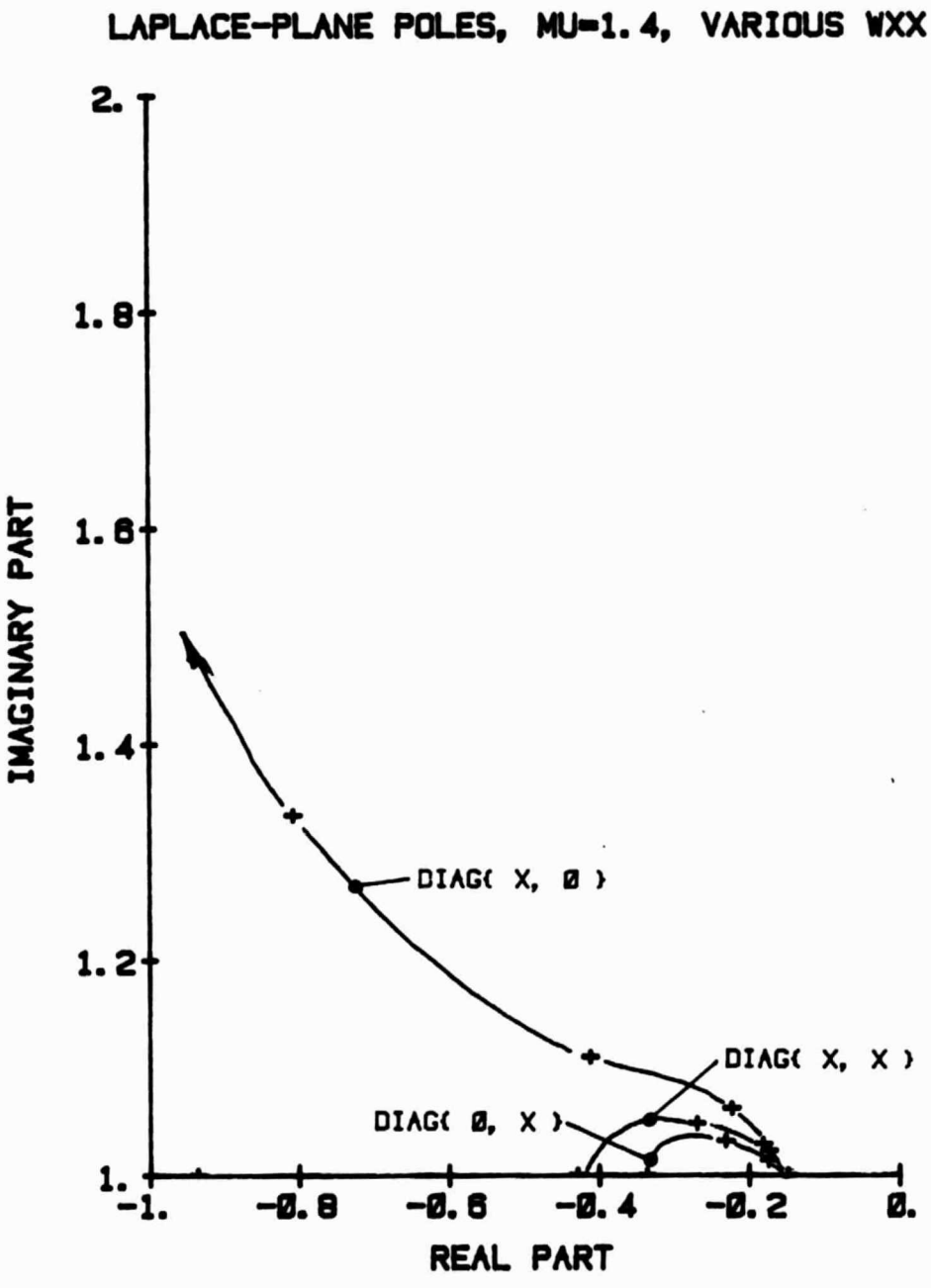

Fig. 3.9a: Laplace-plane poles, mu=1.4, various weightings

ORIGINAL PAGE IS
OF POOR QUALITY

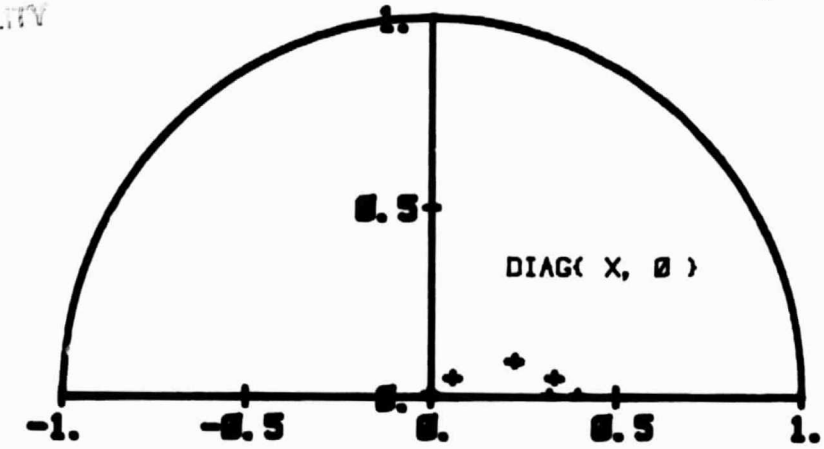

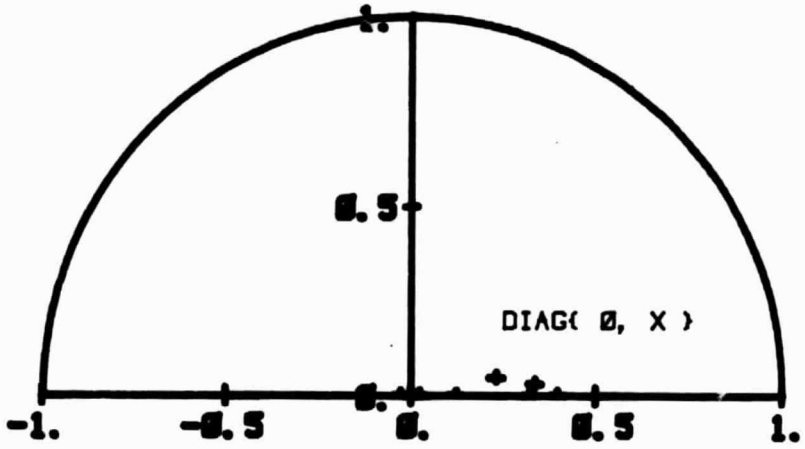

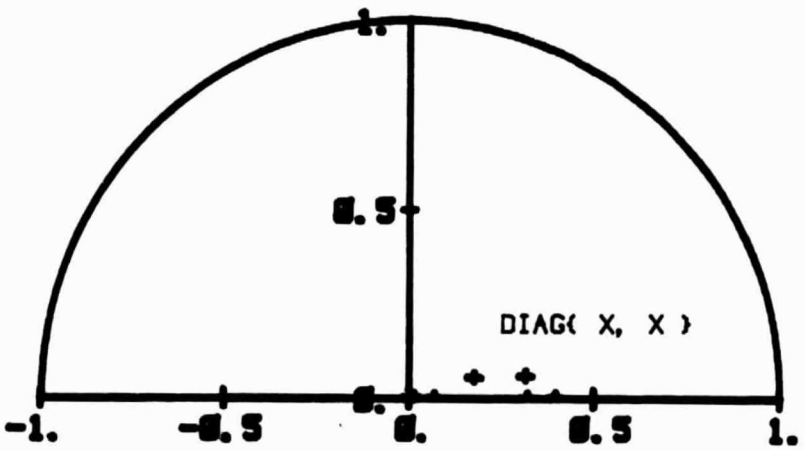

Fig. 3.9b: Floquet-plane poles, mu=1.4, various weightings

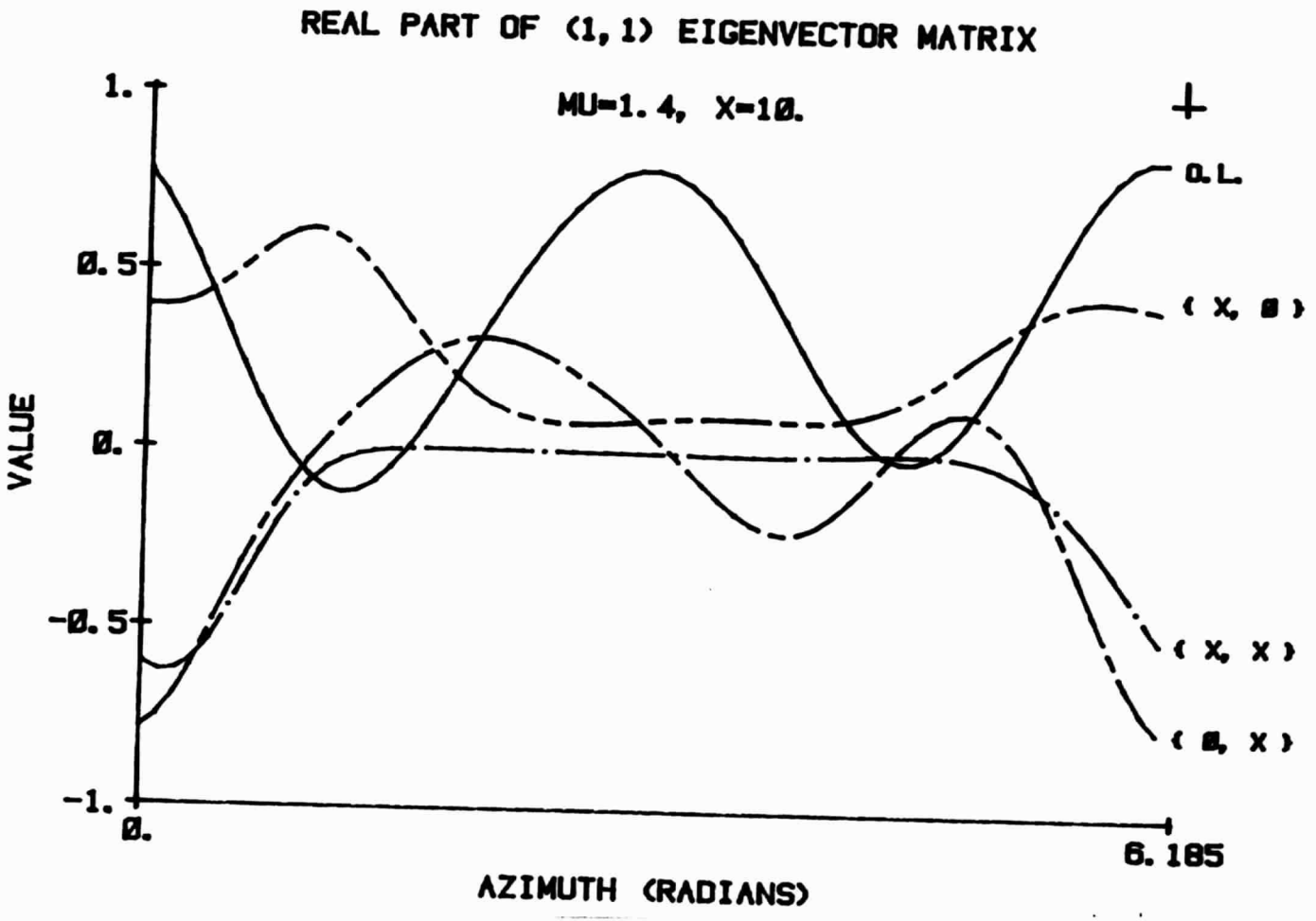

Fig. 3.10a: Real part of eigenvector component, various weighting forms

ORIGINAL PAGE IS
OF POOR QUALITY

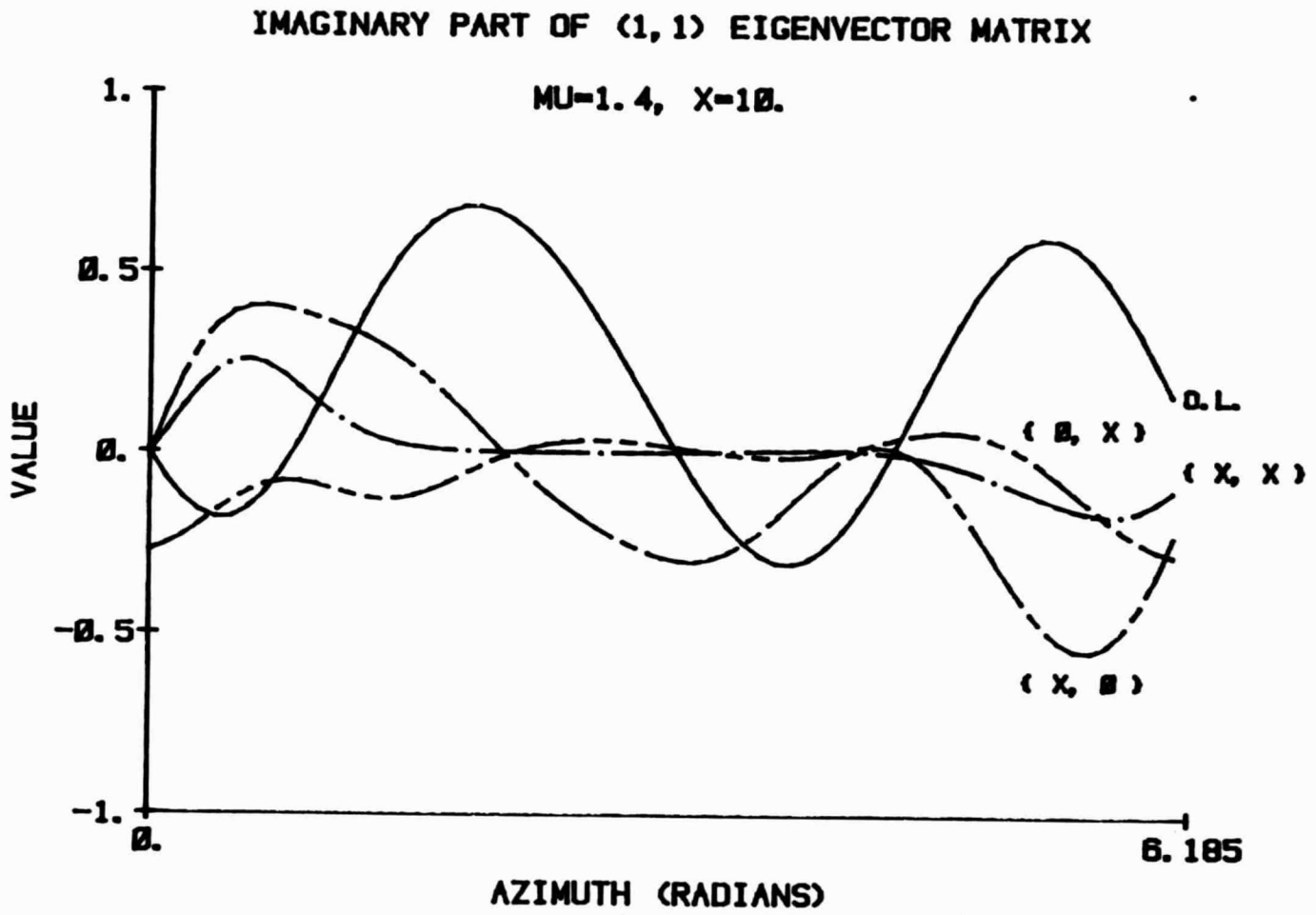

Fig. 3.10b: Imaginary part of eigenvector component various weighting forms

ORIGINAL PAGE IS
OF POOR QUALITY

ORIGINAL PAGE IS
OF POOR QUALITY

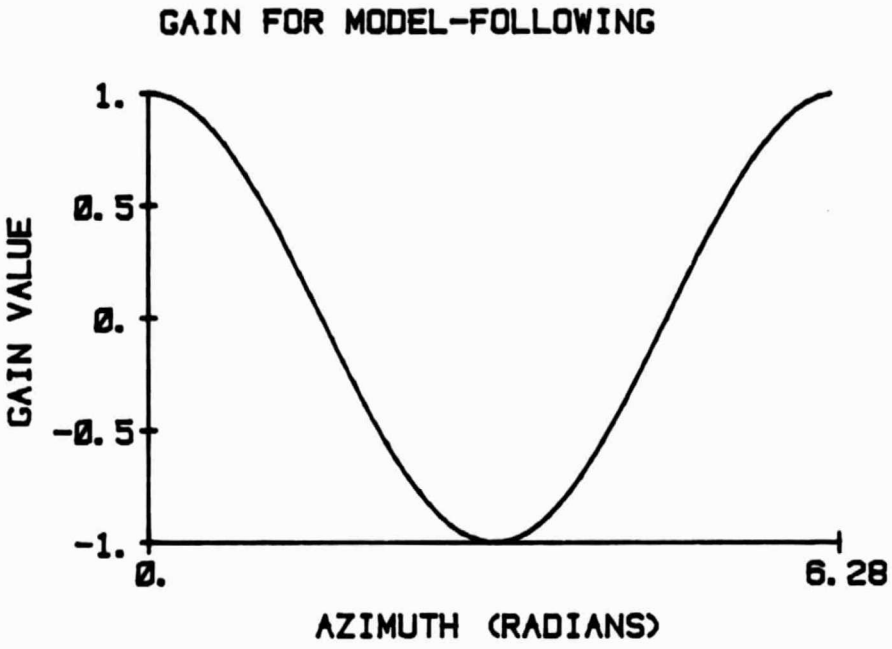

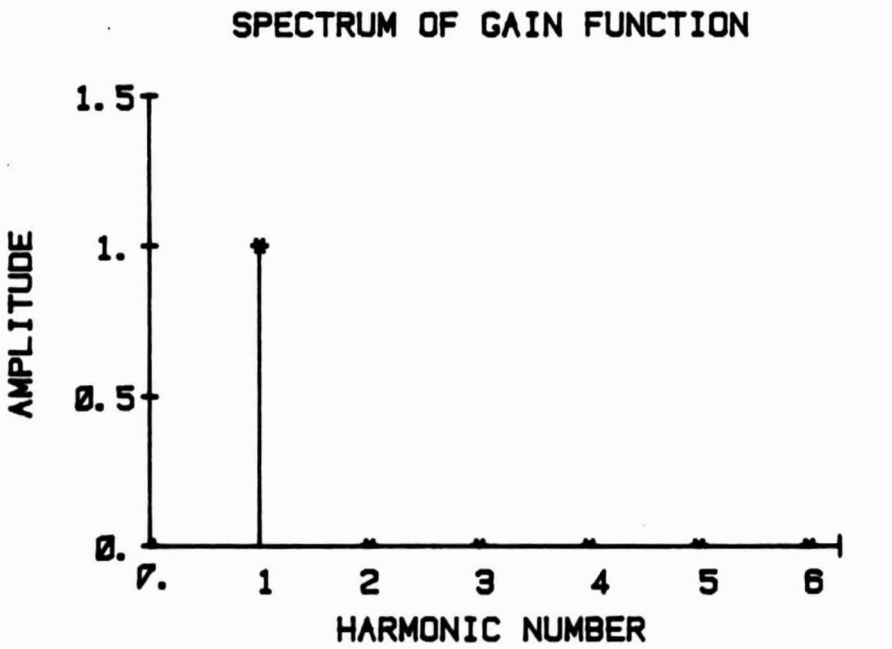

Fig. 3.11: Gain function for scalar model-following ex.

ORIGINAL PAGE IS
OF POOR QUALITY

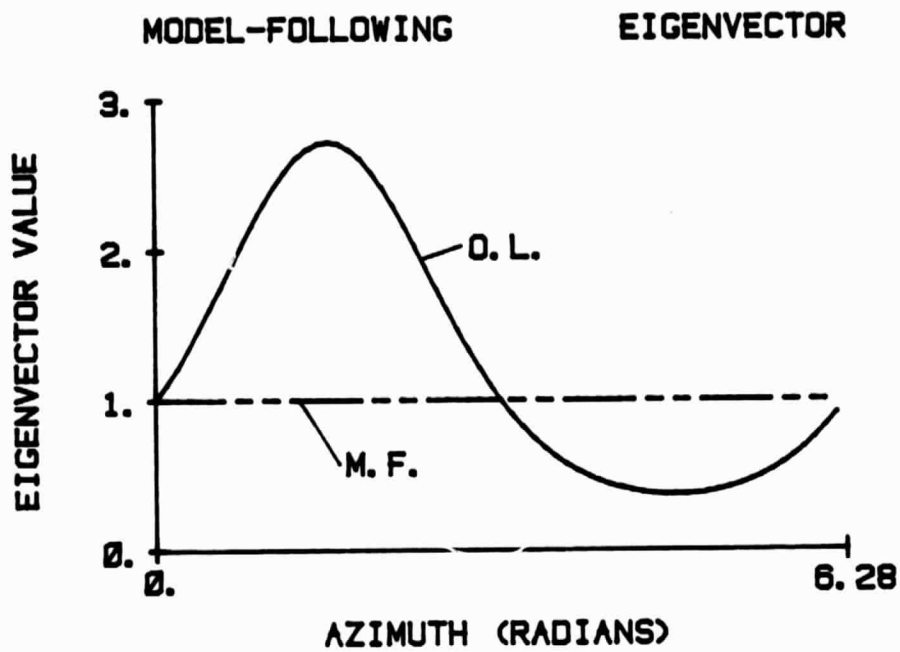

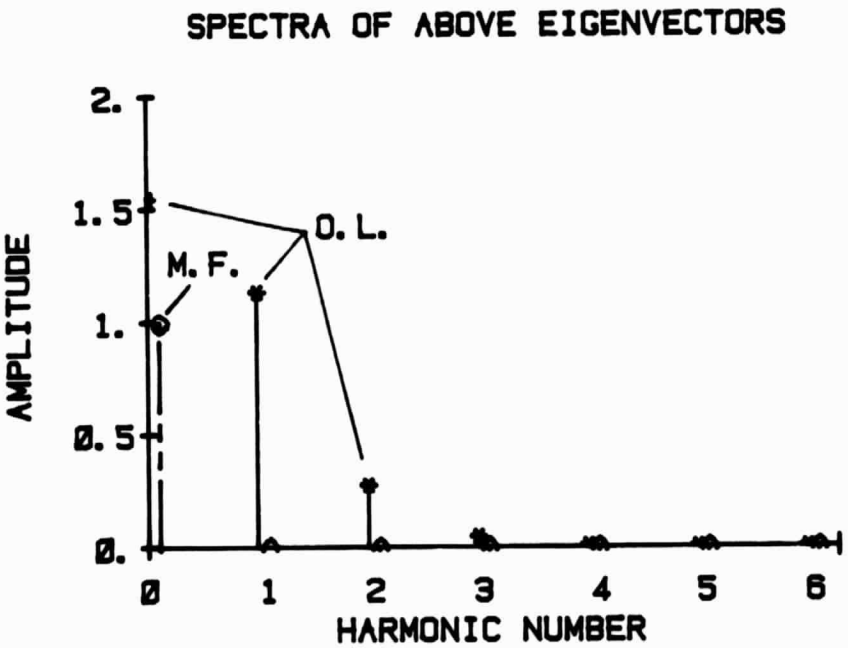

Fig. 3.12: Open- and closed-loop eigenvector for scalar model-following example

ORIGINAL PAGE IS
OF POOR QUALITY

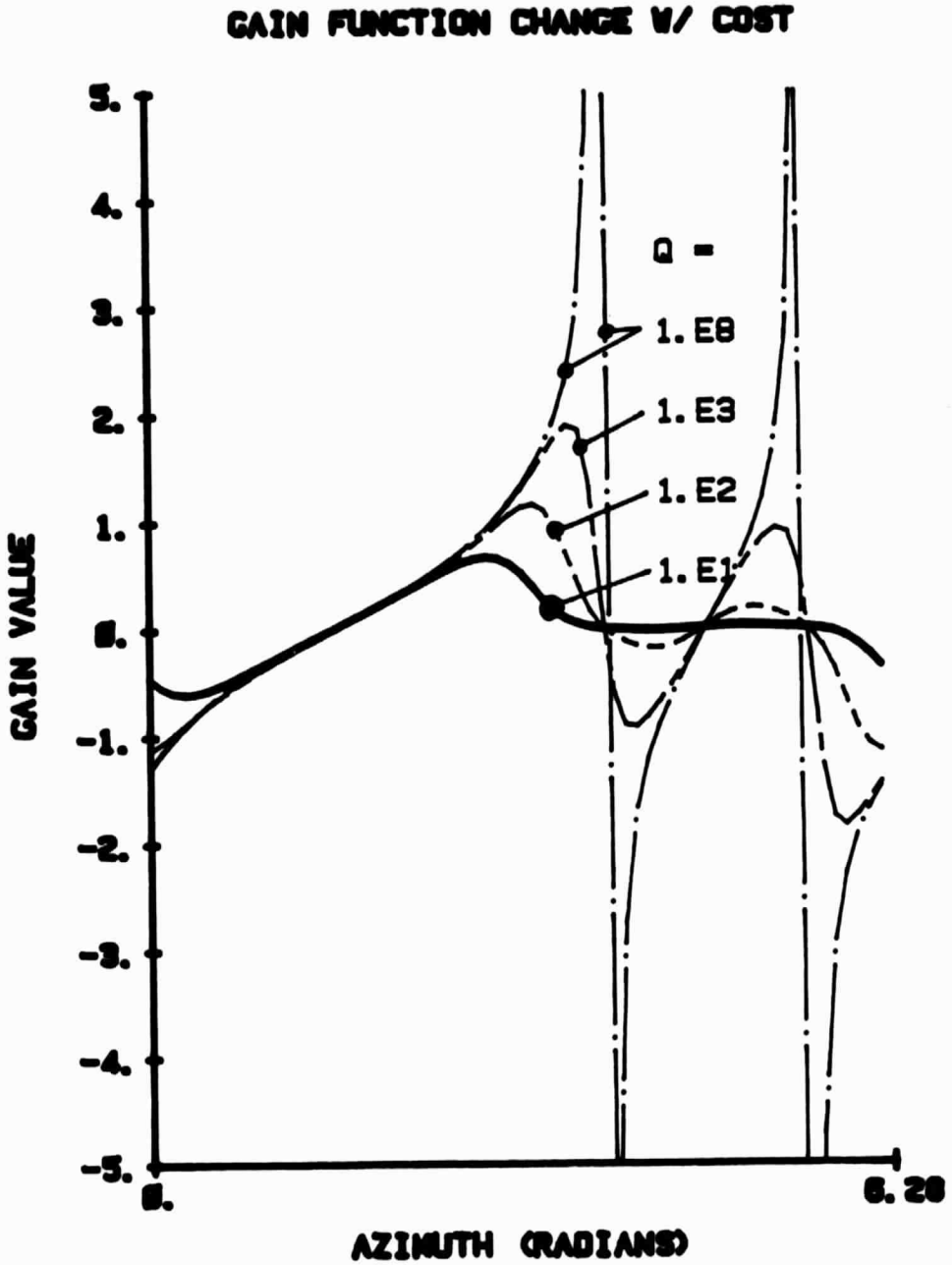

Fig. 3.13: Gain function for various cost values at μ=1.4

ORIGINAL PAGE IS
OF POOR QUALITY

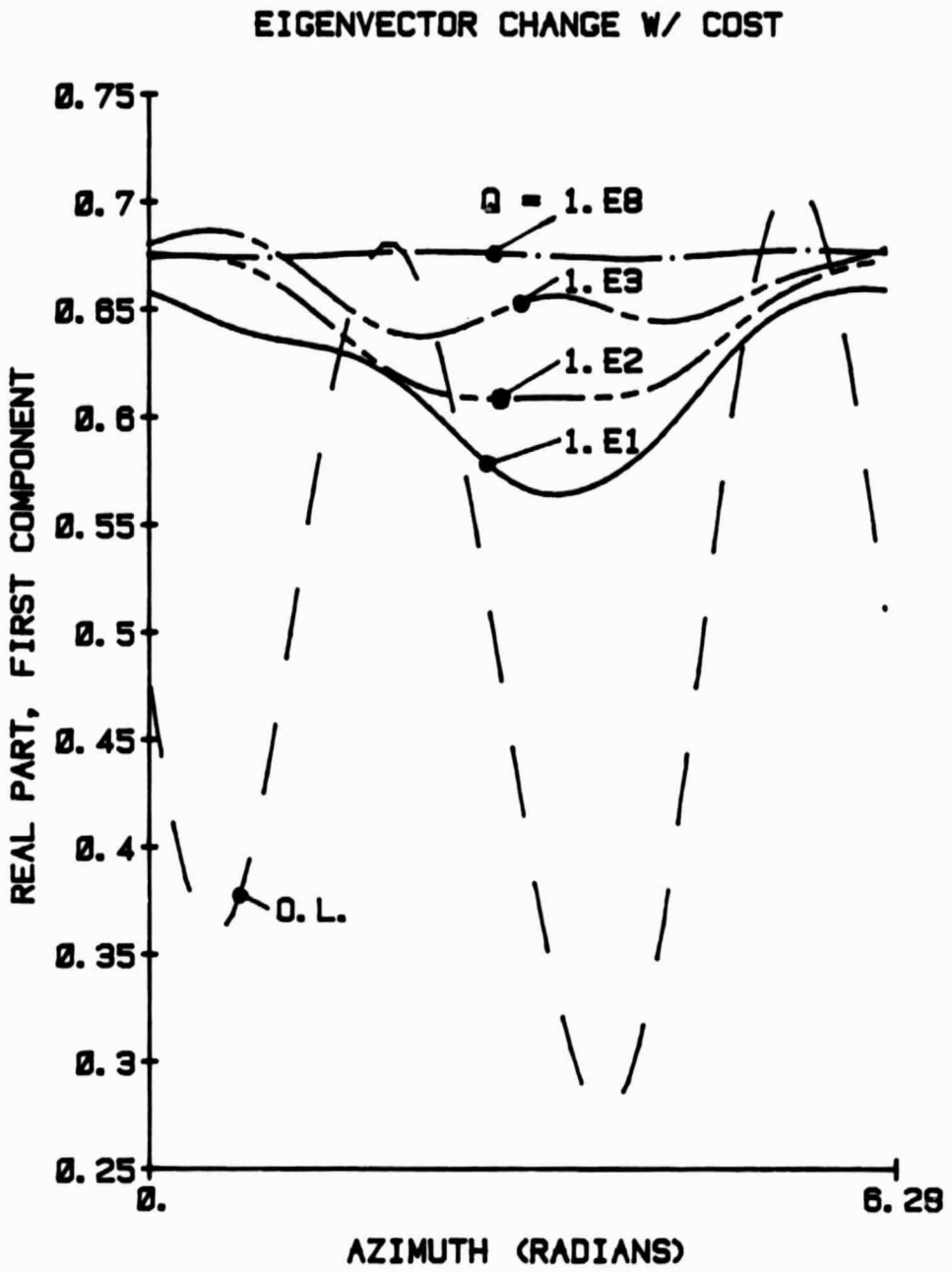

Fig. 3.14: Eigenvector component for μ =1.4 with increasing levels of model-following cost

ORIGINAL PAGE IS
OF POOR QUALITY

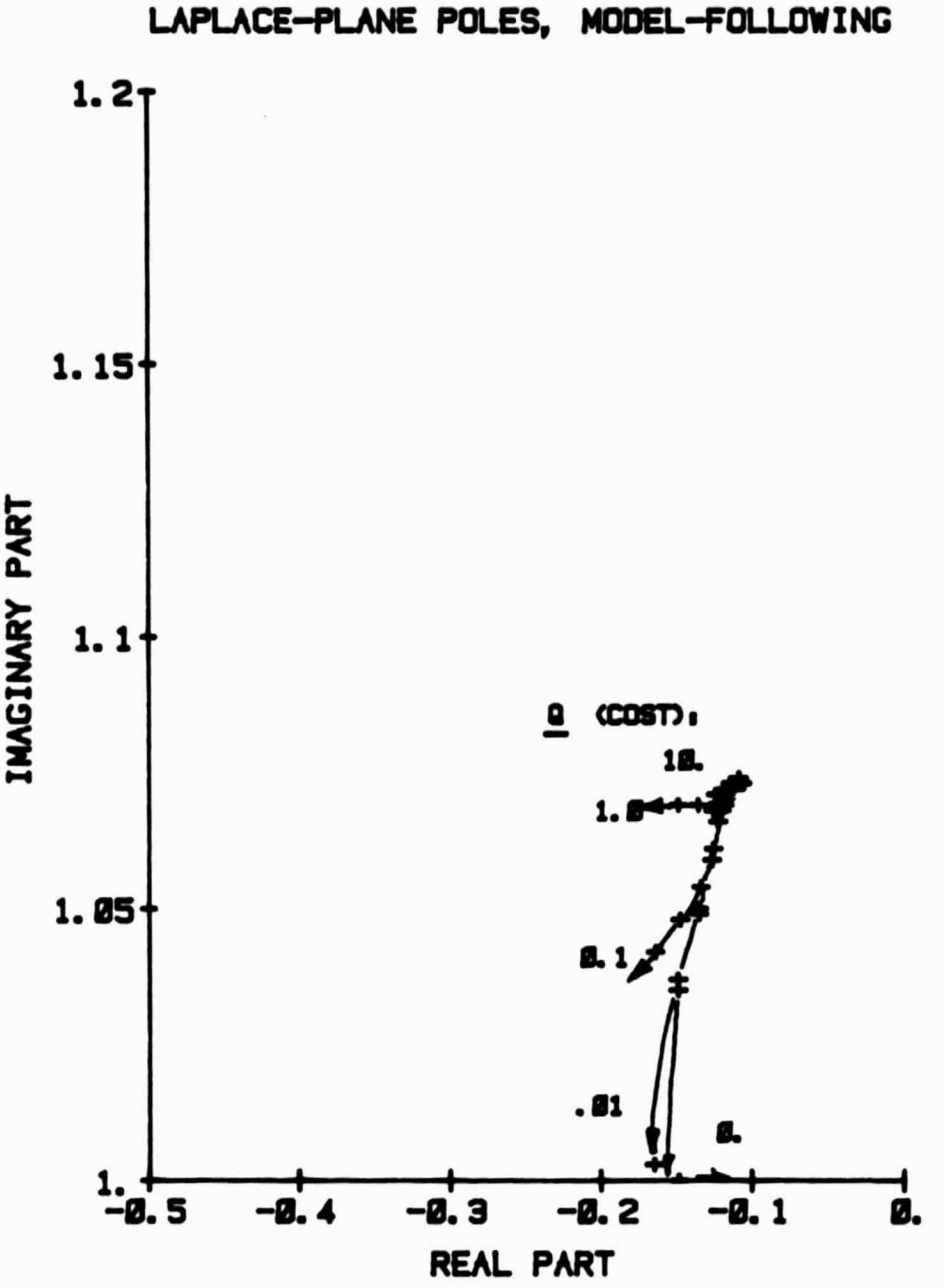

Fig. 3.15a: Laplace-plane root loci for increasing advance ratio at a fixed model-following cost

ORIGINAL PAGE IS
OF POOR QUALITY

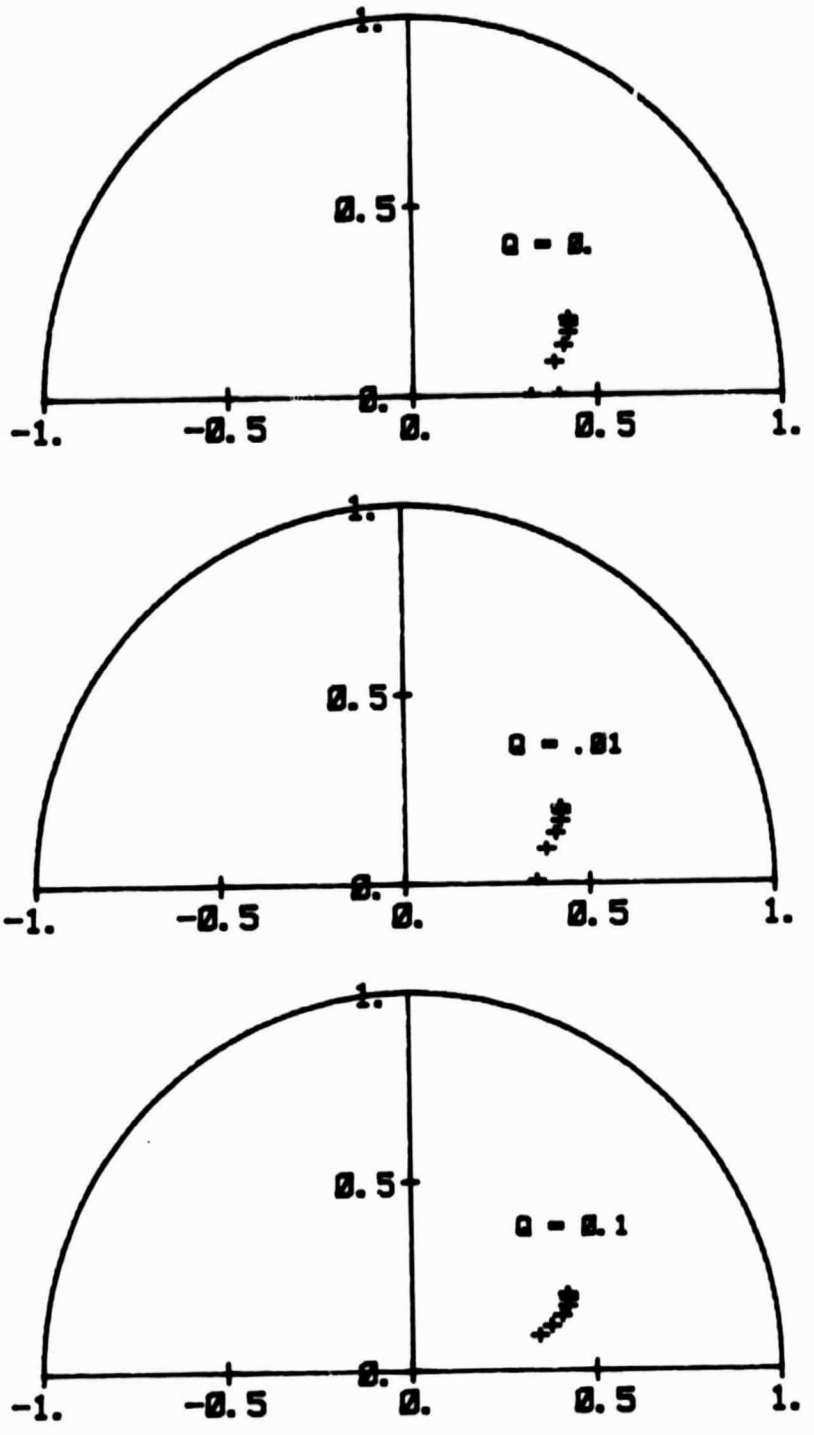

Fig. 3.15b: Floquet-plane root loci for increasing advance ratio at a fixed model-following cost

ORIGINAL PAGE IS
OF POOR QUALITY

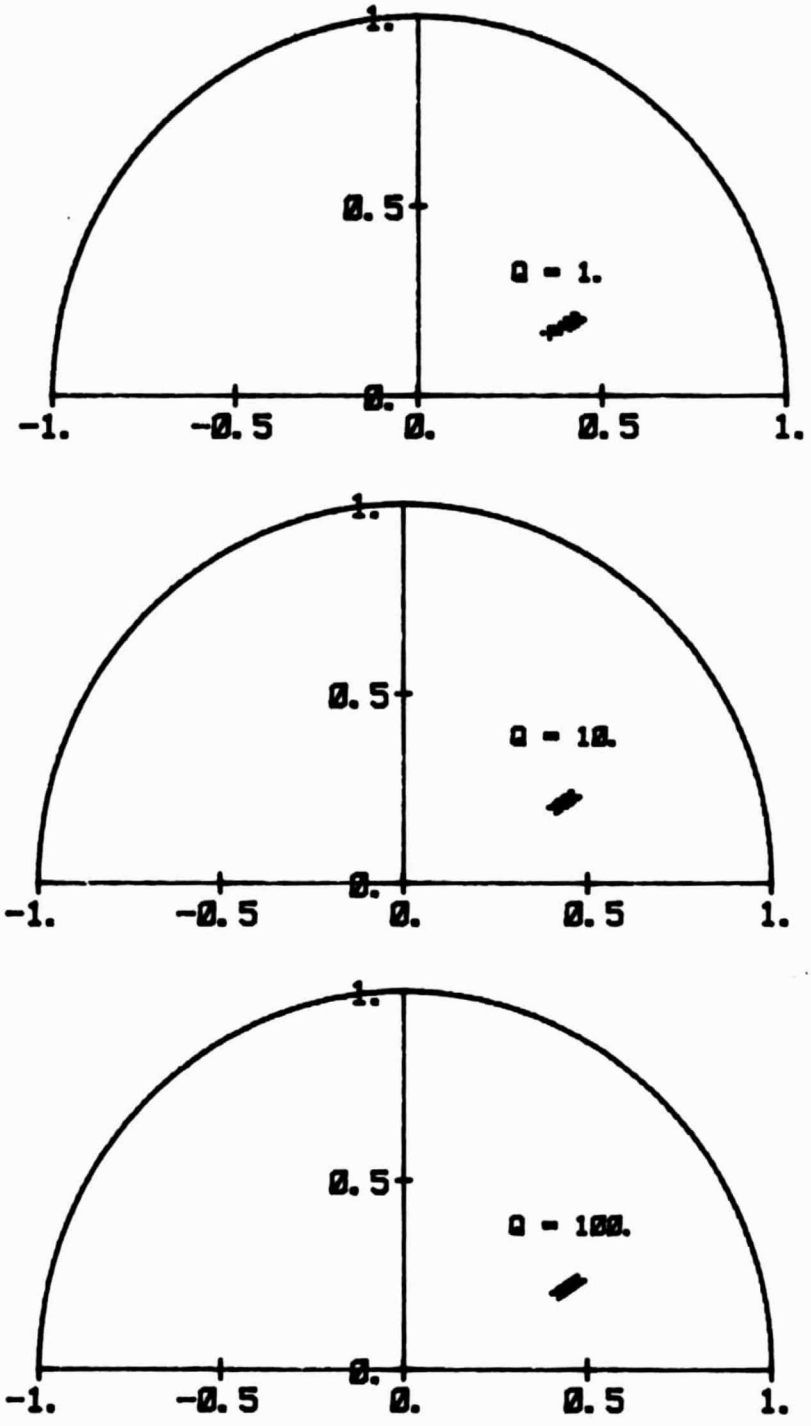

Fig. 3.15c: Floquet-plane root loci for increasing advance ratio at a fixed model-following cost

ORIGINAL PAGE IS
OF POOR QUALITY

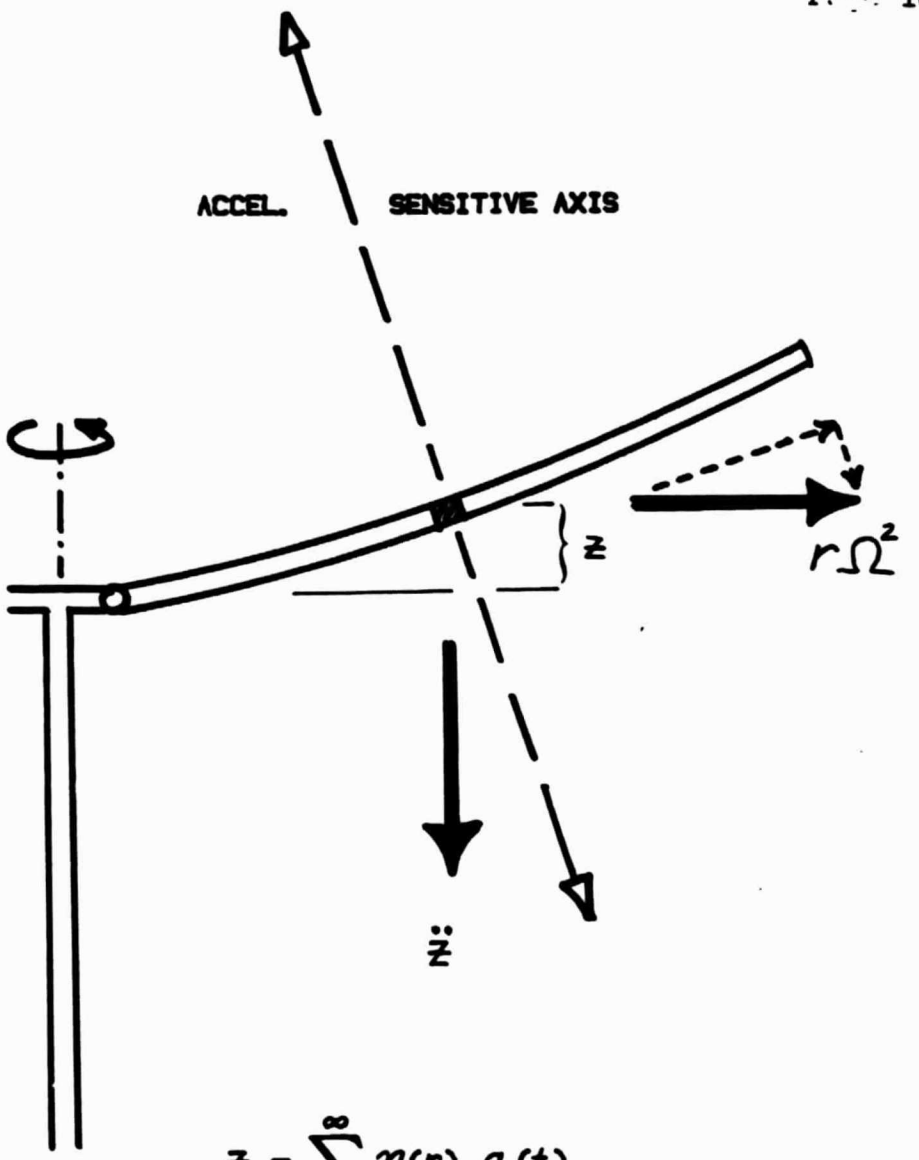

$$z = \sum_{K=1}^{\infty} \eta_K(r)\, q_K(t)$$

$$\text{ACCEL} = \sum_{K=1}^{\infty} \left\{ \eta_K \ddot{q}_K + r\Omega^2 \frac{d}{dr}\eta_K q_K \right\}$$

Fig. 4.1: Sensor dynamics for tip accelerometer

ORIGINAL PAGE IS
OF POOR QUALITY

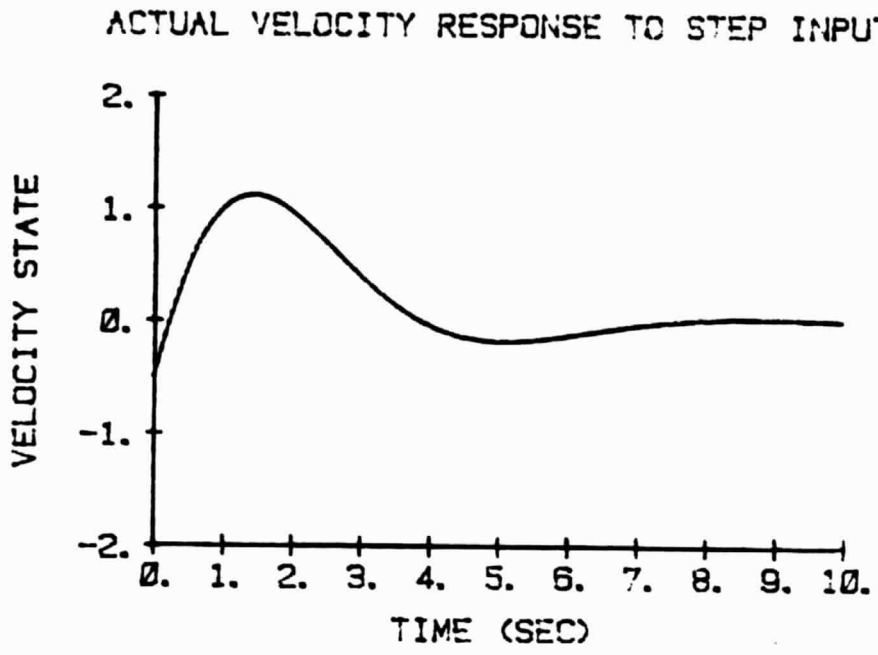

Fig. 4.2a: Velocity state of digital simulation

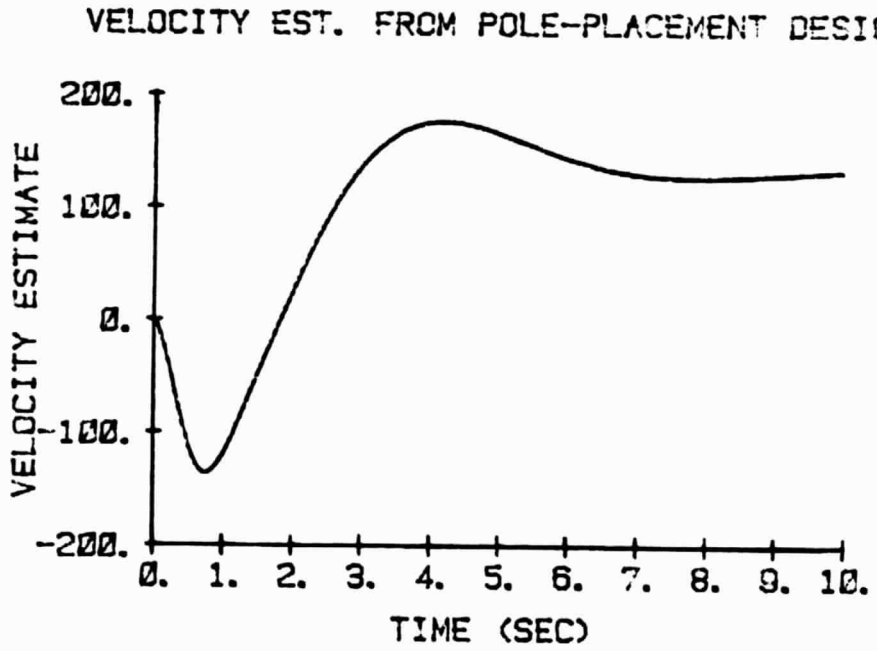

Fig. 4.2b: Velocity estimate using pole-placement

ORIGINAL PAGE IS
OF POOR QUALITY

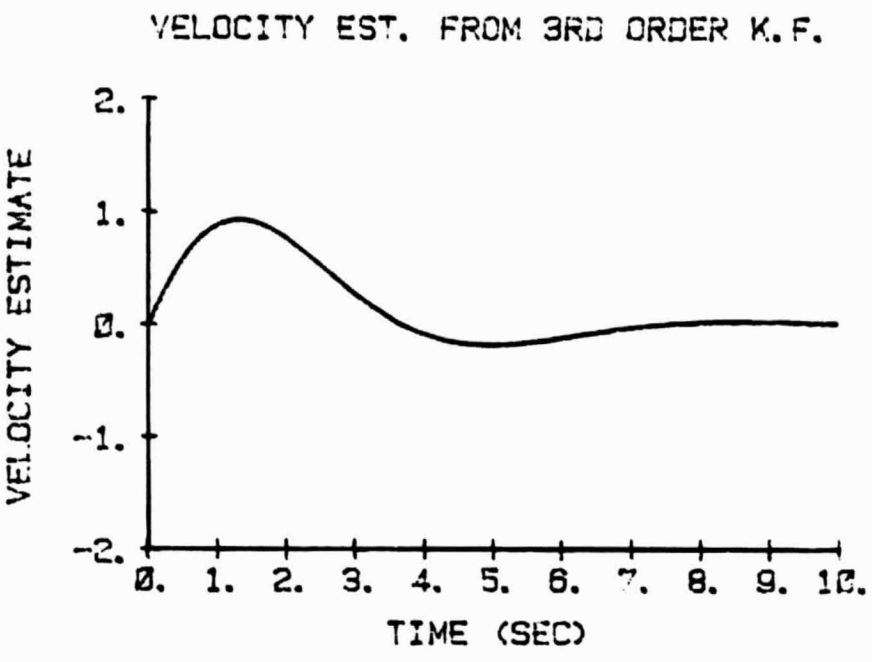

Fig. 4.2c: Velocity estimate using third-order Kalman Filter

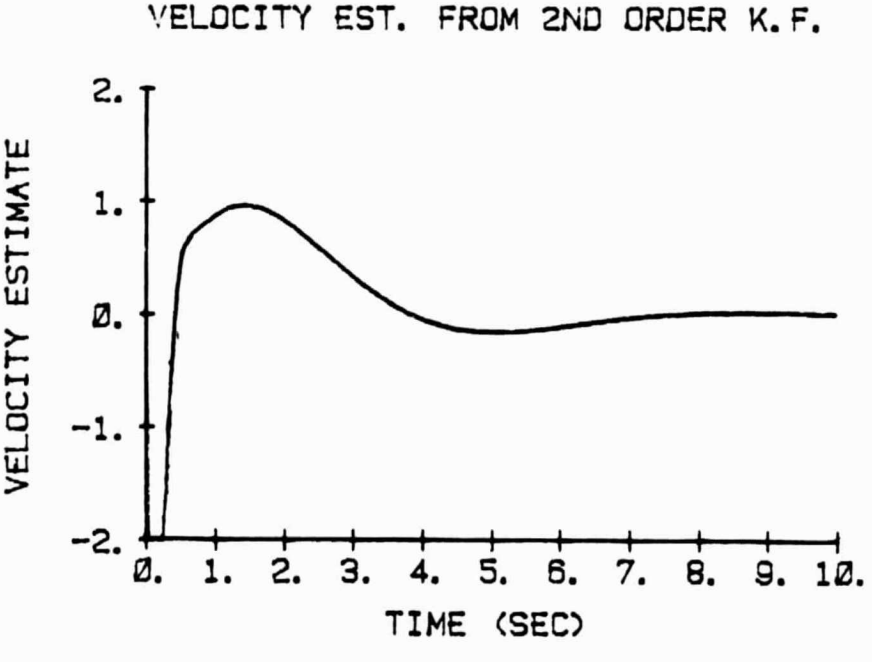

Fig. 4.2d: Estimated velocity using second-order Kalman Filter

ORIGINAL PAGE IS
OF POOR QUALITY

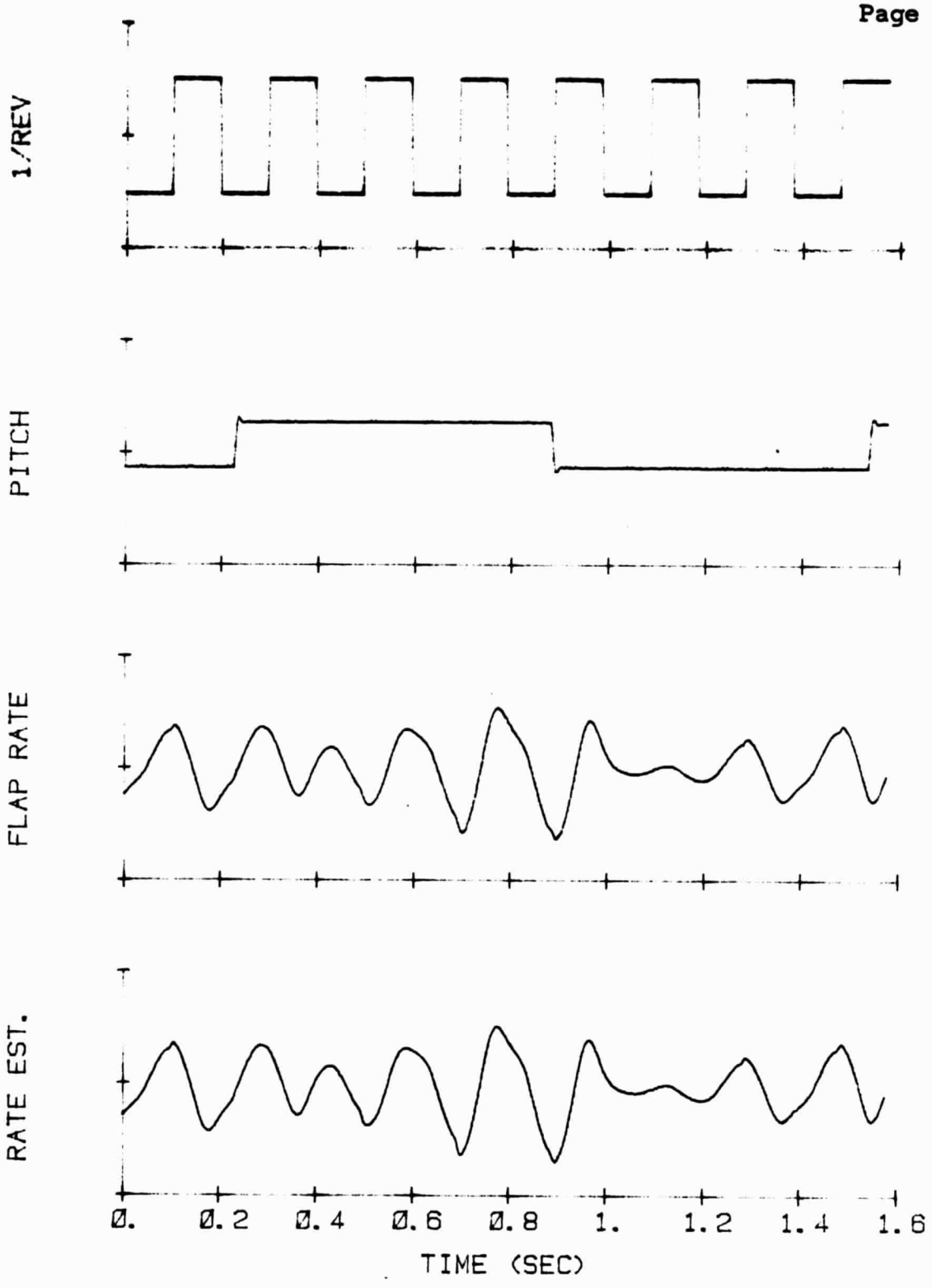

Fig. 4.3: Comparison of actual and estimated flapping rate estimate for analog simulation, μ =1.14

ORIGINAL PAGE IS
OF POOR QUALITY

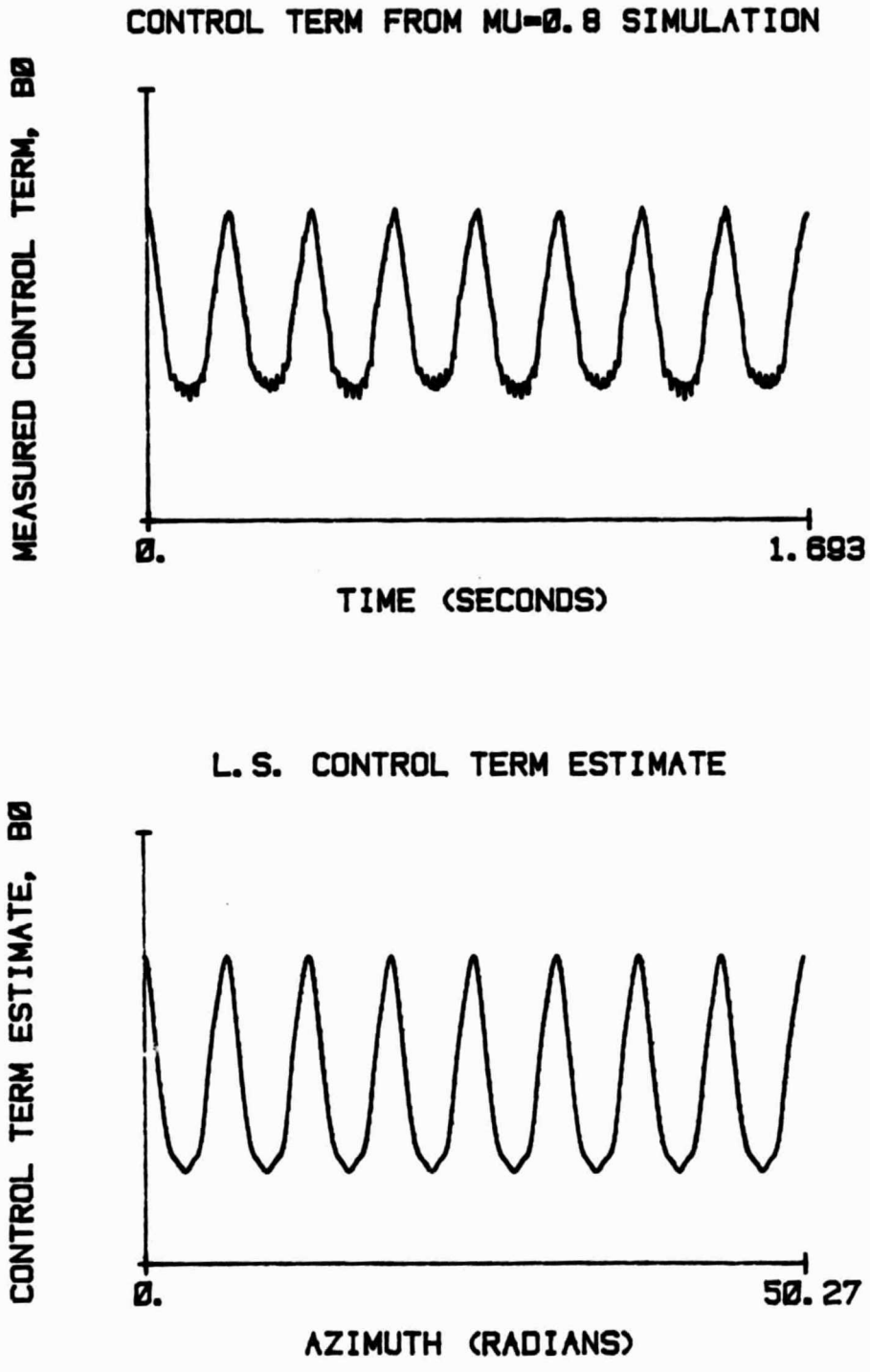

Fig. 4.4a: Comparison of actual and estimated periodic control term from parameter regression

ORIGINAL PAGE IS
OF POOR QUALITY

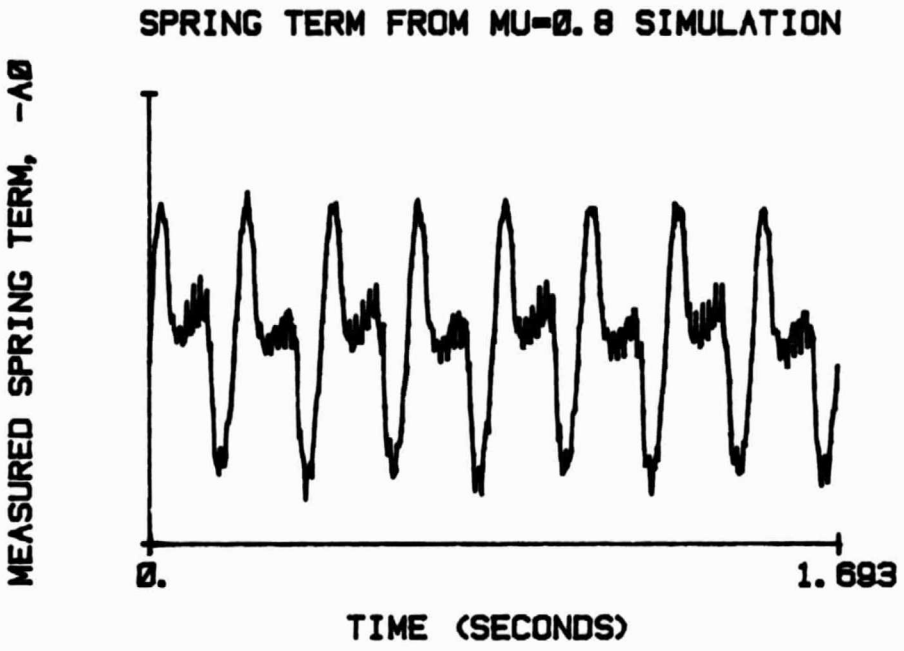

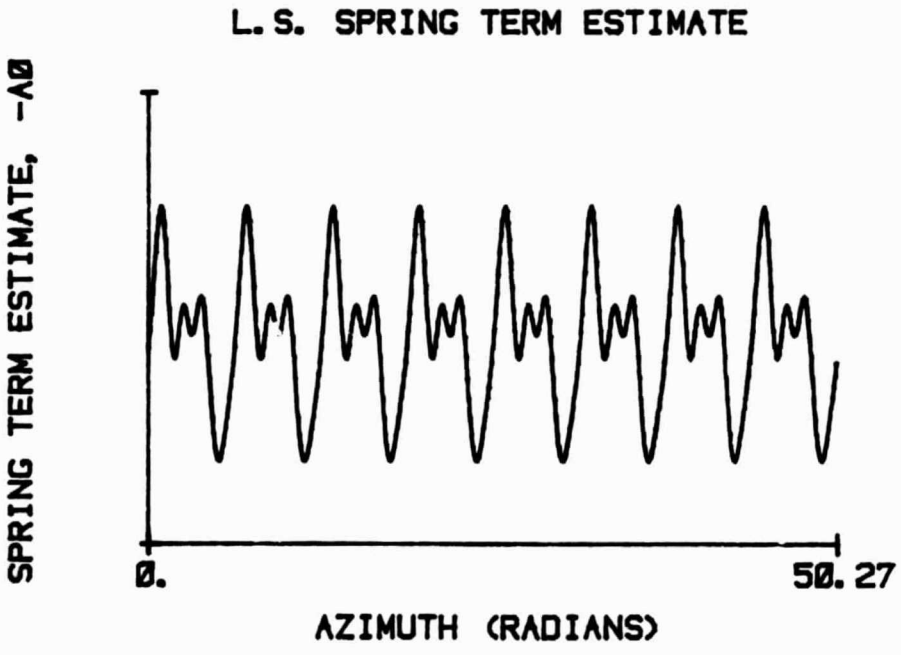

Fig. 4.4b: Comparison of actual and estimated periodic spring term from parameter regression

ORIGINAL PAGE IS
OF POOR QUALITY

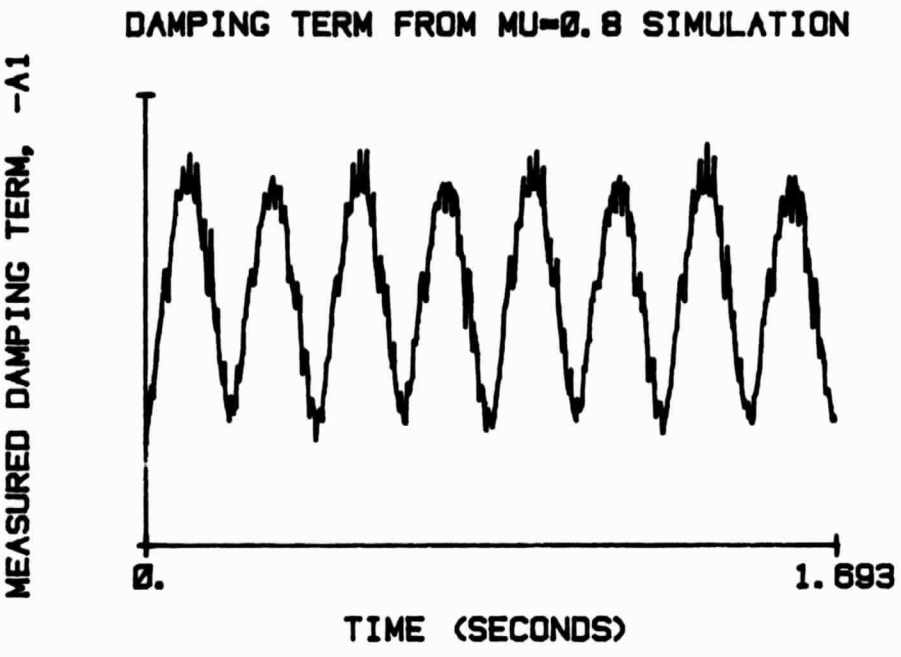

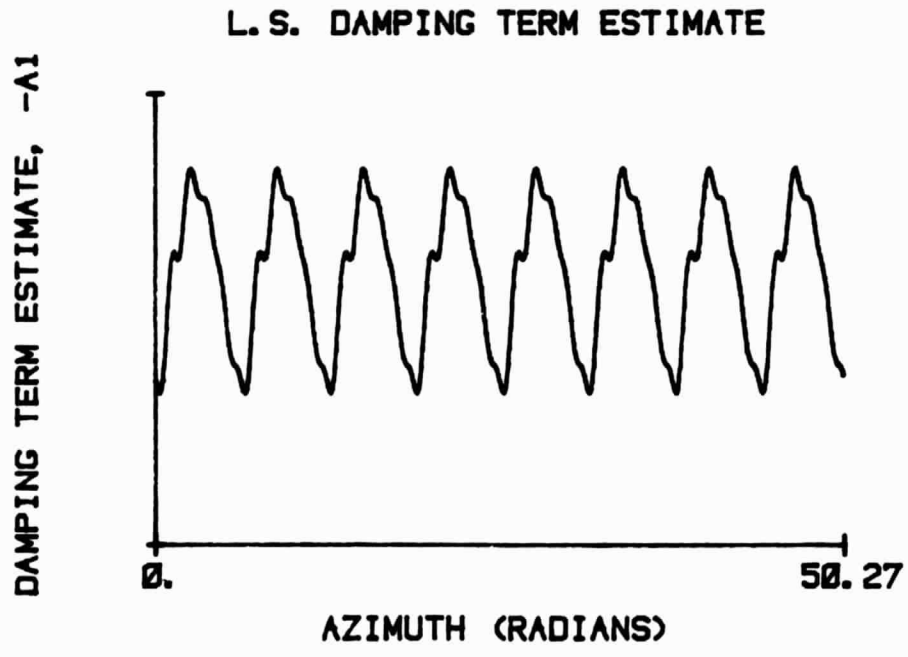

Fig. 4.4c: Comparison of actual and estimated periodic damping term from parameter regression

ORIGINAL PAGE IS
OF POOR QUALITY

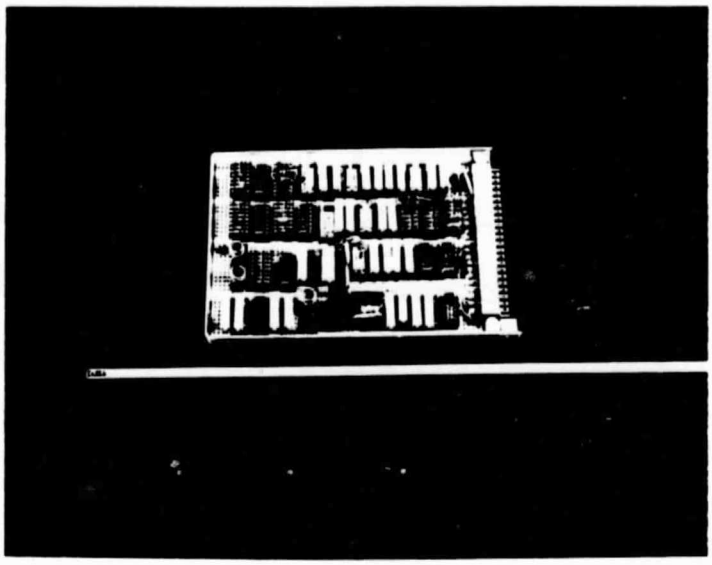

Fig. 5.1: Photograph of analog computer simulation card

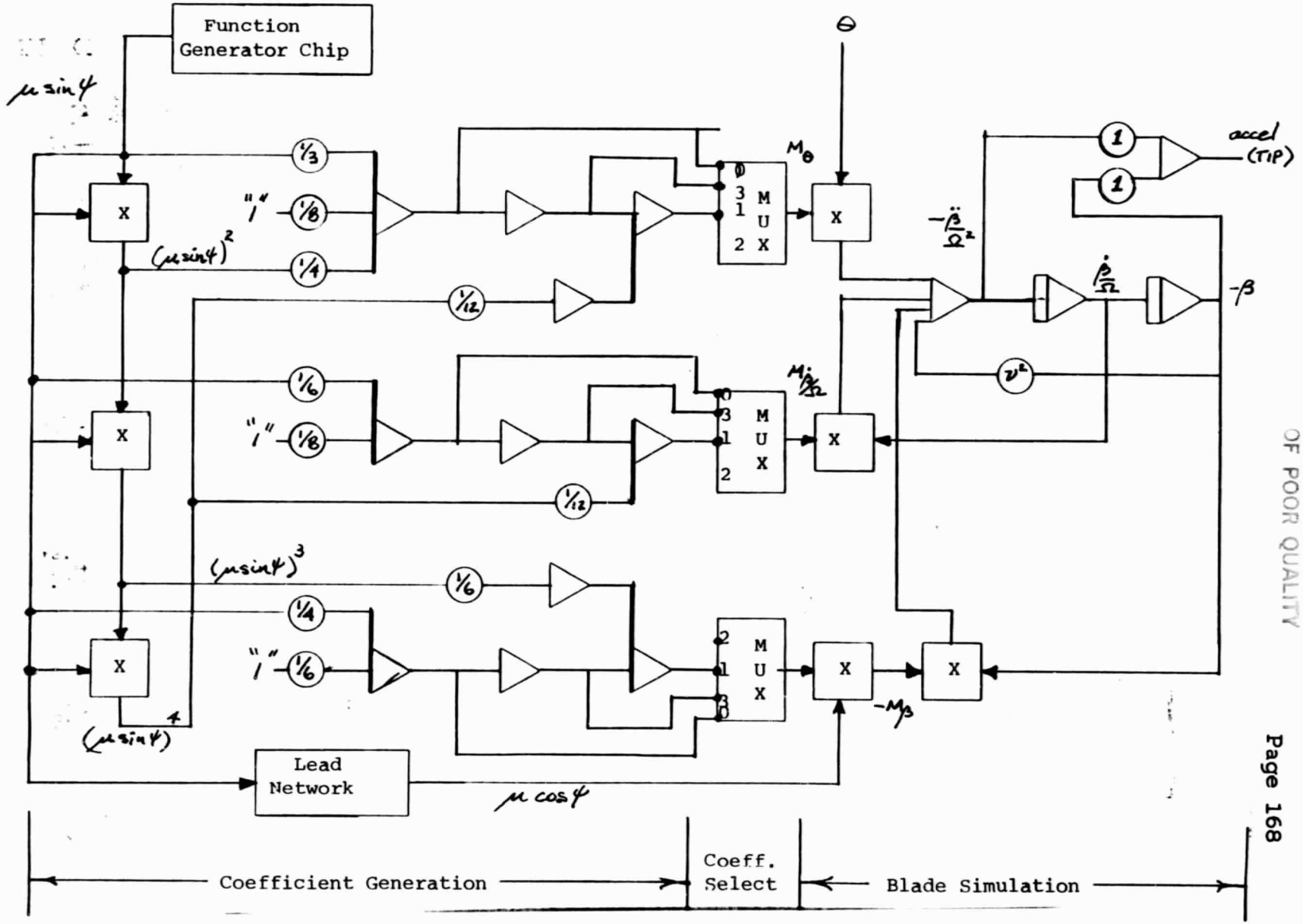

Fig. 5.2: Functional block diagram of analog simulation

ORIGINAL PAGE IS OF POOR QUALITY

ORIGINAL PAGE IS
OF POOR QUALITY

Fig. 5.3: Model rotor blade specifications

γ = 3.01 Section = NACA 0012 *8 deg linear twist

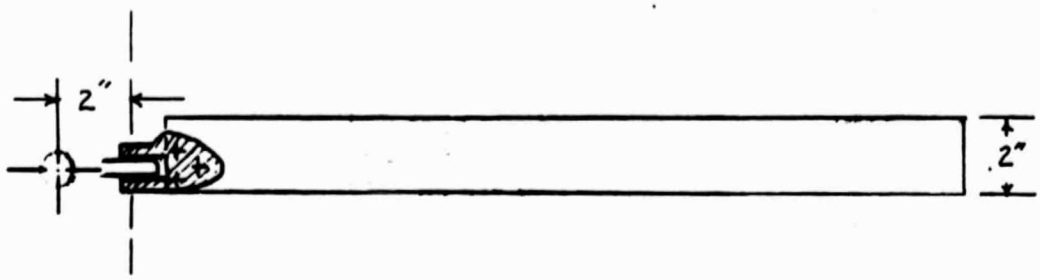

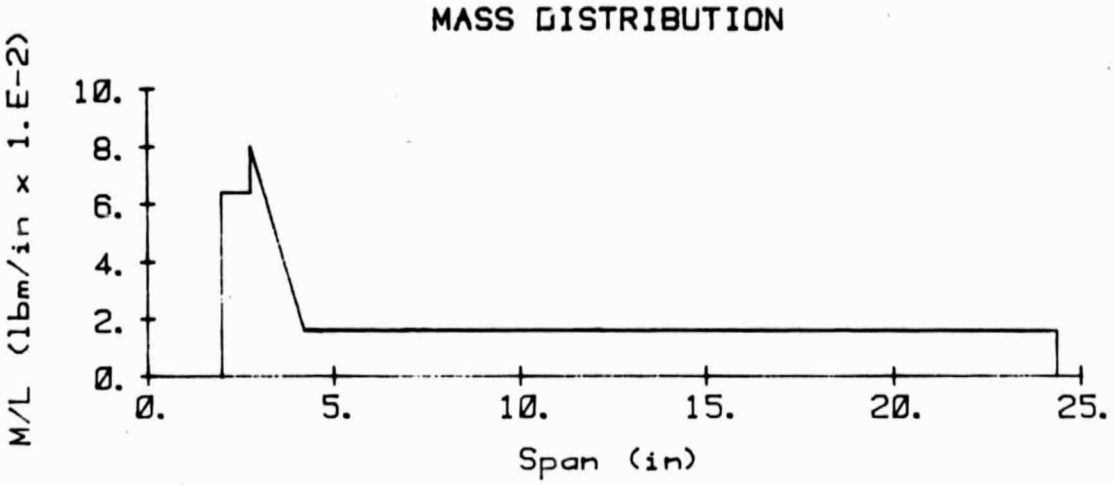

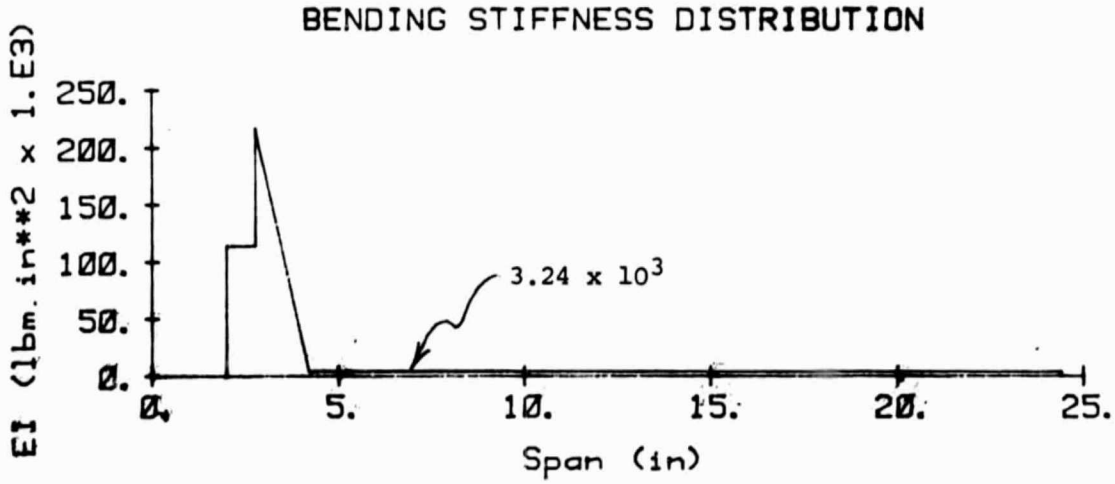

ORIGINAL PAGE
OF POOR QUALITY

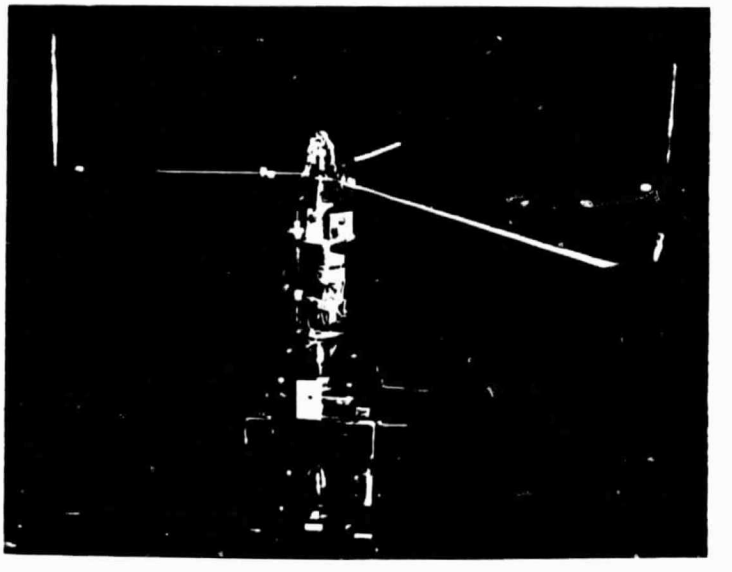

Fig. 5.4: IBC model rotor installed in acoustic tunnel

ORIGINAL PAGE IS
OF POOR QUALITY

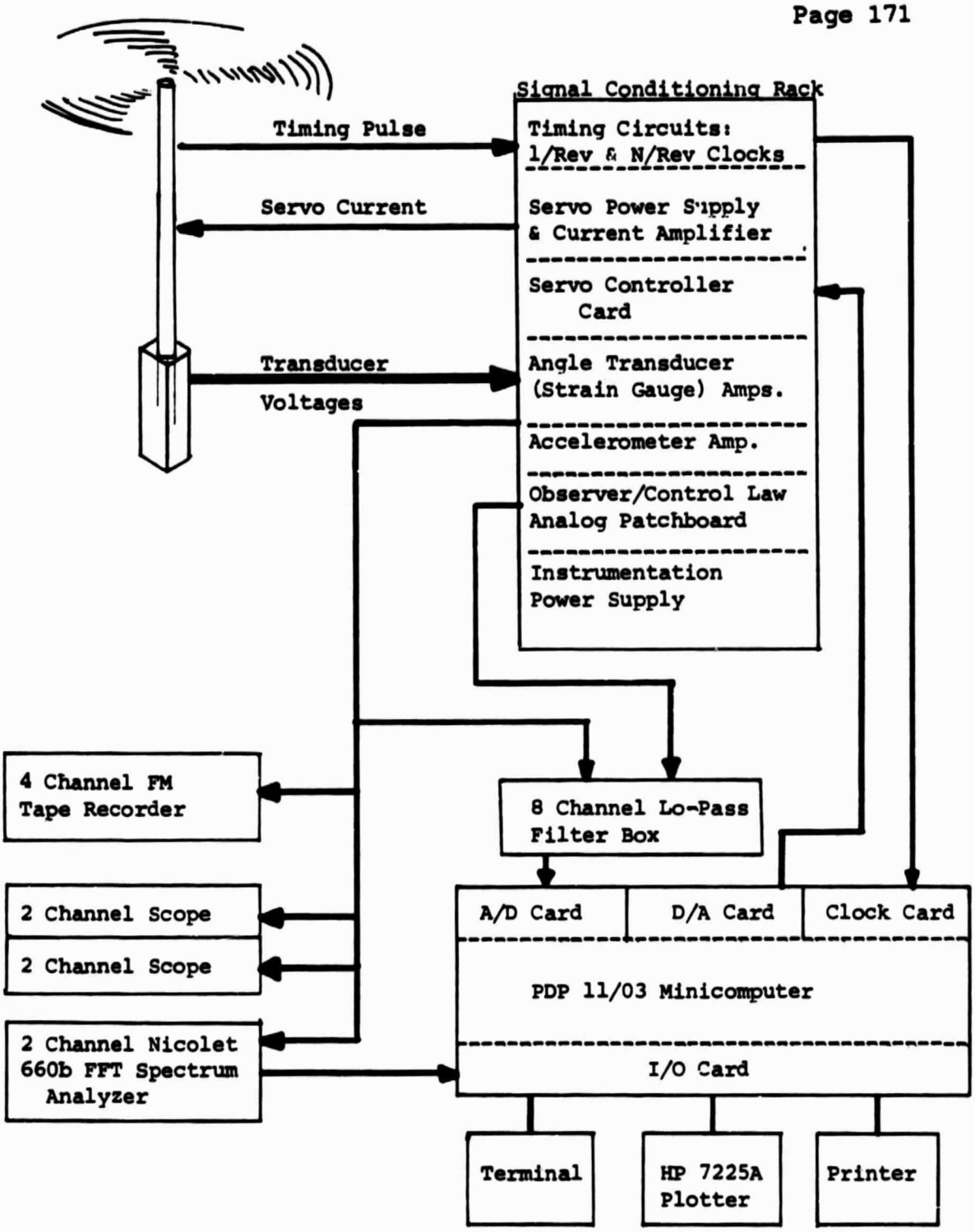

Fig. 5.5: Instrumentation schematic for data collection

ORIGINAL PAGE IS
OF POOR QUALITY

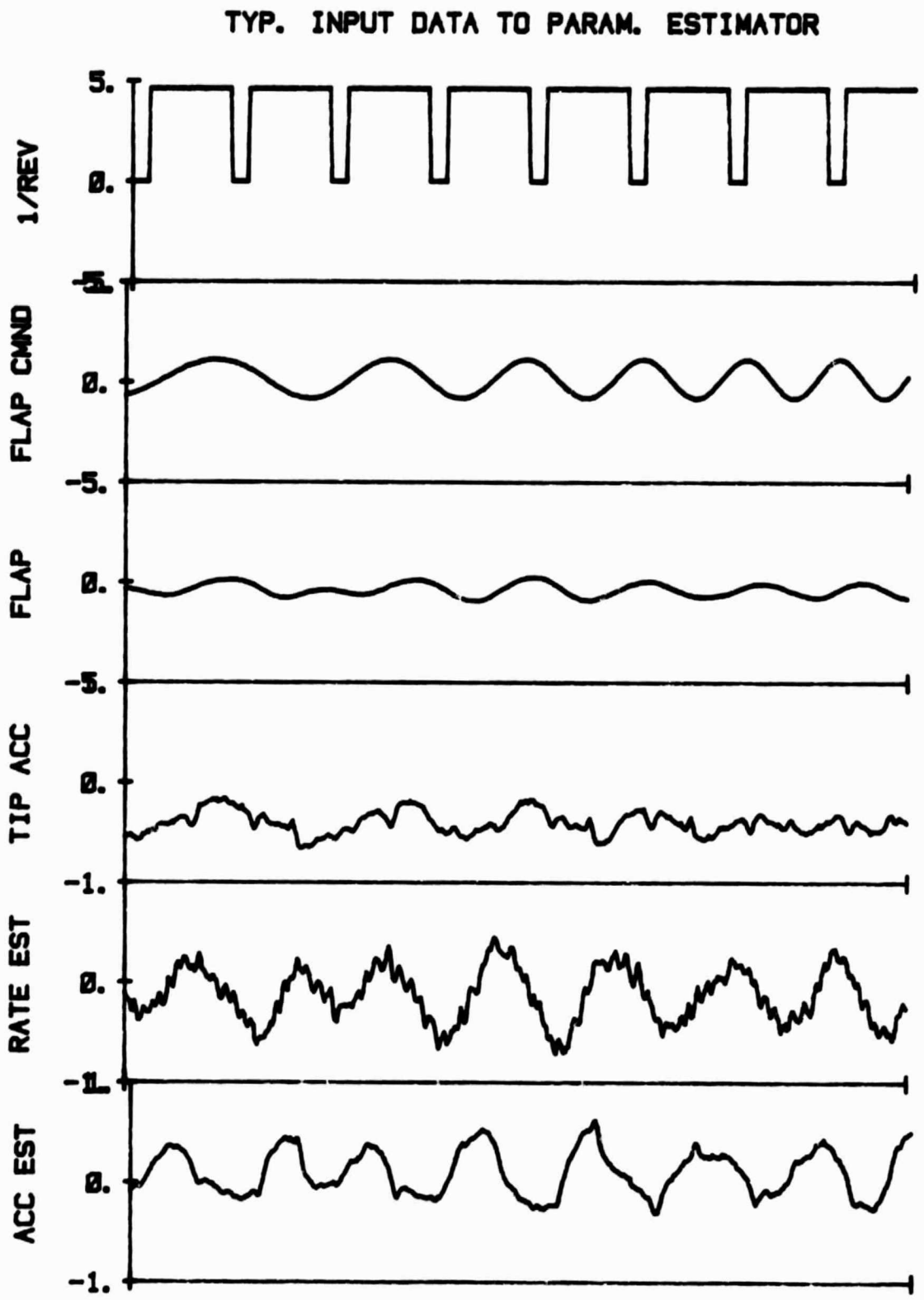

Fig. 6.1: Typical data set for parameter identification

ORIGINAL PAGE IS
OF POOR QUALITY

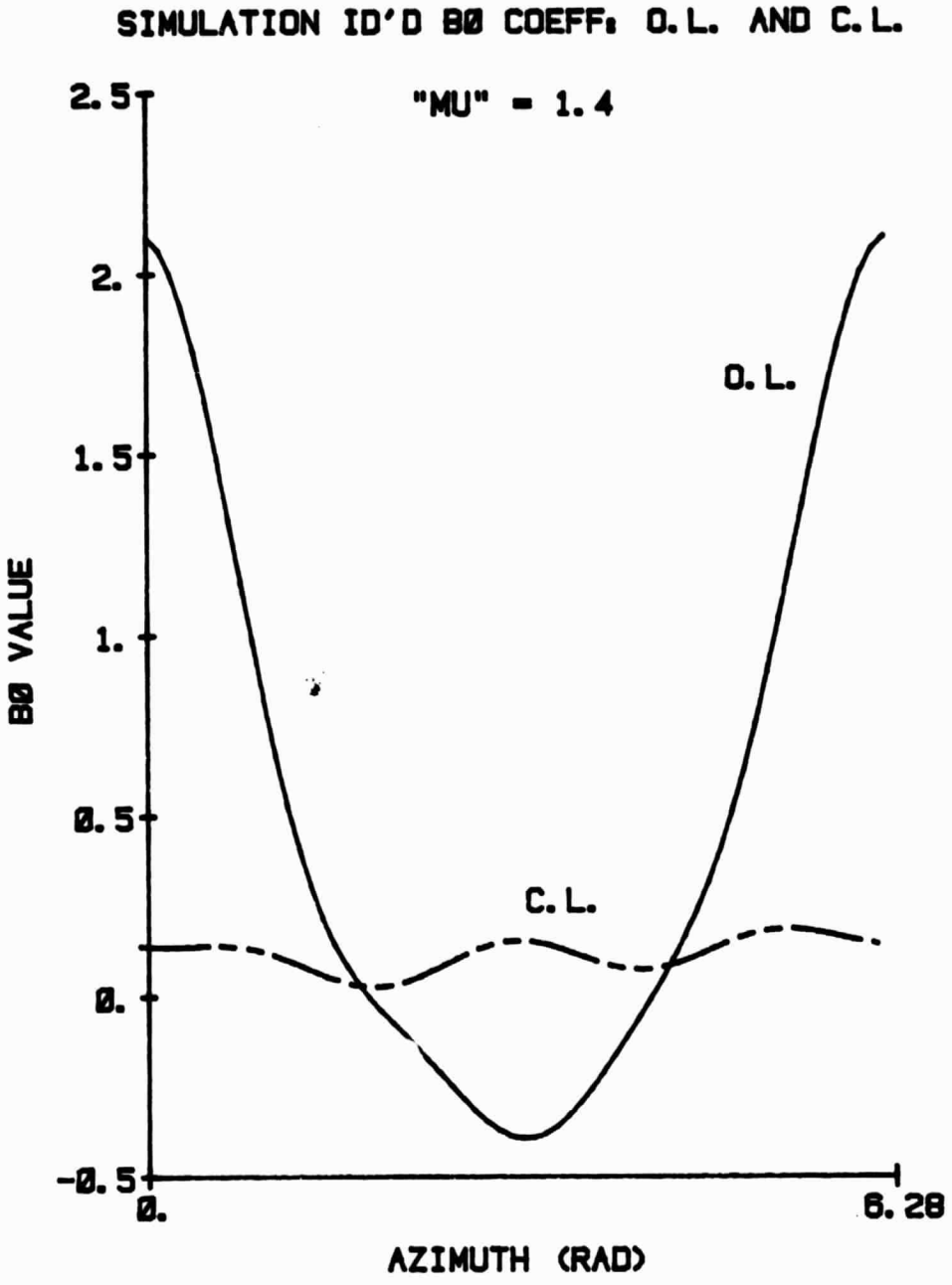

Fig. 6.2a: Estimated control power for simulation, open- and closed-loop

ORIGINAL PAGE IS
OF POOR QUALITY

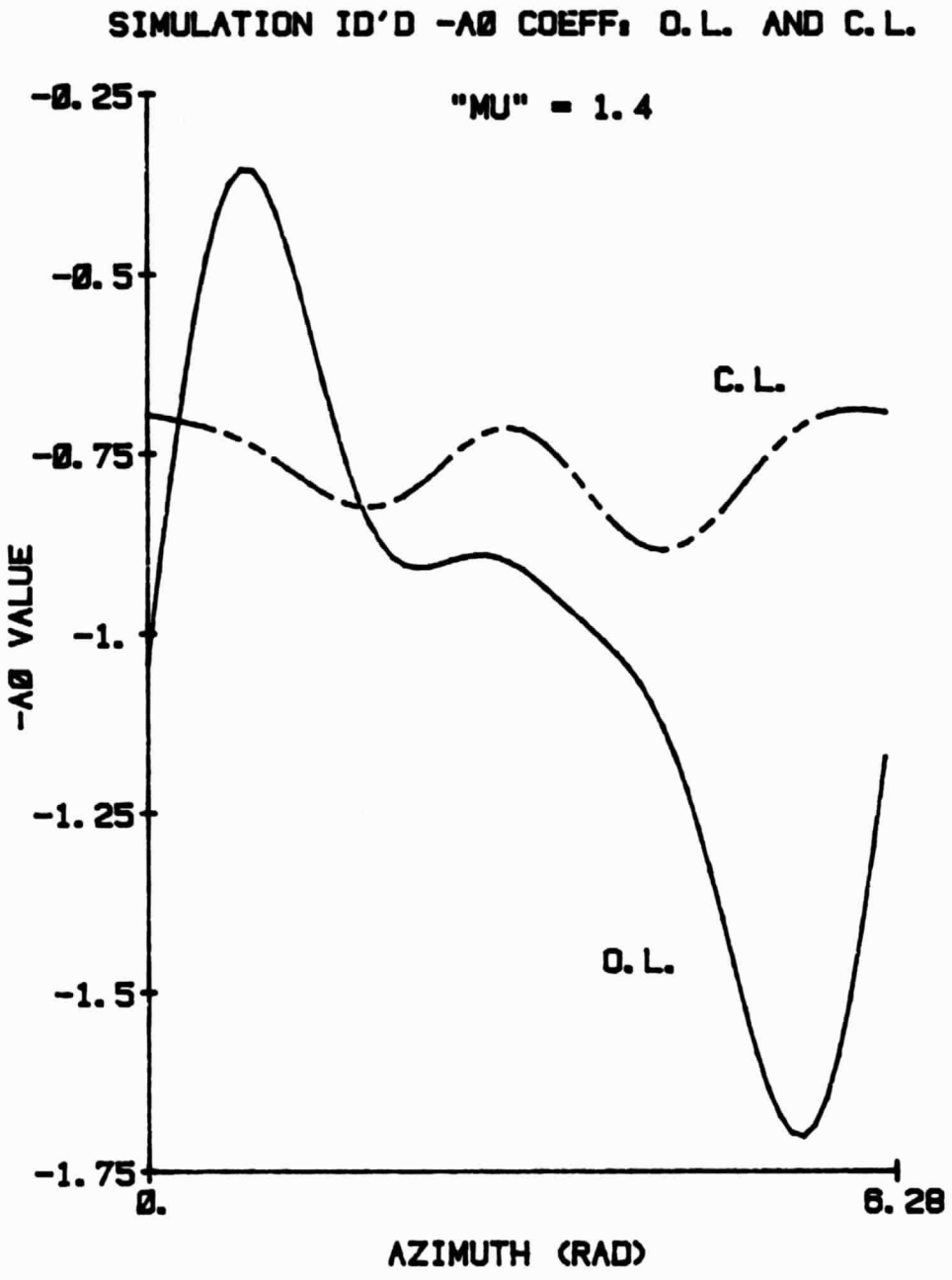

Fig. 6.2b: Estimated spring term for simulation, open- and closed-loop

ORIGINAL PAGE IS
OF POOR QUALITY

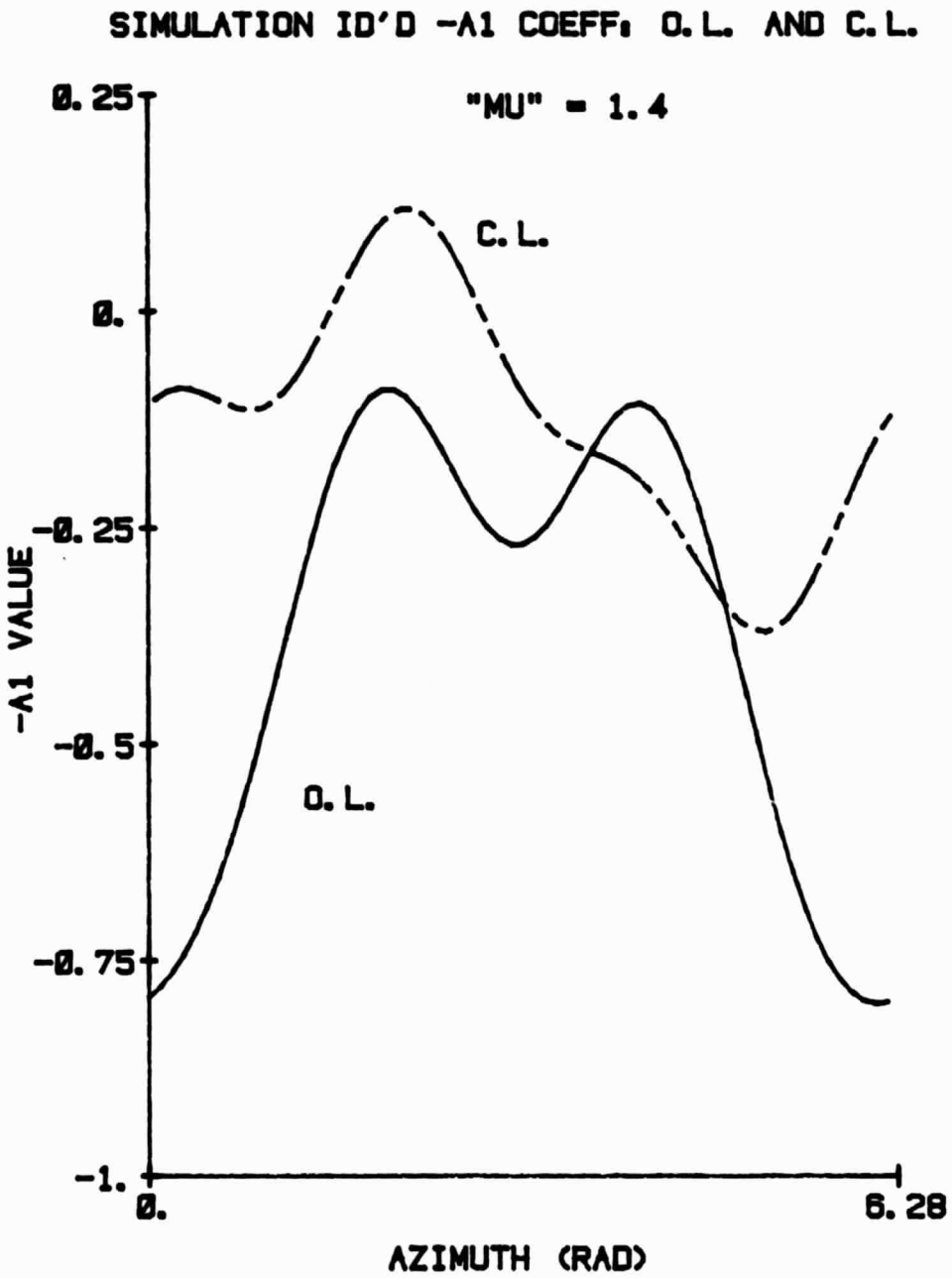

Fig. 6.2c: Estimated damping term for simulation, open- and closed-loop

ORIGINAL PAGE IS
OF POOR QUALITY

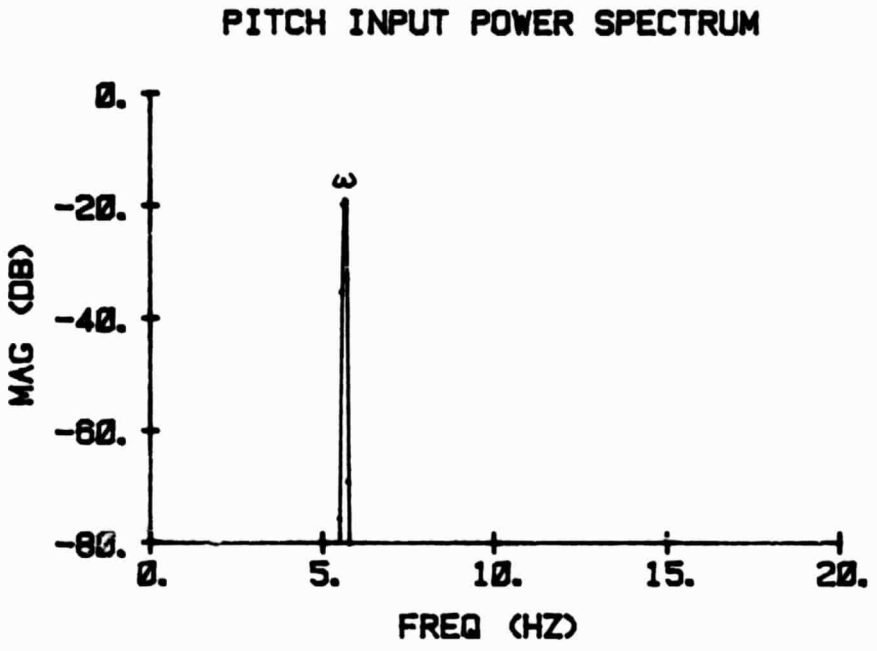

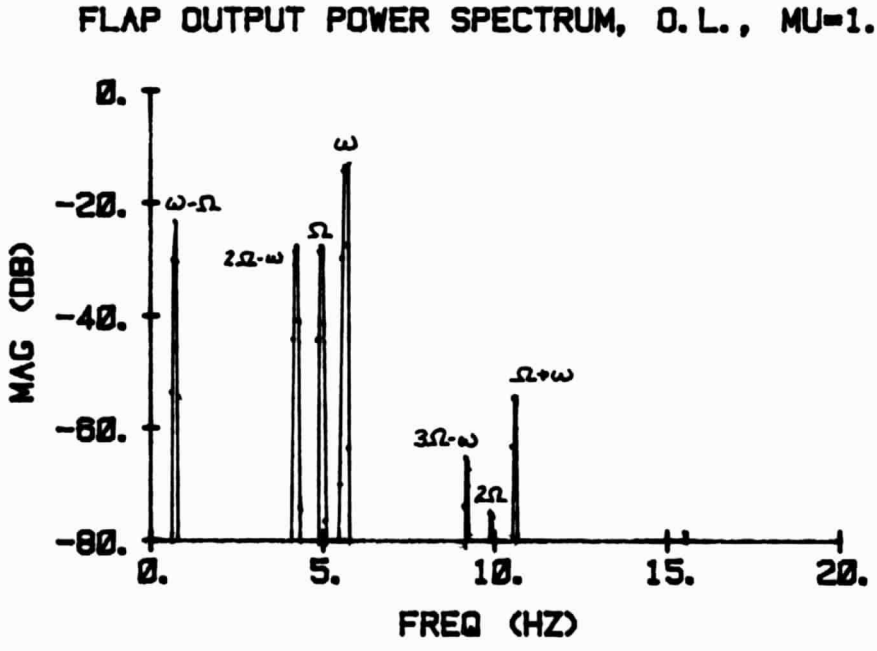

Fig. 6.3a: Open-loop power sprectra for simulation of excitation and response

ORIGINAL PAGE IS
OF POOR QUALITY

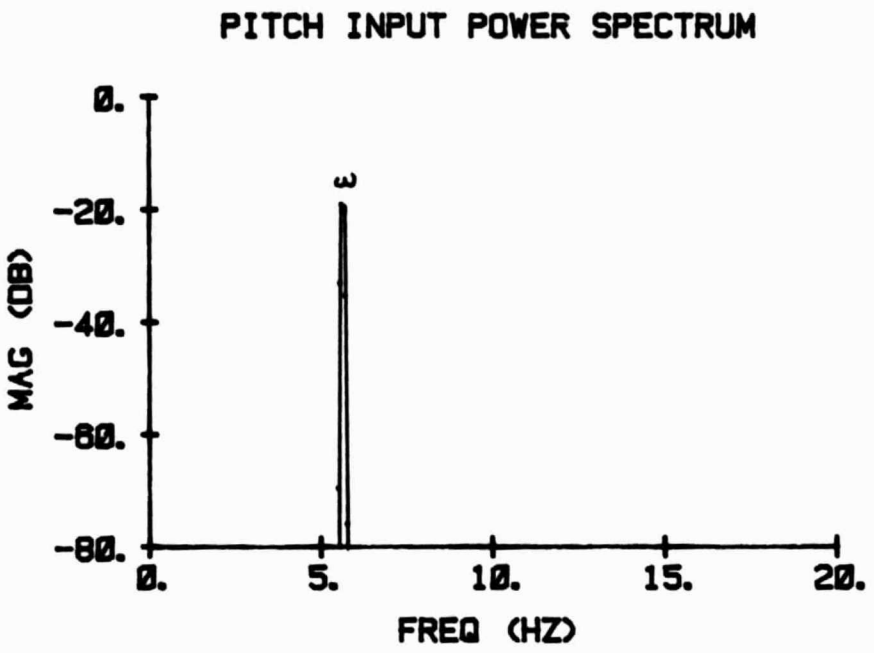

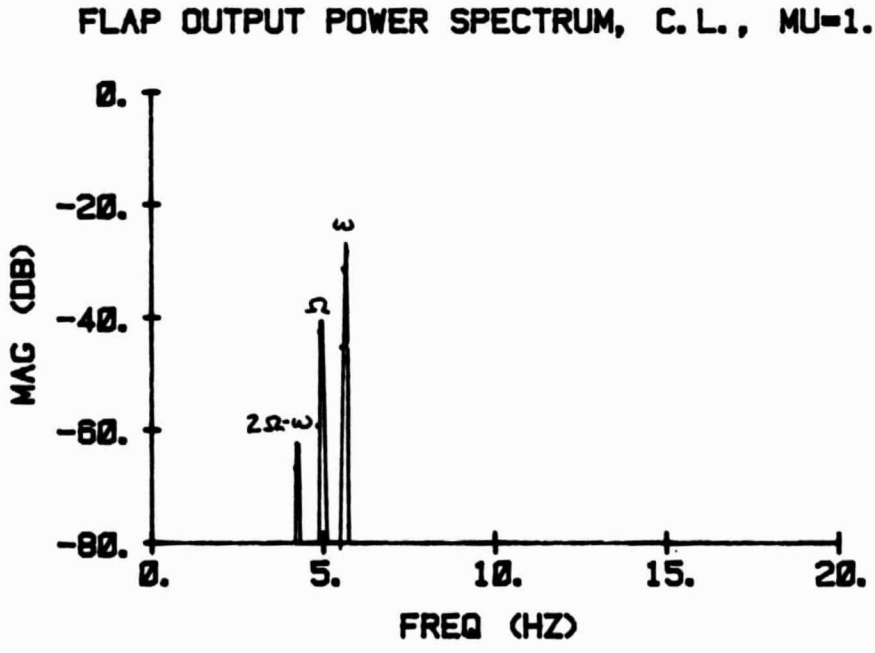

Fig. 6.3b: Closed-loop power spectra for simulation of excitation and response

ORIGINAL PAGE IS
OF POOR QUALITY

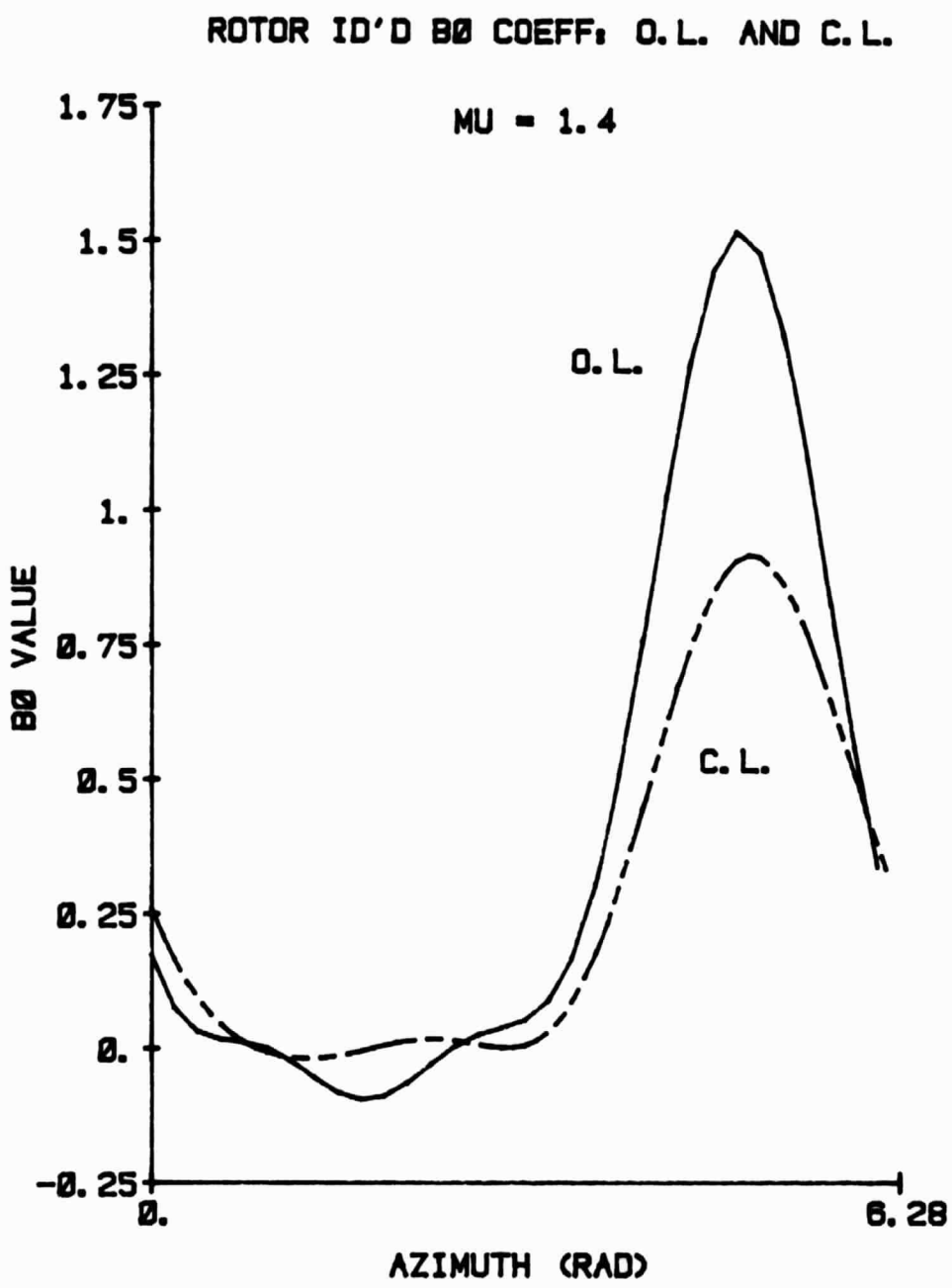

Fig. 6.4a: Estimated control power for rotor, open- and closed-loop

ORIGINAL PAGE IS
OF POOR QUALITY

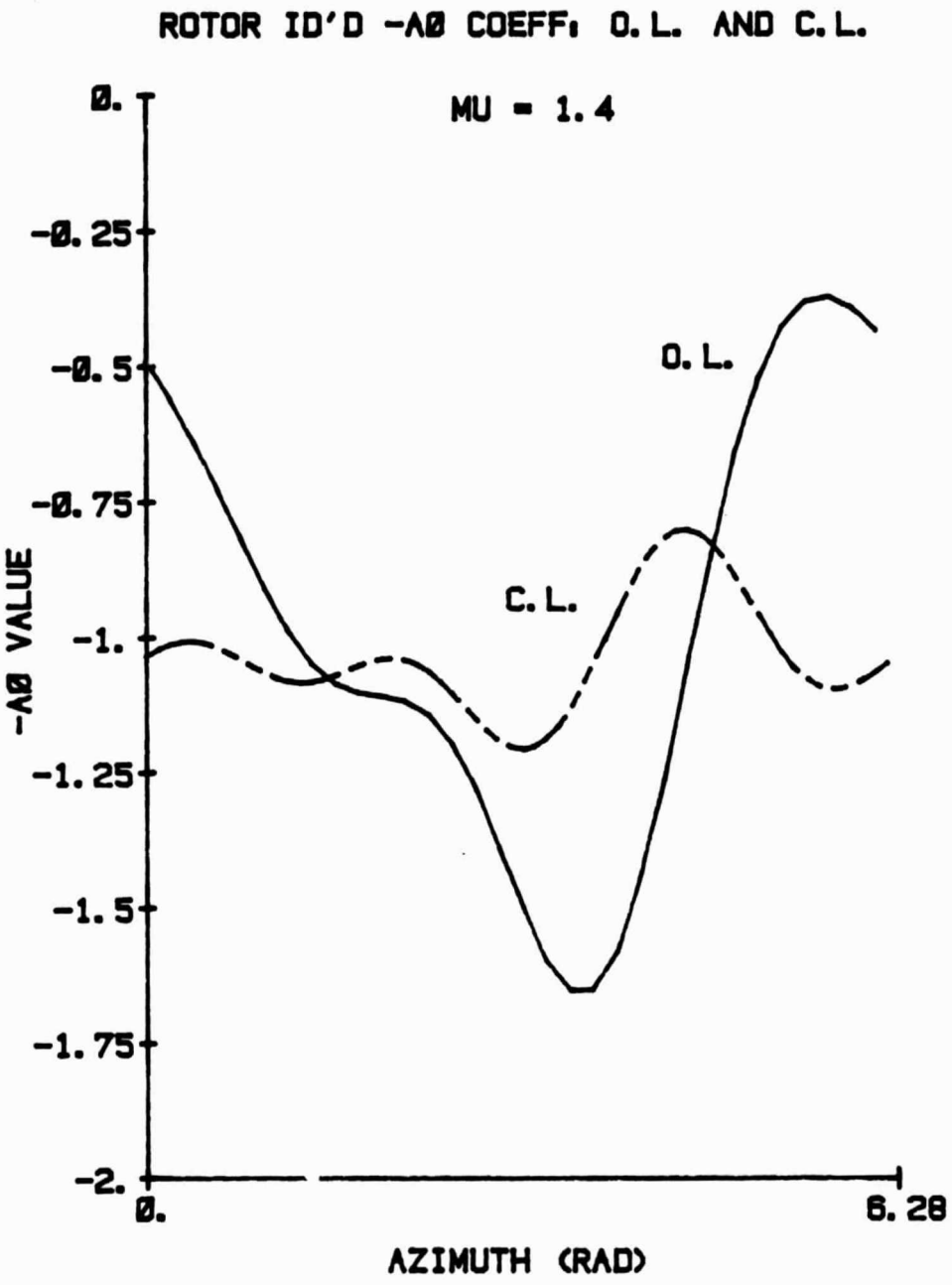

Fig. 6.4b: Estimated spring term for rotor, open- and closed-loop

ORIGINAL PAGE IS
OF POOR QUALITY

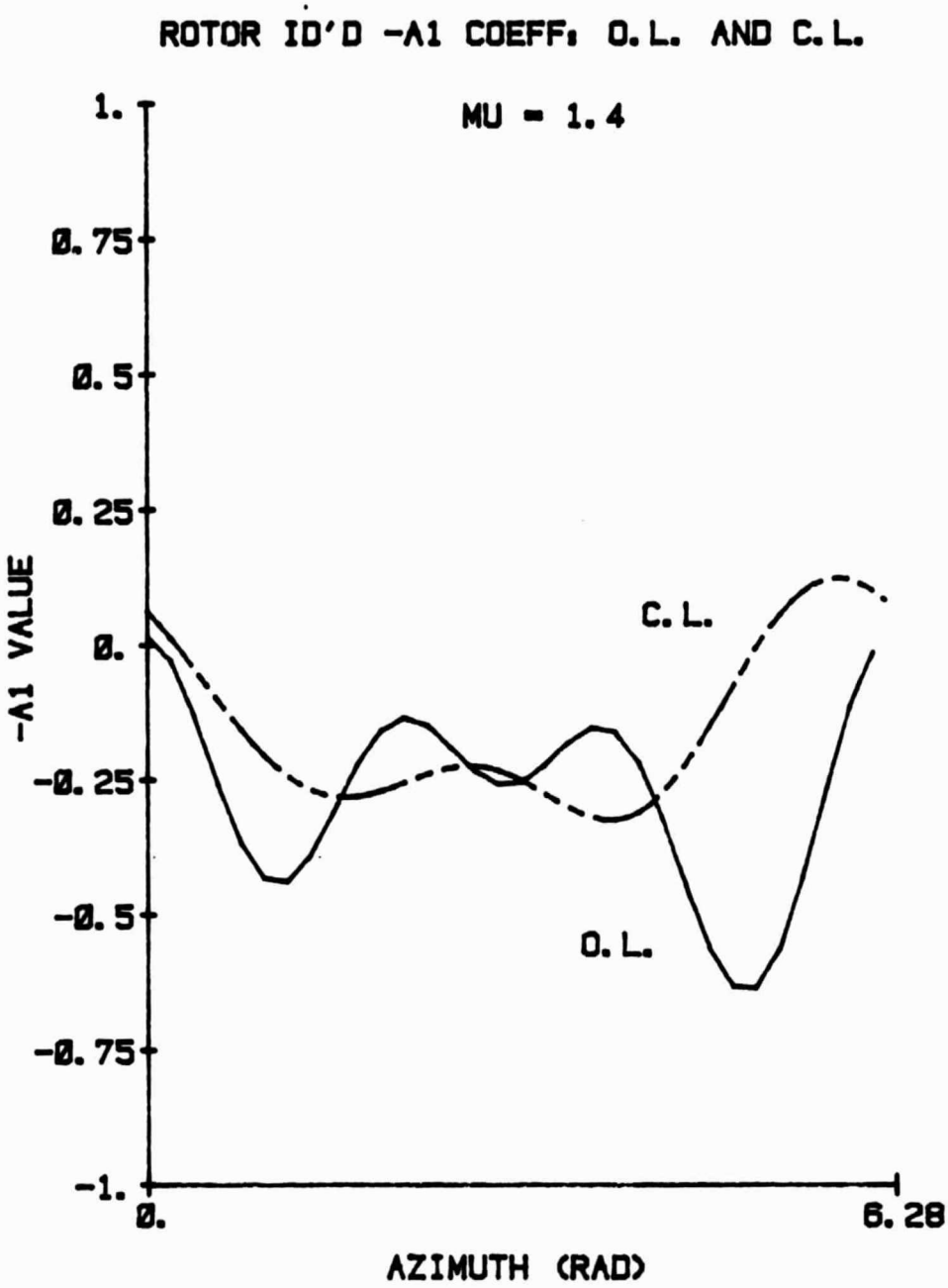

Fig. 6.4c: Estimated damping term for rotor, open- and closed-loop

ORIGINAL PAGE IS
OF POOR QUALITY

APPENDIX - Digital controller computer program listing

```
        .LIST   TTM
        .TITLE  CNTRL
;
;       CNTRL(NPTS,NCHANS,TABLE,CHNLST,ISHFT)
;               MACRO ROUTINE TO OUTPUT THE
;       SUM OF THE PRODUCTS OF GAINS IN 'TABLE'
;       WITH VALUES FROM THE A/D CONVERTER.
;
;       THIS ROUTINE WILL CYCLE THROUGH ITSELF AND REPEAT
;       INDEFINITELY UNTIL A KEY IS STRUCK ON THE TERMINAL, WHICH
;       WILL CAUSE AN EXIT. ALSO, IT IS ASSUMED THAT THIS ROUTINE
;       IS CALL FROM A FORTRAN MAINLINE, AND THUS NO REGISTERS
;       ARE SAVED.
;
;       THE I*2 DATA TABLE IS ASSUMED TO BE IN A 'PACKED' FORM;
;       THAT IS, THERE ARE NO CHANNELS TO BE SKIPPED -- THE
;       FIRST CHANNEL FOR THE NEXT POINT IMMEDIATELY FOLLOWS
;
        .GLOBL  CNTRL
        .MCALL  .REGDEF
        .REGDEF
;***************************************************************
;
;       CNTRL(NPTS,NCHANS,TABLE,CHNLST,ISHFT) ---
;
CNTRL:  MOV     @2(R5),NPTS     ;SAVE NPTS
        MOV     @4(R5),NCHANS   ;AND # OF CHANNELS
        MOV     6(R5),TABLE     ;SAVE TABLE POINTER
        MOV     8.(R5),R1       ;SAVE CHANNEL POINTER
        MOV     @10.(R5),ISHFT  ;SAVE NO. OF SHIFTS
;
;       DISABLE TERMINAL INTERRUPTS AS WAS DONE FOR
;       'TBLDMP.MAC'
;
        MOV     @RCSR,TTCSR             ;SAVE OLD TTY CNTL REG
        CLR     @RCSR                   ;DISABLE KBD INT FOR NOW
        MOV     @XCSR,LPCSR             ;SAVE LP CONTROL REG
        CLR     @XCSR                   ;DISABLE PRINTER INT
        MOV     @#60,HAND               ;PUSH OLD KBD HANDLER LOC
        MOV     @#62,STAT               ;AND STATUS ONTO STACK.
;
;       NOW LOAD  OWN TERMINAL KEYBOARD INTERRUPT HANDLER.
;       UPON SENSING A PRESSED KEY, R0 WILL BE LOADED WITH
;       A ZERO VALUE, SO INITIALIZE IT NOW.
;
        MOV     #1,KFLAG                ;INITIALIZE KBD INT FLAG
        MOV     #KBDSRV,@#60            ;LOAD KBD SERV HANDL ADDR
        MOV     #340,@#62               ;SET PRIORITY TO 7
        MOV     #100,@RCSR              ;ENABLE KBD FOR INT'S.
;
;       SET UP A/D CHANNEL TABLE
;
SETUP:  MOV     NCHANS,R5               ;COPY CHAN COUNT
        MOV     #CHNLST,R2              ;POINT TO CHANNEL LIST
        MOV     (R1)+,@R2               ;GET CHAN NO. AND
        SWAB    @R2                     ;PUT IN BITS 8-11.
        BIS     #120,(R2)+              ;SET FOR ST#1 START
                                        ;ON FIRST CHANNEL.
        DEC     R5                      ;BUMP CHAN COUNT
        BEQ     LOAD                    ;BRANCH IF ONLY 1 CHANNEL
MVCHN:  MOV     (R1)+,@R2               ;GET CHAN NO. AND
        SWAB    @R2                     ;PUT IN BITS 8-11.
        BIS     #101,(R2)+              ;ENABLE DONE INTERRUPTS
        SOB     R5,MVCHN                ;FINISH OFF ALL CHANS
```

ORIGINAL PAGE IS
OF POOR QUALITY


```
;
;       SET UP INTERRUPTS AND CONTROL WORDS
;
;       > SET UP CLOCK ST#2 TRIGGER HANDLER
;
LOAD:   MOV     #ST2SRV,@ST2VEC         ;POINT TO ST#2 HANDLER
        MOV     #200,@ST2PSW            ;WITH PRIORITY OF 4.
;
;       > AND THE A/D DONE HANDLER ...
;
        MOV     #ADSRV,@ADVEC           ;A/D DONE INT HANDLER
        MOV     #200,@ADPSW             ;PRIORITY LEVEL 4
        MOV     TABLE,R1                ;POINT TO TABLE BASE ADDR
        MOV     NPTS,COUNT              ;SET POINT COUNT
        MOV     #CHNLST,R0              ;POINT TO 1ST A/D CHAN
        MOV     NCHANS,R5               ;SET CHANNEL COUNT
        MOV     #STABT,R4               ;SET A/D STACK POINTER
        CLR     SIGHI                   ;CLEAR SUMMATION BUF
        CLR     SIGLO                   ;HI AND LO WORDS.
;
;       START CLOCK AND CONVERSIONS
;
        MOV     #60002,@KWCSR           ;SET CLOCK FOR ST2 INT ENA
WAIT:   TST     KFLAG                   ;WAIT FOR KEYBOARD INPUT
        BNE     WAIT                    ;BRANCH IF NONE FOUND
;
        MOV     HAND,@#60               ;HAND FOR KBD INTO PLACE,
        MOV     STAT,@#62               ;POP OLD KBD STAT REG
        MOV     TTCSR,@KCSR             ;RESTORE KBD CNTL REG
        MOV     LPCSR,@XCSR             ;RESTORE LP CNTL REG
        CLR     @KWCSR                  ;CLEAR CLOCK
        CLR     @ADCSR                  ;AND A/D
        RTS     PC                      ;RETURN FROM CNTRL.MAC
;***************************************************************
;
;       KEYBOARD INTERRUPT HANDLER: ZERO ALL D/A
;       CHANNELS AND THEN DISABLE
;       INT REQ AND SET RO TO ZERO.
;
KBDSRV: MOV     #4,R5                   ;COUNTER FOR D/A CHANS
        MOV     #DACBUF,R2              ;POINT TO D/A REGS
KLP:    MOV     #2048.,(R2)+            ;ZERO EACH ONE
        SOB     R5,KLP                  ;FOR ALL FOUR CHANS
        CLR     @KCSR                   ;DISABLE INTERRUPT REQ
        CLR     @KWCSR                  ;DISABLE CLOCK INT TOO
        CLR     KFLAG                   ;SET KBD FLAG = 'YES'
        RTI
;***************************************************************
;
;       ST#2 EVENT INTERRUPT HANDLER:
;       START A/D, THEN RESET TABLE POINTER
;       AND POINT COUNTER. THIS IS IN EFFECT THE
;       RE-SYNCHRONIZATION ROUTINE.
;
ST2SRV: MOV     (R0)+,@ADCSR            ;POINT TO MUX ADDRESS
        BIS     #1,@ADCSR               ;AND START CONVERSION.
        CLR     @KWCSR                  ;DISAPLE ST#2 INT REQ
        RTI                             ;RETURN FROM ST#2 INT.
;***************************************************************
;
;       A/D DONE INT HANDLER:
;
ADSRV:  MOV     @ADBPR,-(R4)            ;PUSH CONVERSION ON STACK
        DEC     R5                      ;BUMP CHAN COUNT
        BEQ     1$                      ;BRANCH IF ALL CHAN DONE,OR
        MOV     (R0)+,@ADCSR            ;START NEXT CHAN
```

ORIGINAL PAGE IS
OF POOR QUALITY


```
        RTI                             ;AND EXIT.
10$:    MOV     NCHANS,R5               ;RESET CHAN COUNT
20$:    MOV     (R4)+,R2                ;GET LAST CONVERSION
        SUB     #4000,R2                ;SUBTRACT OFFSET
        MUL     (R1)+,R2                ;MULTIPLY BY GAIN
        ADD     R3,SIGLO                ;ADD IN LOWER WORD
        ADC     SIGHI                   ;AND CARRY, THEN
        ADD     R2,SIGHI                ;ADD IN HIGH WORD
        SOB     R5,20$                  ;DO FOR ALL CHANS
        MOV     SIGLO,R3                ;COPY LO WORD OF SUM
        MOV     SIGHI,R2                ;AND HI WORD OF SUM,
        ASHC    ISHFT,R2                ;MULT. BY 2**ISHFT, AND
        NEG     R2                      ;FLIP SIGN AND
        ADD     #4000,R2                ;ADD IN OFFSET
        MOV     R2,@D2ABUF              ;DUMP TO D/A CHANNEL
        CLR     SIGHI                   ;ZERO SUMMATION
        CLR     SIGLO                   ;BUFFER WORDS
        MOV     NCHANS,R5               ;RE-RESET CHAN COUNT
        MOV     #CHNLST,R0              ;POINT TO TOP OF CHNLST
        DEC     COUNT                   ;BUMP POINT COUNT
        BEQ     40$                     ;BRANCH IF NPTS DONE
        MOV     (R0)+,@ADCSR            ;OK RESET A/D FOR ST1.
        RTI                             ;AND EXIT.
40$:    CLR     @ADCSR                  ;TURN OFF A/D INT
        MOV     TABLE,R1                ;POINT TO TABLE BASE ADDR
        MOV     NPTS,COUNT              ;SET POINT COUNT
        MOV     #60002,@KWCSR           ;SET CLK FOR ST2 INT ENA
        RTI
;***************************************************************
;
;       STORAGE AND LOCATION DEFINITIONS
;
ADVEC:  400                             ;A/D DONE INT VEC ADDR
ADPSW:  402                             ;A/D INT PSW
KWVEC:  440                             ;CLK INT VEC ADDR
KWPSW:  442                             ;CLK INT PSW
ST2VEC: 444                             ;ST2 INT VEC ADDR
ST2PSW: 446                             ;ST2 INT PSW
ADCSR:  170400                          ;A/D CONTROL REG
ADBPR:  170402                          ;A/D BUFFER REG
D2ABUF: 170440                          ;D/A CHAN "A" OUTPUT BUF
KWCSR:  170420                          ;CLOCK STATUS REG
KWBPR:  170422                          ;CLOCK BUFFER REG
RCSR:   177560                          ;KEYBD CNTL STAT REG
XCSR:   177564                          ;PRINTER CNTL STAT REG
;
TTCSR:  .WORD   0                       ;STORAGE FOR RCSR
LPCSR:  .WORD   0                       ;STORAGE FOR XCSR
HAND:   .WORD   0                       ;OLD KEYBOARD HANDLER
STAT:   .WORD   0                       ;OLD KEYBOARD STATUS
;
NPTS:   .WORD   0                       ;NO. PTS/REV
NCHANS: .WORD   0                       ;NO. A/D INPUT CHANS
TABLE:  .WORD   0                       ;ADDR OF DATA TABLE
CHNLST: .BLKW   16.                     ;MODIFIED CHANNEL LIST
ISHFT:  .WORD   0                       ;GAIN=(2**ISHFT)/65536.
COUNT:  .WORD   0                       ;COUNTER FOR # POINTS
KFLAG:  .WORD   0                       ;KEYBOARD INT REQ FLAG.
SIGLO:  .WORD   0                       ;SUMMATION BUF LO WORD
SIGHI:  .WORD   0                       ;SUMMATION BUF HI WORD
;
STKTP:  .BLKW   8.                      ;STORAGE FOR A/D BUF STACK
STKBT:  .WORD   0                       ;BOTTOM OF A/D STACK
;
        .END
```